Papers presented to the

NINTH SYMPOSIUM

ON ANTARCTIC METEORITES

22-24 March 1984

NATIONAL INSTITUTE OF POLAR RESEARCH,
TOKYO

国立極地研究所

The Ninth Symposium on Antarctic Meteorites

Programme

22 - 24 March, 1984

National Institute of Polar Research, Tokyo

Thursday, March 22, 1984

0900-1200 Registration Auditorium (6th Floor)

* Speaker

1000 - 1005 Takesi Nagata : Opening address

Chairmen: Naoki Onuma and Mineo Kumazawa

1 1005 - 1020 Katsushima T.* Nishio F. Ohmae H. Ishikawa M. and Takahashi S.
Collection of Yamato Meteorites from Antarctica in 1982-83

2 1020 - 1035 Nishio F.* Ohmae H. Ishikawa M. Katsushima T. and Takahashi S.
Bedrock Topography and Occurrence of Meteorites in the Meteorite Ice Field near the Yamato Mountains

3 1035 - 1050 Tajima K.* and Nishio F.
Exact Solution of Radar Equation for Detecting Meteorites Buried within the Ice by Radio Echo Sounding

4 1050 - 1105 Tazawa Y.* and Fujii Y.
Anormalously Sm Enriched Perovskite Spherules and Other Types of Spherules from the JARE-15 Ice Core at Mizuho Station

5 1105 - 1120 Matsumoto Y.* Jyo N. and Kojima H.
Classification of Several Yamato-75 Chondrites (V)

6 1120 - 1135 Kojima H.* and Yanai K.
Classification of the Pebble Size Meteorites in the Yamato-74 Collection

7 Prinz M. Nehru C. E. Weisberg M. K. Delaney J. S. and Yanai K.
Yamato-691, A Type 3 Enstatite Chondrite: Relationship with Other Unequilibrated Enstatite Chondrites (UEC's)

8 1135 - Takeda H.* Mori H. Ikeda Y. and Yanai K.
Yamato-79 Howardites and their Primitive Crust

9 - 1205 Takeda H.* Ishii T. Mori H. Wooden J. E. Prinz M. Delaney J. S. and Nyquist L. E.
Consortium Studies on Yamato-74, 75 and 79 Eucrites, and their Relationship

1205 - 1300 Lunch Time

Chairmen: Ken-ichiro Aoki and Nobuo Morimoto

10 1300 - 1315 Kojima H.* Ikeda Y. and Yanai K.
Classification of the Yamato Carbonaceous Chondrites

11 1315 - 1330 Jakes P.* and Bukovanska M.
New Czechoslovakian L-5 Chondrite: Usti Nad Orlici-Kerhartice

12 1330 - 1345 Yanai K.* Kojima H. Prinz M. Nerhu C. E. Weisberg M. K. and Delaney J. S.
Petrologic Studies of Three Primitive Achondrites from the Yamato Mounatins, Antarctica

13 1345 - 1415 Scott E. R. D.* Taylor G. J. and Keil K.
Matrix Material in Type 3 Ordinary Chondrites - Composition and Relationship with Chondrules

14 1415 - 1440 Fredriksson K.* and Specht S.
Electron and Ion Probe Determinations of Some Element Partitions in Individual Chondrites

15 1440 - 1455 Ikeda Y.* and Takeda H.
Petrology of the Y-7308 Howardite

16 1455 - 1510 Delaney J. S. O'Neill C. Nehru C. E. Prinz M. Stokes C. P. Yanai K.* and Kojima H.
Classification of Some Basaltic Achondrites from the Yamato-79 Meteorite Collection Including Pigeonite Cumulate Eucrites, a New Group

1510 - 1540 Tea Time

Chairmen: Ichiro Sunagawa and Yukio Ikeda

17 1540 - 1555 Yanai K.* and Kojima H.
Lunar Meteorite in Japanese Collection of the Yamato Meteorites

18 1555 - 1610 Matsunami S.*
Chemical Compositions of Matrices and Chondrule-Rims of Unequilibrated Ordinary Chondrites

19 1610 - 1625 Kimura M.*
Coarse-Grained Lithic Fragments in Unequilibrated Ordinary Chondrites

20 1625 - 1640 Watanabe S.* Kitamura M. and Morimoto N.
Analytical Electron Microscopy of a Chondrule (L3: ALH-77015) Including Relict Olivine

21 1640 - 1655 Kitamura M.* Isobe H. Watanabe S. and Morimoto N.
Thermal History of 'Relict Pyroxene' in the Allende Meteorite

22 1655 - 1710 Mori H.* and Takeda H.
An Analytical Transmission Electron Microscopic Study of Shock-Produced Veins in the Tenham Chondrite

23 1710 - 1725 Miura Y.* and Tomisaka T.
Composition and Structural Substitution of Meteoritic Plagioclases

24 1725 - 1750 Smith D. G. W.* Launspach S. and Miura Y.
Ni, Fe and Co Variation Patterns of Twelve Antarctic Chondrites

1800 - 2000 Reception (Lecture Room, 2nd Floor in Research Building)

Friday, March 23, 1984

Chairmen: Hiroshi Takeda and Hiroichi Hasegawa

25 0945 - 1000 Akai J.*
Mineralogical Characterization of Matrix Materials in Carbonaceous Chondrite Yamato-793321 and Belgica-7904 by HREM

26 Yanxi M. and Shuyuan Z.
High Resolution Electron Microscopy of Pyroxenes from Jilin and Shuangyang Chondrites

27 1000 - 1015 Takahashi E.* Matsui Y. and Ito E.
Melting Phase Relations of Various Chondrites at High Pressures

28 1015 - 1030 Takahshi E.*
On the Origin of Pallasite

29 1030 - 1045 Suzuki T.* Akimoto S. and Fukai Y.
Iron Hydride and Origin of Earth: Can E-Chondrite Make Earth?

30 1045 - 1100 Nakazawa K.* and Hayashi C.
Origin of the Moon

31 1100 - 1115 Fukuoka T.* and Suzuki E.
Chemical Compositions of Yamato Polymict Achondrites

32 1115 - 1130 Nagata T. Masuda A. Taguchi I.* and Ono Y.
Chemical Studies on Distribution of Germanium and Gallium in Antarctic Iron Meteorites

33 1130 - 1150 Michel-Levy M. C. Bourot-Denise M. Danon J.* Scorzelli R. B. and Souza-Azevedo I.
Unusual Metal Phases in the Tuxtuac LL Chondrite

1150 - 1300 Lunch Time

Chairmen: Akimasa Masuda and Akira Shimoyama

34 1300 - 1315 Nishikawa Y.* Nakamura N. and Hutchison R.
Precise Determination of REE, Ba, Sr, Rb, K, Ca and Mg Abundances in the Individual Chondrules of H-Chondrites

35 1315 - 1330 Ebihara M.*
Neutron Activation Analysis of Rare Earth Elements for Some Meteorites Including Antarctic Meteorites

36 1330 - 1345 Masuda A. Takahashi K.* and Shimizu H.
Studies of REE Abundances and Major Element Compositions of Kapoeta, Juvinas and Roda Achondrites

37 Gibson Jr. E. K. Cronin J. R. Kotra R. K. Primas T. R. and Moore C. B.
Amino Acids, Carbon and Sulfur Abundances in Antarctic Carbonaceous Chondrites

38 1345 - 1400 Shimoyama A.* and Harada K.
Search for Amino Acids Indigenous to the Yamato-793321 and Belgica-7904 Carbonaceous Chondrites

39 1400 - 1415 Murae T. Masuda A. and Takahashi T.
Studies on Organic Components in Carbonaceous Chondrites, Allende, ALH-77307, and Y-74662, by Direct Pyrolysis.

40 1415 - 1445 Clayton R. N.* Mayeda T. K. and Yanai K.
Oxygen Isotopes in Yamato Meteorites

41 1445 - 1500 Okano O.* Nakamura N. Misawa K. Honma H. and Goto H.
Rb-Sr Systematics and Trace Element Abundaces Studies of the Antarctic LL-Chondrites

1500 - 1530 Tea Time

Chairmen: Nobuo Takaoka and Noboru Nakamura

42 1530 - 1545 Ozima M.* Takayanagi M. Zashu S. and Amari S.
Anomalous $^{3}He/^{4}He$ Ratio in Pacific Ocean Sediments -- Evidence for Meteorite Debris or Cosmic Dust Fallout?

43 1545 - 1600 Matsuda E.* and Kigoshi K.
Carbon-14 Ages of Antarctic Meteorites

44 Bhandari N. Goswami J. N. and Shukla P. N.
Cosmogenic Tracks and Spallation Products in Antarctic Meteorites and their Terrestrial Ages

45 1600 - 1615 Kaneoka I.*
Relationship between the Type of Meteorite and the Characteristics of Ar-Degassing

46 1615 - 1630 Takaoka N.*
Isotopic Analysis of Noble Gas in ALH-77257 (Ur)

47 1630 - 1645 Nagao K.* Inoue K. and Ogata K.
Rare Gas Studies of the Antarctic Meteorite: Belgica-7904 C2 Chondrite

48 1645 - 1700 Komura K.* Tan K. L. and Sakanoue M.
Non-Destructive Measurement of Radionuclides in Yamato Meteorites

49 1700 - 1715 Honda M.* Nagai H. Yamamuro K. and Hayashida Y.
Cosmogenic Scandium 45 in Iron Meteorites

50 1715 - Nagata T.* and Funaki M.
Magnetic Properties of Antarctic Polymict Eucrites

51 - 1745 Nagata T.* Funaki M. and Taguchi I.
Magnetic Properties of Antarctic Iron Meteorites

Saturday, March 24, 1984

Chairmen: Masatake Honda and Minoru Ozima

52 0945 - 1010 Zbik M.* Lang B. Grodzinski A. and Stoch L.
Microstructural and Thermoanalytical Characterization of Several Antarctic Meteorites

53 1010 -1025 McFadden L. A. Gaffey M. J. and Takeda H.
Observational Evidence Relating Near-Earth Asteroid Composition to Meteorites

54 1025 - 1045 Hasegawa H.* and Kozasa T.
Grain Formation of Primordial Materials of Meteorites

55 1045 - 1100 Fujii N.* Takeuchi H. Ito K. and Miyamoto M.
Shape Analysis of Fe-Ni Grains among Antarctic Ordinary Chondrites

56 1100 - 1115 Tanaka T.*
Meteorite as a Possible Guiding Star for the Creation of New Materials under Micro Gravity

57 1115 - 1130 Momose K. Nagai H.* and Muraoka Y.
The Martensitic Transformation and Change of the Thermo-Remanent Magnetization

58 1130 - 1150 Sugiura N.* and Strangway D. W.
NRM Directions around a cm-Size Inclusion in Allende

1150 - 1330 Lunch Time

-- Special Lecture --

Chairman: Naoki Onuma

59 1330 - 1530 Clayton R. N. (University of Chicago)

- Isotopic Cosmochemistry of Oxygen and Silicon -

Thursday, March 22, 1984

0900 - 1200	Registration, 6th Floor
1000 - 1005	Opening address, Auditorium
1005 - 1750	Presentation, Auditorium
1800 - 2000	Reception, Lecture Room 2nd Floor

COLLECTION OF YAMATO METEORITES FROM ANTARCTICA IN 1982-83

Katsushima, T.[*1], Nishio, F.[*2], Ohmae, H.[*3], Ishikawa, M.[*3] and Takahashi, S.[*4]

*1 Department of Geology and Mineralogy, Hokkaido University, Sapporo 060
*2 National Institute of Polar Research, Tokyo 173
*3 Institute of Low Temperature Science, Hokkaido University, Sapporo 060
*4 Kitami Institute of Technology, Kitami 090

The inland traverse party of the 23rd Japanese Antarctic Research Expedition visited the Yamato Mountains in 1982-83 in order to search for Yamato Meteorites and to make glaciological and geological investigations. The meteorites were collected from December 1982 to January 1983 on the bare ice fields south of the Yamato Mountains, and the total amount of them are 211. Some of them were found on the bare ice surface near Motoi Nunatak and the Minami-Yamato Nunataks, which were also investigated by the previous parties, whereas more than half of the specimens were collected along the route from the Minami-Yamato Nunataks to 50 km southward, which was surveyed for the first time by the present party. It is noteworthy that more than 50 specimens were found in the area within 1 km around the measurement point, K22, 25 km south of Kuwagata Nunatak of the Minami-Yamato Nunataks. Since the present investigation covered only a small part of the bare ice field south of the Minami-Yamato Nunataks, it is highly probable that a large amount of meteorites will be found in this field.

The collected specimens are mostly ordinary chondrites, but preliminary examination suggests that they comprise also 13 eucrites, 5 diogenites and 10 carbonaceous chondrites, All diogenites are collected in the field around Motoi Nunatak.

2 − 1

Bedrock topography and occurrence of meteorites in the Meteorite Ice Field near the Yamato Mountains

Fumihiko NISHIO*1, Hirokazu OHMAE*2, Masao ISHIKAWA*2,
Takayoshi KATSUSHIMA*3 and Syuhei TAKAHASHI*4
*1 National Institute of Polar Research, Tokyo 173
*2 Institute of Low Temperature Science, Hokkaido University, Sapporo 060
*3 Department of Geology and Mineralogy, Hokkaido University, Sapporo 060
*4 Kitami Institute of Technology, Kitami 090

In the bare ice area of the Meteorite Ice Field near the Yamato Mountains found a large number of meteorites, the conditions of ice flow is characterized as the horizontal surface velocity is gradually decreasing down to zero towards the nunataks, the vertical velocity is emergent flow, i.e., upward velocity of ice, in the region of high meteorite concentrations with an average emergent flow of approximately 5cm/year, and the ablation rate is approximately equal to the upward movement of ice flow. These characteristics of ice flow may be affected by the sub-ice bedrock topography.

To make clear the bedrock and surface topography of the bare ice area in the Meteorite Ice Field, the radio echo sounding was carried out by over-snow sounding during the field season in 1982-1983. In particular the precise topography of the bedrock and surface in the area up-stream of Motoi Nunatak is investigated because previous oversnow traverse covered this area for studying the ice flow and a large number of meteorites were found. The continuous records of radio echo sounding was obtained at a spacing of 2-3km along a traversed line in the grid of 10x10km as shown in Fig. 1. In the area up-stream of Motoi Nunatak, more than 400 specimens were found and collected on the flat bare ice surface. In Fig. 1, most of meteorite pieces were not found on the steep slope such as ice cliff, but on the flat surface down-stream of the ice cliff which is reflecting on the ice sheet flow. As seen in Fig. 2, high ridge of bedrock topography is created up-stream of the ice cliff, and the bare ice surface is comparatively flat in the up-stream and down-stream of the ice cliff. The horizontal velocity in the up-stream of the ice cliff is larger than in the down-stream of it. It appears, therefore, that the ice flow is governed by the presence of ridge.

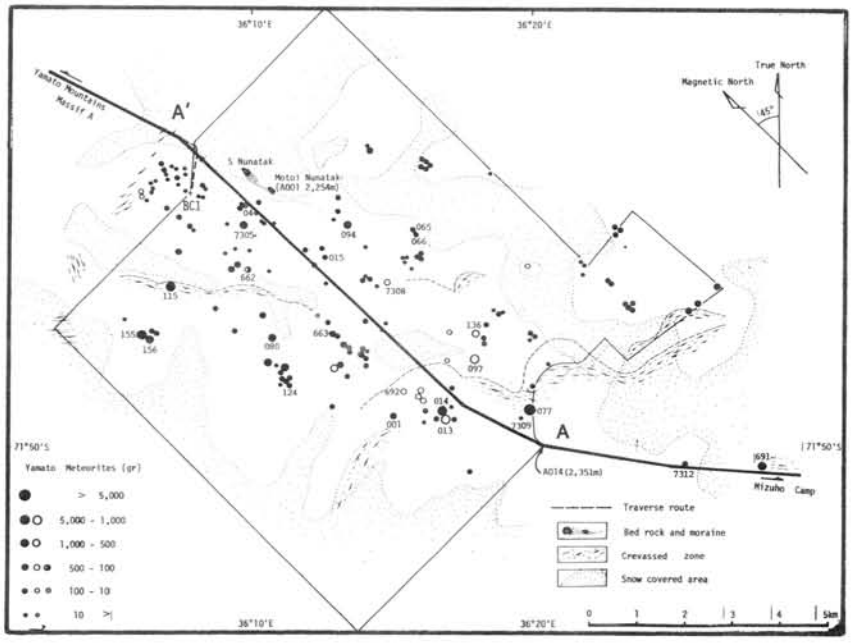

Fig. 1. Surface features of the bare ice and locations of the Yamato meteorites in the Meteorite Ice Field near the Motoi Nunatak, southern end of the Yamato Mountains. Those Yamato meteorites were collected in 1969 and 1973.

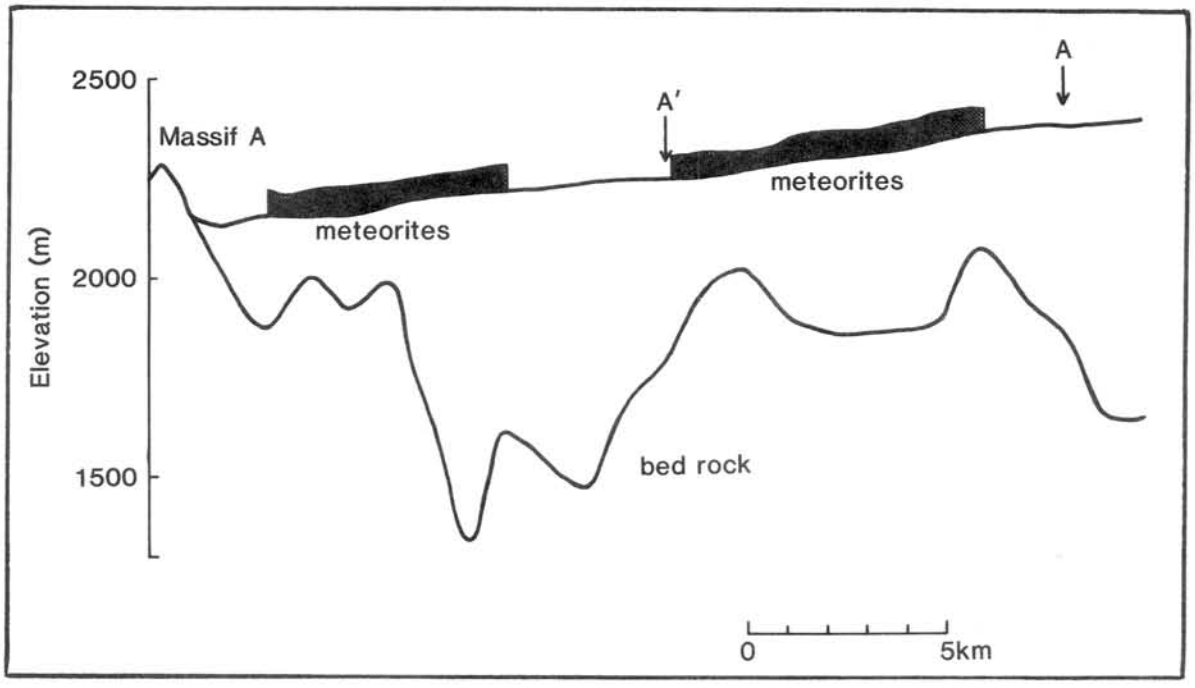

Fig. 2. The south-east to north-west cross-section of the ice surface and bedrock elevation from Motoi Nunatak to Massif A, Yamato Mountains. The line AA' shows traverse route in Figure 1. Shaded area indicate the meteorite concentration area on the bare ice surface.

3 − 1

Exact solution of radar equation for detecting meteorites buried within the ice by radio echo sounding

Katsusuke TAJIMA
(Institute of Interdisciplinary Research, Faculty of Engineering, The University of Tokyo)
and
Fumihiko NISHIO
(National Institute of Polar Research)

Recovery of large numbers of Yamato meteorites and Allan Hills meteorites in Antarctica led us to postulate the presence of meteorite pieces still buried in the ice. If meteorites buried within the ice could be detected by radio echo sounding, it may be significant to clarify the concentration mechanism of a large number of meteorites, and also if meteorites buried in the ice are taken out together with the surrounding ice, valuable information on chronological problems of both meteorite and ice will be obtained.

NISHIO and others (1981) proposed the possibility of locating of meteorites buried in the ice by means of radio echo sounding, assuming that meteorite pieces are spherical in shape, and that the dielectric constant of stony meteorite is equal to that of granite (8.0) and iron meteorites is a conductive sphere. For simplification, it is also assumed that a small number of meteorite pieces are dispersed uniformly in the ice in the isolate form and the strength of the electric field is not attenuated throughout the ice, and that the scattering mechanism will predominate the Rayleigh scattering because the most of the diameter of meteorite pieces are smaller than wavelength used by radio echo sounder.

However, we have to consider that the strength of electromagnetic wave will be attenuated throughout the ice. Also we should calculate in more detail the relation between the detectable depth and the diameter since, when

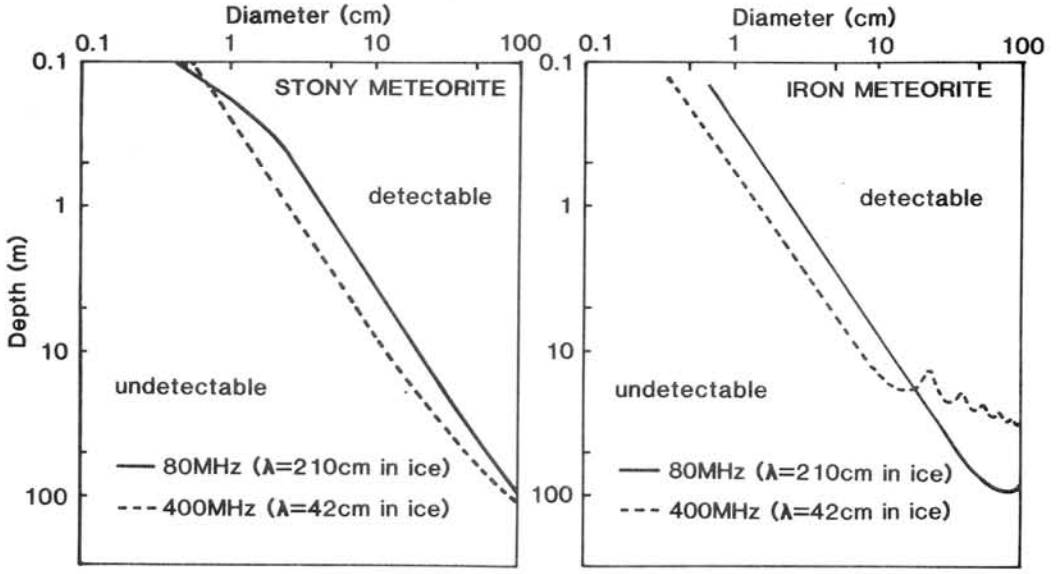

Fig. 1. Relation between the depth of ice and the diameter of spherical meteorite for the iron meteorites and the stony meteorites when electromagnetic wave having frequency of 80MHz(λ=210cm in ice) and 400MHz(λ=42cm in ice) are respectively radiated into the ice.

the electromagnetic wave of the high friquency such as 400MHz is used, the back scattering due to iron meteorites causes the Mie scattering.

It is, therefore, shown that the exact solution of the radar equation should be obtained for detecting meteorites buried within the ice.

The radar equation can be applied to the iron meteorite as conductive sphere and the stony meteorite as dielectrical sphere, respectively.

(1) Radar equation for iron meteorite

Under the assumption that the iron meteorite is a conductive sphere and the electromagnetic wave is incident on a conductive sphere as plane wave insted of spherical wave in the vicinity of the spherical meteorite. Then the radar equation may be given in the following,

$$\frac{P_r}{P_i} = \frac{\lambda^2 G_0^2 e^{-j2kr}}{64(\pi k r^2)^2} \left\{ \sum_{n=1}^{\infty} j^n (2n+1) \left[\frac{\hat{J}_n'(ka)}{j\hat{H}_n^{(2)'}(ka)} \hat{H}_n^{(2)}(kr) + \frac{\hat{J}_n(ka)}{\hat{H}_n^{(2)}(ka)} \hat{H}_n^{(2)}(kr) \right] \right\}^2 \times (TT')^2 \quad (1)$$

$$k^2 = \omega^2 \varepsilon \mu \quad (2)$$

$$\varepsilon = \varepsilon(1 - j\tan\delta) \quad (3)$$

where Pr is the power at the ice-air interface reflected from spherical meteorite, Pi the transmitted power from air to ice, Go the antenna gain, λ the wavelength of electromagnetic wave used, k the propagation constant in ice, a the radius of the spherical meteorite, ε the permittivity of ice, T the transmissivity from air to ice, T' the transmissivity from ice to air, $\hat{J}n$, $\hat{H}n^2$ the spherical Bessel function of the first and second kind, respectively.

(2) Radar equation for stony meteorite

It is assumed that stony meteorite is spherical meteorite as the dielectrical sphere and that the Rayleigh scattering occurs since there is no finding of the stony meteorite pieces larger than 50cm in diameter. In the case of the Rayleigh scattering, for ka<<1, the radar equation may be approximately given in the following,

$$\frac{P_r}{P_i} = \frac{\lambda^2 G_0^2 |e^{-j2kr}|}{16\pi^2 r^2} \times (TT')^2 \times \left| \frac{jk^2a^3}{r} \times \frac{\varepsilon_r - 1}{\varepsilon_r + 2} \times \hat{H}_1^{(2)'}(kr) \right| \quad (4)$$

$$\varepsilon_r = \frac{\varepsilon_m}{\varepsilon_{ice}} \quad (5)$$

where εm is the permittivity of the stony meteorite (εm=8.0) and εice the permittivity of the ice.

Based on the detailed calculation of the radar equation of (1) and (4), Figure 1 shows the criteria for detectable and undetectable meteorites as a function of diameter, depth and frequency of electromagnetic wave of 80MHz and 400MHz. The detectable domains indicate that the intensity of echo reflected from the meteorite buried in the ice is sufficient to be detected

by the present radio echo sounding apparatus taking Go=2 as the antenna gain and $Pr/Pi=10^{-10}$ as the maximum sensitivity of the back-scattered power from spherical meteorite.

As shown in Fig. 1, the detectable domain for iron meteorite is larger than that for stony meteorite, indicating that if the diameter is identical, the detectable depth for iron meteorite must be deeper than that for stony meteorite. The detectable domain extends to smaller diameter of meteorite and larger depth with using higher frequency in the case of the Rayleigh scattering, but it should be noted that for iron meteorite, the frequency dependence on the detectable domain becomes reciprocal and shows resonance phenomena for the 400MHz at the diameter larger than about 10cm where the scattering aspect due to meteorite pieces dispersed in the ice changes from the Rayleigh scattering into the Mie scattering.

In the maximum frequency of diameter of meteorite, about 20cm for the iron meteorite and 1cm for the stony meteorite, the detectable domain shows resonance phenomena for the iron meteorite by the electromagnetic wave of 400 MHz in the depth of 10m, while for the stony meteorite the detectable domain is within 1m in depth. Therefore, it should be applied to the higher frequency to detect the stony meteorite.

Anomalously Sm enriched perovskite spherules and other types of spherules from the JARE-15 ice core at Mizuho Station.

Yuji TAZAWA and Yoshiyuki FUJII
Dept. Physics, Kyoto Univ. & Natl. Inst. Polar Res., Tokyo

In the previous work, two Ca-Ti- (perovskite-like) spherules (CTS) and one Fe-Cr-Ni spherule (FCN) were obtained from a portion of the Mizuho ice core ranged from 32m to 33.5m in depth, and they showed peculiar rare-earth-element concentrations: Sm was enriched by a factor of 10 relative to terrestrial perovskite. In this work, we have studied forty-two spherules from ten portions of the Mizuho ice core (shallower than 43m in depth) by instrumental neutron activation analysis (INAA) and scanning-electron microscopy with energy-dispersive X-ray microanalysis (SEM/EDXMA). Every portion of the ice core contained CTS and FCN (relative frequencies of these types occurrence are approximately 2:1, other types are 1).

All of CTS show the same concentrations of major and trace elements, e.g. Ca,Ti,Cr,Fe, REE,etc., as the previous CTS's values (Fig.1 and Table 1). FCN also show similar concentrations to the previous ones, except REE do not exist.

Pemarkable results are: two cases that the different types of spherules stick together: the one case is a large Zircon spherule stuck with two CTS (Fig.1a) and the other is a large FCN stuck with a CTS (Fig.1b). Especially, the Zircon spherule is constructed from a eccentric Zircon core and a glassy clust.

This clust corsists of Ca, Ti, Cr, Fe, Zr and Si, seems to be a mixture of Zircon and perovskite. It must be important eviden-- ces to confirm the origin of the Mizuho spherules. INAA result of REE and siderophile element are shown in Fig.2.

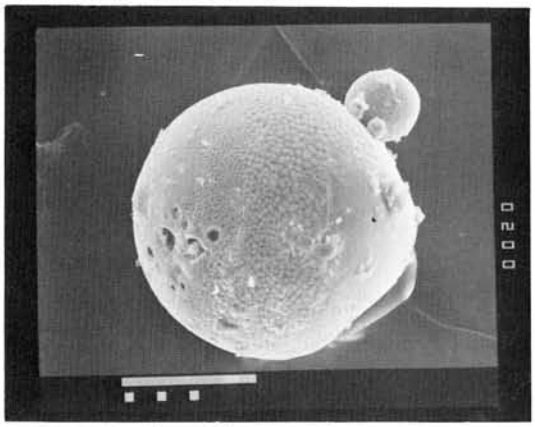

Fig. 1a ZIRCON + CTS (MZ-II-04)

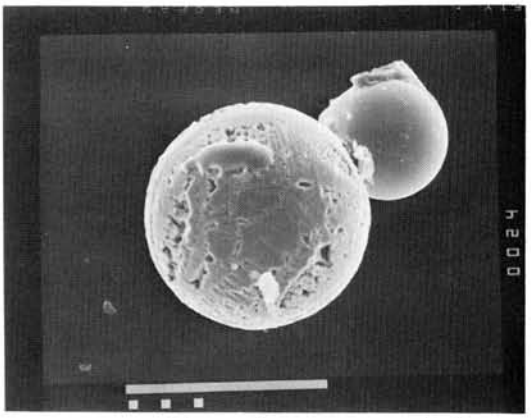

Fig. 1b FCN + CTS (MZ-II-14)

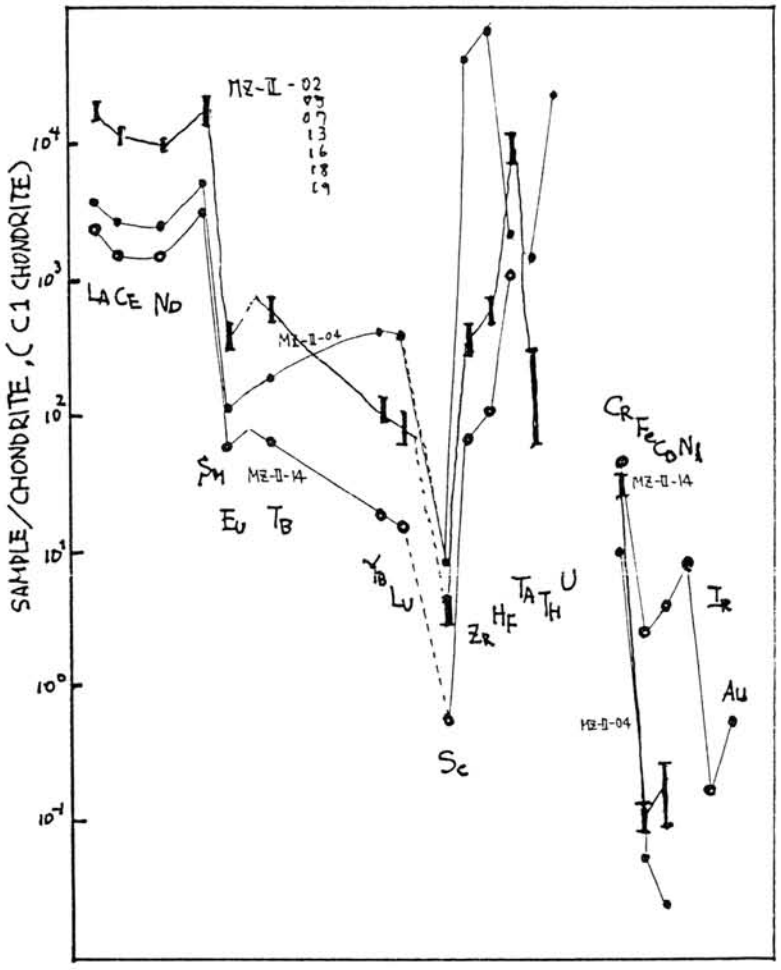

Fig.2
INAA Results of TRACE ELEMENTS in CTS

Classification of several Yamato-75 chondrites (V)

Matsumoto Yukio*, Jyo Nobuyuki* and Hideyasu Kojima**
* Department of Mineralogical Sciences and Geoligy, Faculty of Science, Yamaguchi University, Yamaguchi 753, Japan
** National Institute of Polar Research, Tokyo 173, Japan

Nineteen specimens of Yamto-75 meteorites have been analyzed by using a JXA-50A EPMA of the department of Mineralogical Sciences, Yamaguchi University and a JXCA-733 of National Institute of Polar Research.

These meteorites have been classified as follow;

H3: Y-75029 (83.9g)
H4: Y-75096 (91.8g), Y-75269 (87.2g), H4-5: Y-75291 (23.5g)
H5: Y-75012 (69.9g), Y-75259 (70.0g), H5-4: Y-75262 (47.2g), H5-6: Y-75267 (38.1g)
H6: Y-75100 (85.0g), Y-75277 (99.0g), Y-75304 (22.1g)
L4: Y-75019 (22.7g), L4-5: Y-75297 (20.5g)
L5: Y-75017 (87.2 g), Y-75270 (26.9g), Y-75288 (93.9g), Y-75289 (50.9g)
L6: Y-75071 (6.9g),
LL6: Y-75258 (971.0g).

Table 1. Mean composition and percent mean diviation (%M.D.) of olivines and orthopyroxenes

Sample No.	Olivine					Pyroxene						
	No.	Mg	Fe	M.D.	%M.D.	No.	Ca	Mg	Fe	M.D.	%M.D.	Remarks
Y-75012,92	27	80.7	19.3	0.43	2.2	8	1.1	81.7	17.2	1.10	6.5	H5
Y-75029,92	29	81.6	18.4	1.53	8.3	28	1.3	82.2	16.5	2.12	12.9	H3
Y-75096,91	27	82.8	17.2	0.35	2.0	23	1.2	82.9	15.9	1.26	7.9	H4
Y-75100,92	21	81.2	18.8	0.41	2.2	14	1.5	82.1	16.4	0.28	1.7	H6
Y-75259,92	24	80.2	19.8	0.31	1.6	22	1.5	81.4	17.1	0.25	1.5	H5
Y-75262,62	26	81.2	18.8	0.70	3.7	21	1.4	81.9	16.7	0.76	4.5	H5-4
Y-75267,91	24	81.3	18.7	0.56	3.0	26	1.5	81.9	16.0	1.28	8.0	H5-6
Y-75269,92	33	81.3	18.7	0.25	1.3	27	0.6	83.6	15.8	0.64	4.1	H4
Y-75277,92	31	80.8	19.2	0.31	1.6	16	1.4	81.8	16.8	0.36	2.2	H6
Y-75291,73	58	81.5	18.5	0.89	4.8	10	0.9	83.0	16.1	0.55	3.4	H4-5
Y-75304,71	57	81.5	18.5	0.63	3.4	20	1.3	82.4	16.3	0.54	3.3	H6
Y-75017,91	25	75.5	24.5	0.20	0.8	9	1.0	78.7	20.3	0.62	3.1	L5
Y-75019,91	63	75.7	24.2	0.42	1.7	19	0.9	77.3	21.8	1.71	7.9	L4
Y-75071,81	22	74.7	25.3	0.39	1.5	7	1.5	77.7	20.8	0.36	1.7	L6
Y-75270,93	32	74.2	25.7	0.40	1.5	19	1.2	77.0	21.9	0.57	2.6	L5
Y-75288,92	26	75.2	24.8	0.38	1.5	12	1.4	77.8	20.8	0.33	1.6	L5
Y-75289,71	40	75.0	25.0	0.45	1.8	10	1.4	77.7	20.9	0.45	2.2	L5
Y-75297,72	49	75.9	24.0	0.38	1.6	10	1.3	78.2	20.6	0.96	4.7	L4-5
Y-75258,97	46	68.1	31.2	0.53	1.7	10	2.3	73.6	24.1	0.26	1.1	LL6

Table 2. Fequency distribution of iron contents of olivines

Sample No.	Atomic % Fe 11	12	13	14	15	16	17	18	19	20	21	22	23	24	25	26	27	28	29	30	31	32	35
						-------H------							-----L-----						-----LL-----				
Y-75012								+	++	+													
Y-75029	-					-	+	+	+	-	-												
Y-75096					-	+	++																
Y-75100								++	+	-													
Y-75259								-	++	+													
Y-75262							+	++	+	-	-												
Y-75267							+	++	+	-	-												
Y-75269								++	+														
Y-75277								+	++														
Y-75291						-	++	+	+	-	-				-								
Y-75304							+	++	+			-											
Y-75017													-	++									
Y-75019													+	++	+								
Y-75071														+	++	-							
Y-75270														-	++	+							
Y-75288													-	++	+								
Y-75289														++	+			-					
Y-75297												-	++	++	-								
Y-75258																			-	++	++	-	-

Table 3. Fequency distribution of iron contents of orthopyroxene

Sample No.	Atomic % Fe 5	6	7	8	9	10	11	12	13	14	15	16	17	18	19	20	21	22	23	24	25	26
											---H----				---L----				---LL---			
Y-75012												++			+							
Y-75029	-		-						-		+	++	-	-		-						
Y-75096					-	-				-	++	+	-								-	
Y-75100											+	++	-									
Y-75259												++	++									
Y-75262											+	++	-	-	-							
Y-75267											++	+	+	-		-						
Y-79269									-	-	++	+			-							
Y-75277												++	+	-								
Y-75291										+	+	++	+									
Y-75304											+	++	+	-								
Y-75017														+	+	++	+					
Y-75019															+	+	+		-	+	-	
Y-75071																++	+					
Y-75270																-	++	+	+			
Y-75288															-	++	+					
Y-75289																++	+					
Y-75297													+		+	++	+		+			
Y-75258																			++	++		

10% > - ; 10 - 40% + ; 40%< ++

Classification of the Pebble Size Meteorites in the Yamato-74 Collection

H. Kojima and K. Yanai
National Institute of Polar Research, Tokyo 173

A lot of pebble size specimens of Yamato-74 meteorites have been identified and classified. Most of them are grouped to the chondritic meteorites, belonging to each petrologic type and grade, but several specimens are identified preliminary as unique meteorites. The new identified and classified specimens including one new carbonaceous chondrite, one new ureilite, new one enstatite chondrite(E5) and some unique specimens were presented in the Table 1 with one older lodranite, enstatite chondrite(E3-4) and others. The new carbonaceous chondrite is very fresh specimen with much chondrules and chondrule fragments with less matrix, and was classified as a CO3. The new specimen calssified as a ureilite shows highly recrystallized texture that is very similar to the one of terrestrial quartzite. This ureilite consists of mainly fine-grained olivine and less amount of an euhedral pyroxene crystal with much less amount of the black material than all other ureilites. This ureilite differ from all others as it contains much less black materials.

Table 1. Pebble Classifications from the Yamato-74 Meteorites Antarctic Meteorite Collection

NAME	WEIGHT(g)	CLASSIFICATION		%Fa	%M.D.	%Fs	%M.D.
Yamato-74003	15.5	L6	Chondrite	25.2	1.3	21.1	1.7
Yamato-74004	8.05	H5	Chondrite	19.0	2.1	16.7	1.9
Yamato-74006	35.83	H6	Chondrite	19.1	1.6	16.5	2.0
Yamato-74008	14.31	H	Chondrite	18.5	2.0	16.2	3.8
Yamato-74009	8.97	L5	Chondrite	24.5	1.8	20.6	1.4
Yamato-74016	11.54	H6	Chondrite	19.1	1.7	16.8	2.4
Yamato-74017	3.23	H6	Chondrite				
Yamato-74018	5.25	LL6	Chondrite	29.8	1.1	24.1	0.8
Yamato-74019	6.02	H4	Chondrite	18.8	1.9	16.1	2.8
Yamato-74020	0.56	L6	Chondrite				
Yamato-74023	6.30	L6	Chondrite	22.9	2.7	19.4	1.8
Yamato-74025	14.0	Unique		1.6	9.6	2.2	6.1
Yamato-74026	5.24	H6	Chondrite	19.6	1.5	17.0	1.1
Yamato-74027	35.7	L6	Chondrite	25.4	1.7	15.6	2.0
Yamato-74029	4.3	H4	Chondrite	17.9	1.6	15.6	2.0
Yamato-74030	7.82	L6	Chondrite	25.3	1.2	21.2	2.0
Yamato-74032	14.1	H3	Chondrite	19.0	1.5	16.8	1.4
Yamato-74033	2.9	L3	Chondrite	16.5	33.4	22.5	12.1
Yamato-74034	27.6	H4	Chondrite	19.1	1.4	16.3	1.8
Yamato-74040	35.17	L6	Chondrite	24.4	1.9	20.5	2.4
Yamato-74041	1.79	H5	Chondrite	18.6	2.2	16.9	3.1
Yamato-74042	2.85	H4	Chondrite	18.1	3.0	15.5	2.8
Yamato-74043	5.19	H3	Chondrite	19.0	4.1	15.4	27.3
Yamato-74045	39.82	L6	Chondrite	25.1	1.6	21.1	0.9
Yamato-74046	2.22	H6	Chondrite	25.0	1.5	20.9	1.7
Yamato-74047	2.22	L4	Chondrite	23.2	1.8	19.9	4.4
Yamato-74063	35.41	Unique		10.9	1.8	10.9	2.8
Yamato-74067	4.0	H6	Chondrite	19.2	2.2	16.6	3.3
Yamato-74068	5.41	H5	Chondrite	19.0	1.9	16.9	5.0

6 − 2

NAME	WEIGHT(g)	CLASSIFICATION		%Fa	%M.D.	%Fs	%M.D.
Yamato-74069	18.57	H6	Chondrite	19.9	1.2	17.2	2.4
Yamato-74071	17.55	H5&6	Chondrite				
Yamato-74072	29.0	H	Chondrite				
Yamato-74075	5.05	H6	Chondrite				
Yamato-74076	20.36	L6	Chondrite	24.5	1.3	20.3	2.1
Yamato-74078	15.88	H4	Chondrite	19.5	1.7	17.0	1.1
Yamato-74083	3.31	H4	Chondrite				
Yamato-74084	2.1	H	Chondrite				
Yamato-74085	30.5	H4	Chondrite				
Yamato-74086	0.97	H5	Chondrite				
Yamato-74087	0.78	H6	Chondrite	24.9	1.4	20.8	1.5
Yamato-74088	14.28	H4	Chondrite				
Yamato-74089	43.36	H4	Chondrite				
Yamato-74090	1.01	H	Chondrite				
Yamato-74091	2.30	L6	Chondrite	24.5	1.7	20.8	1.4
Yamato-74092	3.23	L6	Chondrite	19.3	1.6	16.7	1.7
Yamato-74093	6.59	L6	Chondrite	24.8	1.8	20.8	1.6
Yamato-74095	65.92	H6	Chondrite	25.2	1.6	20.8	2.6
Yamato-74098	9.10	H5	Chondrite	18.9	2.0	16.9	
Yamato-74099	27.36	H5	Chondrite	18.6	1.4	16.2	1.6
Yamato-74100	15.45	L6	Chondrite	25.8	1.7	20.9	
Yamato-74101	9.10	H5	Chondrite	18.9	2.2	16.5	2.4
Yamato-74102	2.99	H5	Chondrite	18.8	1.9	16.4	2.3
Yamato-74103	21.59	H6	Chondrite	19.3	1.4	17.2	1.7
Yamato-74104	21.8	H5	Chondrite	19.4	1.9	16.8	2.0
Yamato-74105	25.66	H6	Chondrite				
Yamato-74112	45.52	L6	Chondrite				
Yamato-74113	28.21	L6	Chondrite				
Yamato-74114	42.28	L5	Chondrite				
Yamato-74119	4.36	L5	Chondrite				
Yamato-74121	8.53	H6	Chondrite				
Yamato-74122	53.89	H4	Chondrite				
Yamato-74126	14.52	Diogenite (A)					
Yamato-74127	19.20	L6	Chondrite	24.7	1.4	20.6	2.3
Yamato-74128	40.98	L5	Chondrite	25.0	1.5	21.1	
Yamato-74129	6.57	L6	Chondrite				
Yamato-74131	18.06	H5	Chondrite				
Yamato-74132	2.37	H4	Chondrite				
Yamato-74133	3.36	H4	Chondrite				
Yamato-74134	3.08	H4	Chondrite				
Yamato-74135	7.75	C3	Chondrite				
Yamato-74137	26.32	H6	Chondrite				
Yamato-74143	4.89	H6	Chondrite				
Yamato-74145	0.6	H6	Chondrite				
Yamato-74146	8.55	L	Chondrite				
Yamato-74147	5.93	L4	Chondrite				
Yamato-74148	1.02	H5	Chondrite				
Yamato-74149	0.70	H6	Chondrite				
Yamato-74152	3.92	H4	Chondrite				
Yamato-74153	6.17	L4	Chondrite				
Yamato-74154	2.83	Ureilite		2-16		6-13.1	
Yamato-74161	42.09	L6	Chondrite				
Yamato-74168	1.59	E5	Chondrite	24.8	1.6	20.5	1.7

NAME	WEIGHT(g)	CLASSIFICATION		%Fa	%M.D.	%Fs	%M.D.
Yamato-74171	4.65	L-LL3	Chondrite				
Yamato-74172	47.1	L4,L6	Chondrite				
Yamato-74174	20.9	L6	Chondrite				
Yamato-74186	5.17	H4	Chondrite				
Yamato-74189	1.54	L6	Chondrite				
Yamato-74232	1.89	L6	Chondrite				
Yamato-74343	42.38	H5	Chondrite				
Yamato-74345	8.41	H6	Chondrite				
Yamato-74346	82.35	H6	Chondrite				
Yamato-74357	13.8	Lodranite		7.9	3.0	13.8	2.9
Yamato-74358	2.94	L6	Chondrite				
Yamato-74359	1.53	Unique,	Chondrite				
Yamato-74360	3.29	Unique,	Chondrite				
Yamato-74361	0.4	shocked	Chondrite				
Yamato-74363	1.01	L4	Chondrite				
Yamato-74365	0.67	H6	Chondrite				
Yamato-74366	0.25	H6	Chondrite				
Yamato-74369	4.17	H6	Chondrite				
Yamato-74370	42.1	E3-4	Chondrite	0.1		0.9	62.3
Yamato-74373	0.28	H6	Chondrite				
Yamato-74377	10.51	H6	Chondrite				
Yamato-74378	18.44	L5	Chondrite				
Yamato-74437	3.22	L6	Chondrite				
Yamato-74438	42.24	H5	Chondrite				
Yamato-74439	32.74	L6	Chondrite				
Yamato-74440	1.61	L4	Chondrite				
Yamato-74443	6.03	L5	Chondrite				
Yamato-74444	11.81	LL	Chondrite				
Yamato-74446	7.43	L6	Chondrite				
Yamato-74449	4.04	H6	Chondrite				
Yamato-74451	0.80	L6	Chondrite				
Yamato-74453	14.56	H4-3	Chondrite				
Yamato-74456	56.82	H4	Chondrite				
Yamato-74458	37.35	H5	Chondrite				
Yamato-74604	58.57	H4	Chondrite				
Yamato-74607	0.56	H5	Chondrite				
Yamato-74608	2.00	L4	Chondrite				
Yamato-74611	7.40	L6	Chondrite				
Yamato-74612	2.46	L6	Chondrite				
Yamato-74639	89.5	L5	Chondrite	24.1	1.6	20.4	2.6
Yamato-74643	38.01	H5	Chondrite				
Yamato-74644	20.45	L5	Chondrite				
Yamato-74645	35.6	H4-L4	Chondrite	21.1	1.6	17.9	1.6
Yamato-74649	2.83	L6	Chondrite				
Yamato-74651	1.07	L6	Chondrite				
Yamato-74653	1.09	H6	Chondrite				
Yamato-74654	45.02	L6	Chondrite				
Yamato-74655	10.55	L6	Chondrite				
Yamato-74656	12.52	L4	Chondrite				
Yamato-74657	8.94	L5	Chondrite				
Yamato-74658	11.07	H6	Chondrite				
Yamato-74660	27.2	LL3	Chondrite	10.5	63.4	8.9	78.4
Yamato-74661	5.31	L6	Chondrite				

7 – 1

Yamato-691, a Type 3 enstatite chondrite: Relationship with other unequilibrated enstatite chondrites (UEC's)

M. Prinz[1], C.E. Nehru[1,2], M.K. Weisberg[1,2], J.S. Delaney[1], K. Yanai[3]
(1) Amer. Museum Nat. Hist., NY, NY 10024. (2) Brooklyn College (CUNY), Brooklyn, NY 11210. (3) Nat'l Inst. Polar Res., Tokyo 173, Japan

Okada (1,2) provided an excellent description of the mineralogy and petrology of the Yamato(a) enstatite chondrite, later renamed Yamato-691. Masuda and Tanaka(3) presented REE and related trace element data. Okada classified Y-691 as a Type I (E4) enstatite chondrite, whereas Sears et al. (4) called it EH4,5. Prinz et al. (5) called it E3, based on published data, and suggested that the E3 group consists of newly recognized unequilibrated enstatite chondrites (USC's) which include Qingzhen, Parsa, Kota-Kota, ALHA 77156 and Galim. This study provides further mineralogical data on Y-691, which supports the E3 classification.

Texturally, Y-691 is similar to the other USC's in that it contains sharply defined glass-bearing chondrules, in contrast to E4 and E6 chondrites which have essentially no chondrules. The abundance of olivine-bearing chondrules is Y-691 is also characteristic of E3 chondrites.

Modal data, determined by automated electron microprobe techniques, are presented in Table 1, and compared with E3, E4 and E6 chondrites. The most striking feature is the relatively large abundance of olivine (7.2%) in Y-691 and in other E3 chondrites. The only highly reduced chondrite containing more olivine is the chondritic clast material in Cumberland Falls, which contains 15% olivine (5), and which may also be related to E3's. Olivine is absent in the more equilibrated E4 and E6 condrites, except for rare grains in the E4 Indarch. In Y-691 abundant olivine and silica coexist in chondrules, indicating rapid cooling and disequilibrium. E4 and E6 chondrites contain excess silica, and any olivine which may have been originally present in the assemblage recrystallized as pyroxene.

The atomic Fe/Si and Mg/Si ratios of Y-691 are plotted in Figure 1, and compared with EH(4) and EL(6) enstatite chondrites. Y-691 is clearly intermediate, indicating it does not chemically belong to either group. El Goresy et al. (6) note that Qingzhen is also intermediate between EH and EI, but no data are presented. Other E3's may also have intermediate values distinguishing this group.

Mineralogically, pyroxene is present as enstatite and clinoenstatite. Okada(1) showed that pyroxene ranged from 0.42-1.07% FeO, but our study has revealed enstatite in chondrules with up to 4.6% FeO (Table 2). Enstatite ranges from Wo0.2-0.6En93.0-99.2. Rare grains of Ca-rich pyroxene are also found, with 17% CaO, 0.9% FeO, 24.5% MgO, and 3.4% Al_2O_3.

Okada also reported olivine with 0.83-1.47% FeO, but we have found olivine with up to 4.5% FeO. Olivine ranges from Fo95.6-99.8. The olivine has high Cr, with 0.1-0.8% calculated as Cr_2O_3. Thus the wide range of olivine and pyroxene compositions in Y-691 indicates an E3 classification rather than E4 or E5.

Plagioclase is rare, but feldspathic glass is common. For each glass analysis the molecular Na/Al ratio was calculated and calibrated with the Na/Al ratio in stoichiometric plagioclase, in order to get the An/Ab ratio for plagioclase that would crystallize from the glass. This is based on the assumption that essentially all the Na in the glass resides in the plagioclase component, because only a minor amount is present in the small pyroxene component. The Ca/Al ratio cannot be used because a significant amount

could go with the pyroxene or oldhamite component. Based on these calculations, plagioclase is found to be generally calcic, An32-75. Similar results were found for Parsa (5,7), except that Parsa also contains albitic compositions as well. Abundant calcic plagioclase is also found in the glass of chondrules in unequilibrated ordinary chondrites (unpublished data). Thus it can be concluded that plagioclase in Type 3 E-chondrites is more calcic than in Type 4-6 chondrites, as is also the case for UOC's.

Metal, schreibersite and perryite data for Y-691 are presented in Table 3. Metal is low in Ni (2.9%) and Si (1.78%) in comparison with E4 chondrites, and similar to that found in other E3 chondrites (Table 4). Schreibersite (Table 3) is Ni-rich (18%) in comparison with E4 chondrites (Table 4). Perryite (Table 3) is similar to that found in other E3 chondrites (Table 4); it has not been found in E4 chondrites.

Troilite in Y-691 is similar to that in other E3 chondrites in having low Ti (0.14%) and Cr (1.38%) compared to E4 chondrites. Niningerite in Y-691 is dramatically different from that in E4 chondrites (Table 4), being enriched in Mg and depleted in Fe; it is more similar that in E3 chondrites. Oldhamite and sphalerite are present in Y-691 but the grains are too small for quantitative analysis. No daubreelite, caswellsilverite or djerfisherite was found in the sections studied, but a Ca-rich sulfide too small for quantitative analysis is relatively abundant for a minor phase. Sulfide data varify the correlation of Y-691 with other E3 chondrites.

Y-691 has been shown to be an E3 chondrite in terms of its texture and mode, the FeO range in olivine and enstatite, in the abundance of olivine, and in the compositional characteristics of the metal, schreibersite, perryite, troilite and niningerite. Its classification as an E3 chondrite by Prinz et al. (5) is supported by the new data presented here. The significance of the newly recognized E3 group and its role as a potential precursor to other enstatite chondrite groups is under investigation.

References: (1) Okada, A. (1975) Mem. NIPR, Spec. Issue No. 5, 14-66. (2) Okada, A. (1975) Mem. NIPR, Spec. Issue No. 5, 67-82. (3) Masuda, A. and T. Tanaka (1978) Proc. 2nd Symp. Ant. Meteorites, Mem. NIPR, Spec. Issue, No. 8. 229-232. (4) Sears, D. W. et al. (1982) Geochim. Cosmochim. Acta 46, 597-608. (5) Prinz, M. et al. (1984) Lunar Planet. Sci. XV. (6) El Goresy, A. et al. (1983) Meteoritics 18, in press. (7) Nehru, C. E. et al. (1984) Lunar Planet. Sci. XV. Funding: NASA NAG 9-32 (M. Prinz, P. I.).

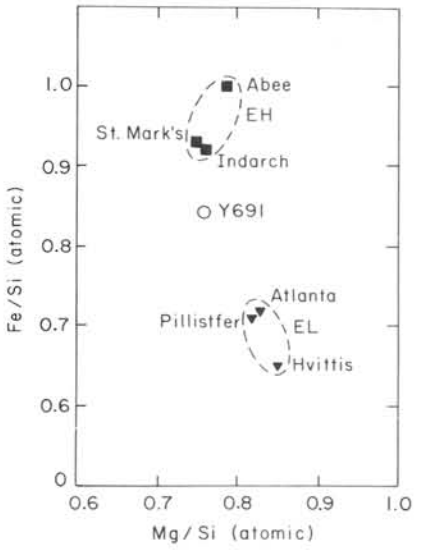

Figure 1. Fe/Si and Mg/Si atomic ratios for Y-691 compared with EH(4,5) and EL(6) chondrites.

Table 1. Modal data (vol.%) of Yamato-691 compared with other E3, E4 and E6 chondrites

		E3		E4		E6	
	Y-691	Kota-Kota	Parsa	Abee	Adhi Kot	Atlanta	ALHA 81021
olivine	7.2	0.7	4.1	-	-	-	-
pyroxene	61.8	67.4	65.1	59.0	59.5	66.1	70.7
plag/glass	5.2	8.5	7.8	9.0	11.5	16.6	10.4
silica	4.8	1.5	2.2	4.5	1.5	0.8	1.0
kamacite	7.7	10.1	6.6	12.6	11.7	9.2	12.3
taenite	0.4	-	1.4	0.7	0.1	tr	-
troilite	8.9	9.9	11.2	11.1	13.0	4.8	4.5
schreibersite	0.7	0.9	0.3	0.2	0.2	1.5	0.5
niningerite	2.8	0.3	0.1	2.6	1.3	-	-
daubreelite	0.1	0.6	0.6	-	-	0.9	0.8
oldhamite	0.4	0.1	0.5*	0.3	1.2	-	-
No. points	1000	1000	2250	1000	1000	1000	1000
Area mm^2	47.2	48.5	41.0	156.3	50.9	462.5	92.8

*Plus traces of perryite, caswellsilverite, Mg-Al spinel.

Table 2. Range of olivine and pyroxene compositions in the Y-691 enstatite chondrite

	Olivine		Enstatite	
SiO_2	40.8	39.2	58.1	56.3
TiO_2	<0.02	<0.02	0.03	0.03
Al_2O_3	<0.02	<0.02	0.08	0.24
Cr_2O_3	0.16	0.80	0.11	1.63
FeO	0.17	4.5	0.38	4.6
MnO	0.06	0.06	0.24	0.07
MgO	59.1	54.7	40.7	36.4
CaO	0.31	0.16	0.13	0.18
Na_2O	<0.02	<0.02	0.03	<0.02
Total	100.60	99.42	99.80	99.45
Wo			0.2	0.3
En Fo	99.8	95.6	99.3	93.0
Fs Fa	0.2	4.4	0.5	6.7

Table 3. Metal, schreibersite and perryite in the Y-691 enstatite chondrite

	Metal	Schreib-ersite	Perryite
Fe	94.6 (91.7 -95.1)	65.7	6.6
Ni	2.9 (2.2 - 5.2)	18.0	77.1
Co	0.19(0.16- 0.22)	<0.02	<0.02
Si	1.78(1.4 - 2.0)	0.12	11.5
P	<0.02	15.2	3.9
Total	99.47	99.02	99.10

Table 4. Mineral Comparisons of Y-691 with E3, E4 and F chondrites

		Qingzhen	Parsa	Kota-Kota	ALHA 77156	Yamato-691	Galim	E4 Average	Cumb. Falls
Enstatite	FeO	up to 8%	1.31	0.2- 5.8	Fs, 0.3-2.1	0.2-4.6	0.8-5.7	0.62 (0.22-1.12)	0.1 - 9.7
Olivine	FeO	n.d.	1.61	0.25-1.2	Fa, 0.1-1.3	0.1-4.5	n.d.	0.56	0.27- 3.6
Plag (glass)	An	n.d.	0-65	0-70	1.5	An32-75	glass	2.2	4.0 -11.2
Kamacite	Ni	2.7-3.4	2.4	3.3	2.8	2.9	n.d.	7.1	4.4 - 5.8
	Si	2.2-2.4	2.3	2.6	2.5	1.8	low	3.4	0.1 - 0.2
Troilite	Ti	1.0	0.22	0.27	n.d.	0.14	0.1	0.42	0.01
	Cr	1.8	0.54	0.60	0.54	1.38	0.1	2.25	0.1 - 0.5
Niningerite	Mg	23.5	26.0	23.5	24.7	33.6	n.d.	13.2	n.d.
	Mn	12.5	11.7	11.6	15.2	3.9		5.9	
	Fe	14.3	12.3	15.6	13.0	14.1		32.8	
	Ca	0.54	0.65	0.39	0.35	0.38		2.1	
Oldhamite	Mg	0.49	0.65	0.90	n.d.	n.d.	n.d.	1.40	n.d.
	Mn	0.45	0.17	0.17				0.32	
Perryite	Si	12.5	11.9	12.1	n.d.	11.5	n.d.	n.d.	n.d.
	P	3.1	3.5	3.4		3.9			
	Fe	9.0	5.1	4.6		6.6			
	Ni	74.5	80.6	81.2		77.1			
Schreibersite	Ni	15.1	10.8	15.1	15.4	18.0	n.d.	9.3	30 -52.5
	P	14.9	13.4	15.4	n.d.	15.2	n.d.	15.5	15.2-16.0

E4 -Incldes Indarch, Adhi Kot and Abee. n.d. - No available data. Sources of data given in (5).

8 − 1

YAMATO-79 HOWARDITES AND THEIR PRIMITIVE CRUST.

Takeda[1,3], Hiroshi, Mori[1], Hiroshi, Ikeda[2,3], Yukio, and Yanai[3], Keizo
[1]Mineralogical Inst., Faculty of Science, Univ. of Tokyo, Hongo, Tokyo 113
[2]Dept. of Earth Sci., Faculty of Science, Ibaraki Univ., Mito 310, and
[3]National Inst. of Polar Research, Kaga, Itabashi-ku, Tokyo 173.

The howardites meteorites have been interpreted to be lithified ejecta deposited by impacts of various sized meteorites and hence various depths of excavation of the layered crust on their parent body (e.g. 1). The study of howardites provides us with information of a variety of components, such as diogenites, cumulate euctites and ordinary eucrites and thier genetic relationship. Because howardites are rare among the known Antarctic meteorite collections (2), we investigated howardite-like specimens listed in "Tentative Catalog of Yamato Meteorites" compiled by Yanai (1983), as a part of the preliminary examination of the Yamato-79 collection. The results have been interpreted in the light of a crystal differentiation model proposed recently on the basis of the Yamato 7308 howardite (3).

Yamato 790727 (120.4g), 791208 (47.9g) and 791492 (41.1g) are three howardites tentatively identified in the Y-79 collection. Three polished thin sections supplied by NIPR have been examined by an optical microscope and a microprobe (JEOL 733 Superprobe at NIPR). The presence of orthopyroxene has been confirmed by the single crystal X-ray diffraction technique. The bulk chemical compositions analysed by H. Haramura (Geol. Inst., Univ. of Tokyo) are similar each other and plots in the middle of the diogenite-eucrite trend in the Al_2O_3 vs. CaO diagram, and are close to that of Binda, the most Mg-rich eucrite. These howardites are different from Y7308, which is the most diogenite-rich howardite.

The thin sections show a complex breccia of angular fragments, up to 2 mm long, of pyroxene, plagioclase and olivines, with some lithic clasts, set in a matrix of comminuted minerals. Accessory chromite and ilmenite and trace amounts of troilite are present. The dominant mineral fragments are diogenitic orthopyroxenes. A considerable amounts of weathering is indicated by rusty staining in Y791208. Microprobe analyses show a wide range in pyroxene composition as are given in Fig. 1. An contents in plagioclase range from 85 to 95 (Y790727), 90 to 93 (Y791208) and 89 to 95 (Y791492). Olivines with Fa_{15-25} are present.

Some characteristic lithic clasts found in thses howardites include: (1) MC: a small fragment of plagioclase An_{91} and partly inverted pigeonite $Ca_{14}Mg_{50}Fe_{36}$ with coase exsolution lamellae of augite on (001) in Y791208, similar to Nagaria, (2) GC: a gabbroic clast consisting of pigeonites $Ca_9Mg_{41}Fe_{50}$ with clouding and fine exsolution lamellae of augite with (001) in common and plagioclase with An_{90}, in Y791208. (3) a partly recrystallized dark aphanitic clast with plagioclase crystals in Y791208. (4) a diogenite clast with fine granoblastic texture and another one with partly melted and recrystallized portions in Y790727. (5) small inverted pigeonite fragments with blebby inclusions of augite similar to Binda in Y791492.

The chemical compositions of the pigeonite in the MC clast are similar to those in the Medanitos cumulate eucrite (4). Such clast has been rare among the known meteorite collections. The bulk composition of the GC pigeonites in Y791208 is more Mg-rich than those in many ordinary eucrites. This clast fills the gap existed between the cumulate eucrites and ordinary eucrites in the non-Antarctic collection. The presence of many other pyroxene fragments intermediate between the diogenites and

ordinary eucrites, in addition to the above unique clasts, is in line with the founding in Y7308 (5, 3), and gives strong support for the crystal fractionation model for the origin of the crust of the howardite parent body. If this hypothesis were accepted, the crust would be the most primitive planetary type crust formed from a shallow magma ocean. The mechanism of formation will provide us useful information to understand the crust formation of the Earth and the Moon.

Although these howardites were found in a region not far from the area where the Yamato polymict eucrites were found in the Yamato meteorite field, they are distinct from the Yamato polymict eucrites and Y7308 howardite. They are rather similar to a group popular in the non-Antarctic collection. We cannot definitely state that three howardites are pieces from a single fall, but there is a possibility. Counting these howardites as one piece, we have four distinct eucrites and two howardites in the Yamato collection. The statistics are not much different from the other collections.

We thank the National Inst. of Polar Res. for meteorite samples.

References:
(1) Takeda H. (1979). Icarus, 40, 445-470.
(2) Mason B., Jarosewich E. and Nelen J. A. (1979). Smithson. Contrib. Earth Sci., 22, 27-45.
(3) Ikeda Y. and Takeda H. (1984). Lunar and Planetary Sciences XV, in press, Lunar and Planetary Institute, Houston.
(4) Delaney J. S., Nehru C. E., Prinz M. (1983). Lunar and Planetary Science XIV, 150-151, Lunar and Planetary Institute, Houston.
(5) Takeda H., Miyamoto M., Ishii T. and Reid A. M. (1976). Proc. Lunar Sci. Conf. 7th, 3535-3548.

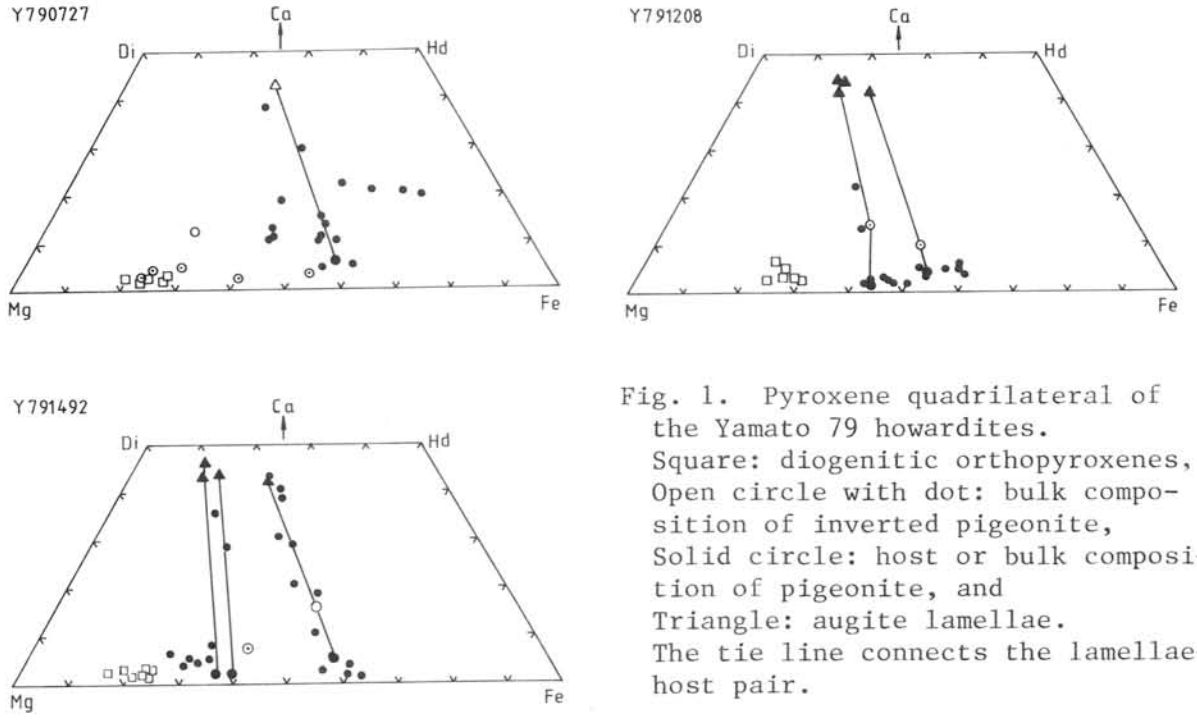

Fig. 1. Pyroxene quadrilateral of the Yamato 79 howardites.
Square: diogenitic orthopyroxenes,
Open circle with dot: bulk composition of inverted pigeonite,
Solid circle: host or bulk composition of pigeonite, and
Triangle: augite lamellae.
The tie line connects the lamellae-host pair.

CONSORTIUM STUDIES ON YAMATO-74,75 AND 79 EUCRITES, AND THEIR RELATIONSHIP

Takeda[1], Hiroshi, Ishii[2], T., Mori[1], H., Wooden[3], J. E., Prinz[4], M., Delaney[4], J. S. and Nyquist[5], L. E..
[1]Mineralogical Inst., Faculty of Science, Univ. of Tokyo, Hongo,Tokyo 113, [2]Ocean Res. Inst., Univ. of Tokyo, Minamidai, Nakano-ku, Tokyo 164, [3]U. S. Geol. Survey, Menlo Park, Calif., [4]Amer. Museum of Natural History, Central Park West at 79th St., New York, N.Y. 10024, [5]NASA Johnson Space Center, Houston, Texas 77058, U.S.A.

International consortium studies on polymict eucrites have been carried out in conjunction with the NASA-NIPR cooperation. Mineralogical and isotopic comparisons of Yamato and Victoria Land polymict eucrites have indicated that the Yamato group most likely represents pieces from a single fall distinct from the Victoria Land groups and that important distinction result from differences in depth of excavation, local rock types, and subsequent thermal reheating events(1,2). Remainders of the several grams of the interior samples of Yamato 74159, 74450, 75011 and 75015, supplied by NIPR and processed at NASA-JSC, have been distributed to other groups for the REE analyses (Prof. Masuda's group) and for INAA (Dr. Fukuoka's group). The results will be given in separate reports. Additional samples from the Y-79 collection have been studied and compaired with the Yamato 74 and 75 polymict eucrites to obtain a better understanding of their relationship.

Polished thin sections (PTS) of some characteristic clasts and matrix portions of Yamato 790007 and Y790020 and a PTS of a new polymict eucrite tentatively identified in Y791000 to Y791500 samples (3), have been investigated by X-ray microprobe analysis and X-ray diffraction techniques.

A coarse-grained mesostasis-rich lithic clast, about 5 mm in diameter in Y790020, is composed of yellowish pyroxenes and white laths of plagioclase up to 1.5 mm in length. The chemical zoning trend of the pyroxene (Fig. 1) and the texture are similar to those of the unique clast in Y75011 (1). A small fragment of this type clast was found in Y790007. Another eucritic clast in Y790007 show chemical variation of pigeonite with fine exsolution lamellae of augite (Fig. 2) similar to ordinary eucrites(4), but the clouding was not observed. Y790007 contains dark glassy clasts with radiating networks of feathery pyroxenes. The glass sometimes penetrates into matrices. The bulk chemical composition of the glass is slightly enriched in SiO_2 and Al_2O_3 than the bulk specimens. The texture and composition suggest that this clast is an impact melt. The composition of the pyroxene fragments (Fig. 3) in both eucrites are not much different from the Y74-75 group and the Binda-like pyroxene clast abundant in the previous PTS for the preliminary examination team (PET) was not found in the new PTS's of Y790007, but was found in Y790020.

A PTS made from an interior sample of Y790266 show a texture identical with the PET sections. The matrix portion appears to be shock metamorphosed and is similar to that of Y790260. Y791186 classified as a polymict eucrite in the curatorial catalog (3) was turned out to be a monomict eucrite with the pyroxene composition slightly more Mg-rich than most of the ordinary eucrites. The pigeonite crystal up to 2 mm long has coase exsolution lamellae of augite (up to 15 μm) and is partly inverted to orthopyroxene. This feature is similar to cumulate eucrites but the plagioclase shows chemical zonings (An_{77-91}) and the lath-shaped crystals have a hollow core of pyroxene. This eucrite is distinct from other Yamato and the non-Antarctic group, but fragments of such pyroxene have

been known in Y790020. It has been one of the missing components of polymict eucrites in the meteorite collection.

In summary, although Y790007 and Y790020 show some features characteristic of the individual sample, the presence of the Y75011-type unique clast and the compositions of the matrix pyroxenes suggest that they may belong to the main Yamato polymict eucrite group. Y790266 is different from this group and may be related to Y790260. Y791186 is not polymict, and is different from the Yamato main group. The composition of pyroxene and partly inverted texture are intermediate between ordinary eucrites and cumulate eucrites.

We thank the National Institute for Polar Res. for the meteorite samples and Ocean Research Inst., Univ. of Tokyo for the microprobe. A part of the work of H.T. was performed at NIPR as a Visiting Assoc. Prof. and a part of research was supported by a scientific grant from Ministry of Education, Japan.

References:

(1) Takeda H., Wooden J. L., Mori H., Delaney J. S., Prinz M. and Nyquist L. E. (1983). Proc. Lunar Planet. Sci. Conf. 14th, Pt. 1, B237-B244 (J. Geophys. Res. 88, Suppl.).
(2) Delaney J. S., Takeda H. and Prinz M. (1983). Mem. Natl. Inst. Polar Res. Spec. Issue 30, in press.
(3) Yanai K. comp. (1983). Tentative Catalog of Yamato Meteorites, Natl. Inst. Polar Res., Tokyo.
(4) Mason B., Jarosewich E. and Nelen J. A. (1979). Smithson. Contrib. Earth Sci., 22, 27-45.

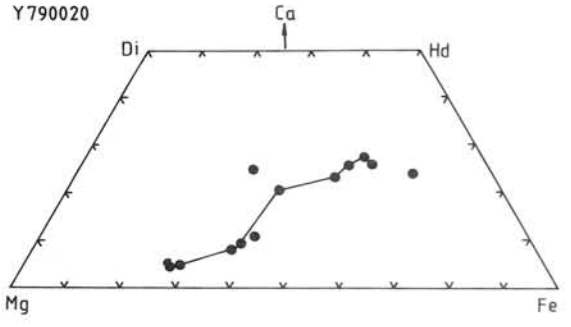

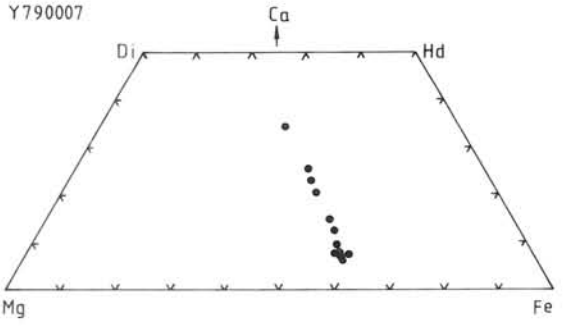

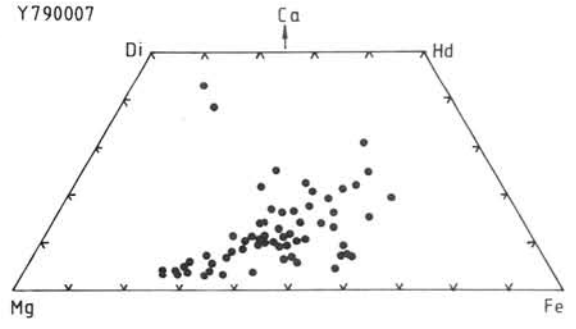

Fig. 1 (top left). Pyroxene quadrilateral showing chemical zoning trends of a coarse-grained mesostasis-rich clast of the Y75011-type found in Y790020.
Fig. 2 (top right). Exsolution trend of a pigeonite in the ordinary eucrite type clast in Y790007.
Fig. 3 (bottom). Chemical variation of pyroxene fragments in the matrix of Y790007.

10

Classification of the Yamato carbonaceous chondrites

Hideyasu Kojima*, Yukio Ikeda** and Keizo Yanai*
* National Institute of Polar Research, Tokyo 173
** Department of Earth Sciences, Ibaraki University, Mito 310

Three newly classified carbonaceous chondrites and six known specimens have been studied petrographically and petrologically to be classified and characterized their alteration state. Major chemical compositions of their matrix, groundmass, AOI and CAI were analyzed using a broad beam of JXCA-733 micro-probe techniques. Ikeda (1983) classified the alteration degrees of chondrule into the four stages. In this study, the alteration state of chondrules have been described on the same criteria.

Nine carbonaceous chondrites have been classified as follow;
CM2: Y-79003, Y-791198, Y-791824, Y-793321, B-7904
CO3: Y-74125, Y-791717
CV3: Y-75260

The alteration state of these specimens varied widely.

i) Y-791717, Y-74135 and Y-75260 are much more fresh than others, but they have been slightly altered partially. Chondrules and chondrule fragments of these have unaltered clean glass and devitrified glass.

ii) Y-793321 have been weakly to moderately altered. Most groundmass of chondrules were altered to brown colored materials, and the polysynthetic low-Ca pyroxenew were partly altered. They were richer in FeO+MgO than these of unalterated one, but less than chondrite. Most of their composition were plotted in the range between chlorite and smectite. Many calsite fragments are recognized in the matrix.

iii) Y-79003 and B-79004 were similar to each other and have been moderately altered. Their groundmass and almost polysynthetic low-Ca pyroxene were altered to brown and yellowish brown colored materials. The compositions of the groundmass enriched in FeO+MgO contents than Y-793321, and were plotted to the near area of chlorite. CaO contents were distinctly poorer than Y-793321, but calcites were recognized only in the dark clasts and/or inclusions.

iv) The alteration state of Y-791198 and Y-791824 was much more intensive than other specimens. The groundmass of their chondrules were altered to yellowish green or green colored materials. Most of olivines were remarkably altered and no polysynthetic low-Ca pyroxene remained in these specimen, but a few fine metal grains were recognized remained only in Y-791198. The groundmass of Y-791824 was enriched in FeO+MgO content and were plotted the same area as them of the matrices.

Name	Weight(g)	Class & Type	*	metal	calcite
Y-791717	25322	CO3	fresh	+	absent
Y-74135	7.7	CO3	fresh	+	absent
Y-75260	4.0	CV3	fresh		absent
Y-793321	379.73	CM2	1	+	common
B-7904	1234.	CM2	2	+	absent
Y-790003	4.29	CM2	2		**
Y-791198	179.77	CM2	3		common
Y-791824	23.28	CM2	4	absent	**

* order of alteration
** free in matrix, but in inclusion and dark clots.

NEW CZECHOSLOVAKIAN L-5 CHONDRITE: ÚSTÍ NAD ORLICÍ-KERHARTICE

Jakeš, P.,[1] and Bukovanská, M.[2]
1 Geological Survey Prague, Czechoslovakia (presently at Dept. of Geology and Mineralogy, Kyoto University, Kyoto 606)
2 National Museum , Prague, Czechoslovakia

Single stone (1260 g) which fell on 12.6.1963 has been studied. It is well equilibriated, slightly brecciated chondrite of L 5 type. The chondrules are of cross-hatched "grid" type built by olivine, (2) radial type, usually built by pyroxene , (3) porphyritic chondrules formed by large pyroxene and olivine crystals set in fine grained matrix, (4) fine grained chondrules of olivine and orthopyroxene composition. Matrix of the chondrite is fine grained with orthopyroxene, olivine, feldspar and opaque minerals.

Within the matrix single piece (7mm in diameter) of fine grained and strongly shocked chonrite has been found. Bulk modal analysis of the studied meteorite shows 52 % orthopyroxene, 19 % olivine, 18% plagioclase, 3 % taenite and kamacite, 7 % troilite, and 1 % of chromite (clinopyroxene is extremely rare).

Variations of mineral compositions (studied by the wave - lenght dispersive electron microprobe -fully automated) are extremely small and are difficult to distinguish from an experimental error of probe analyses. The variations are strikingly regular however, and appear distinctly if mineral grains are analyzed side by side. Fe/Mg ratio vary sympathetically in both olivine and pyroxene. Lowest Fa values were found in olivines from chondrules in clast (Fa 22.9) and within the individual olivines of the clast (Fa 23.1), whereas chondrules of the major portion of meteorite have Fa 23.9 and matrix olivine contains Fa 24.2. Similar relationships were found in Fe/Mg ratios of orthopyroxene; lower contents of Fs in clast (Fs 19.5) and slightly higher ones in the pyroxenes of major portion of meteorite (Fs 20.2). Analyzed clinopyroxene correspond to En 44.6, Fs 7.6, and Wo 48.0. The plagioclase occurs as an interstitial component and its composition corresponds to An 10, Ab 85, Or 5. Also whittlockite has been analyzed (CaO=47.0, Na2O=2.66, MgO= 3.18 , FeO=0.4 , P2O5 =46.4 wt.per cent. Among the opaque phases troilite, taenite, pentlandite, native copper, cubanite, pyrrhotite, chalcopyrite and mackinawite were found. Ni in kamacite varies between 3.3 to 6.2 %, in taenite 35.4 to 58.5 %. Troilite is strictly stoichiometric with Ni, Cu, and V contents less than 0.5%, and chromite with Cr_2O_3=54.75, FeO=31.99, TiO_2= 2.69, Al_2O_3=6.09, MnO=0.93, MgO=2.44, and V_2O_5=0.79 %.

Texture and mineral compositions suggest L 5 clasification.

12－1

Petrologic Studies of Three Primitive Achondrites from the Yamato Meteorites Collection, Antarctica

K. Yanai[1], H. Kojima[1], M. Prinz[2], C.E. Nehru[2,3], M.K. Weisberg[2,3], J.S. Delaney[2].
(1) National Institute of Polar Research, Tokyo 173. (2) Amer. Museum Nat. Hist., NY, NY 10024. (3) Brooklyn College (CUNY), Brooklyn, NY 11210.

Four stony-iron meteorites from the Yamato area Mountain, Antarctica, have been studied in order to determine their mineralogy, petrology and classification, and compare them with members of the supergroup of primitive achondrites described by Prinz et al. (1). Three of these meteorites (Y-74357, Y-75274 and Y-791493) have been briefly noted earlier (2-4), but the present study is more detailed and compares them with related meteorites. The fourth (Y-8002) is first reported here, but is paired with one of the earlier three (Y-75274).

The term primitive achondrites has been previously proposed (5) and is intended to distringuish a large group of primitive meteorites with highly varying ratios of metal to silicates and which have no evidence of present or past chondritic textures. They are distinguished from differentiated achondrites, such as eucrites, etc. which exhibit obvious effects of major igneous fractionation, presumably on a parent body, Iron meteorites which have undergone igneous fractionation, such as IIIAB, are also differentiated achondrites. Primitive achondries have experienced little or no major ingeous fractionation, but some have had sulfide loss and/or reduction (mainly of olivine). They include silicates in IAB and IIICD irons, winonaites, Lodran and Brachina. Oxygen isotopic data appear to be consistent with the concept that these groups can be related for most members of the proposed supergroup (6). Primitive achondries have previously been termed chondritic (e.g., 7), but no chondrules or relics of them have ever been found. The term no chondrites is inappropriate as it also includes differrentiated achondrites. Hence, primitive achondrites is the most appropriate name for the supergroup.

Each of the three meteorites was modally analyzed, using automated microprobe techniques, and the results are shown in Table 1 and Figure 1 and compared with primitive achondrites. Several noteworthy features are found. Y-74357 is by far the most olivine-rich primitive achondrite (except for the unique Brachina (8)). It also has no plagioclase, which is characteristic of Lodran; however, Lodran has strongly reduced olivine on its rims and extremely rare clinopyroxene, whereas Y-74537 has uniform olivine and 3.5% cpx. Y-791493 has 5% phosphate, more than in all other primitive achondries except for the unusually phosphate-rich San Cristobal and Dayton. It aslo contains only 1.6% plag and trace of cpx, both lower than in most primitive achondrites. Y-75274 contains a rare type of phosphate, farringtonite-brianite. Thus, each of the three Yamato primitive achondrites has some unusual modal feature which extends the modal range of this supergroup.

Texturally, these three meteorites are similar to those of other primitive achondrites. They are all equigranular, with some minor grain size variation within a single sample, and appear to be equilibrated. Tiny silica-K_2O-rich melt inclusions have been found in Y-791493 and Y-8002.

Mineralogical data are presented in Table 2 and Figure 2, and compared

with primitive achondries. Y-74357 contains unusually Mg-rich olivine (Fo92), when compared with its coexsting opx (En84). The olivine is homogeneous, and must have been severely reduced in relation to the coexisting pyroxene. Disequilibrium ol-opx assemblages are characteristic of primitive achondrites (1; Fig. 2), but Y-74357 has unusually reduced olivine. Equilibrium ol-opx pairs are shown in Figure 2. Y-791493 is typical of primitive achondrites with ol (Fo88) and opx (En85); plagioclase is An18, also a typical value. The Y-75274/Y-8002 pair have relatively Mg-rich mafics, with ol (Fo96) and opx (En94). Plagiocalse is unusually calcic, An28; other primitive achondrites range up to An22, with only rare garins in Kendall Co. up to An49.

Chromite in the three Yamato primitive achondrites is typical of other primitive achondrites. Each contains chromite high in Zn (0.57-1.30%) and MnO (1.2-2.4%), and high Cr/(Cr+Al) ratios. Phosphate data are given in Table 3. Y-74357 has mainly merrillite, with some coexisting chlorapatite. Y-791493 has large merrillites, and small chlorapatite grains, both with compositions similar to Y-74357. Merrillite and chlorapatite are very similar to those found in most primitive achodnries. Y-75274 has an unusual phosphate which is a combination of farringtonite and brianite; the phosphate in the IIICD iron Carlton (a primitive achodrite) is very similar, and is the only known occurrence of this phosphate composition.

Metal and schreibersite date are presented in Table 4. FeNi metal is generally similar in all three meteorites and similar to that in other primitive achondrites. Bunch et al. (9) showed that metal within silicate inclysions has somewhat lower Ni than in the coexisting metal of the host iron. In the three meteorites studied metal is interspersed with the silicates and the Ni values are similar to the lower Ni values in the inclusions. Schreibersite has variable compositions within each of the three meteorites, as shown in Table 4.

Y-791493 was described as a lodranite (4), and the other two meteorites were tentatively also linked with this classification. However, none of these meteorites has reduced olibine with Mg-enriched rims, the most unique characteristic of Lodran. Since all primitve achondrites have reduced olivine, the only characteristic that is different about Lodran is that has preserved evidence of the process. Lodran also has no plagioclase or phosphate. We suggest that the term lodranite be dropped and that it, as well as three Yamato meteorites described here, be termed primitive achondrites. There are insufficient criteria for the definition of a lodranite to call these new meteorites by that term.

We suggest that primitive achondrite be the group name for all of the meteorites described by Prinz et al. (1) and in this paper. The members of this supergroup can be used as a type name for descriptive purposes, e.g. a winonaite-type primitive achondrite. However, the group name primitive achondrite should be the proper classification regardless of whether or how they are classified on a type level.

References: (1) Prinz, M. et al. (1983) LPS XIV, 616-617. (2) Yanai, K. and H. Kojima (1983) Meteoritics (abs.) 18, in press. (3) Matsumoto, Y., K. Yanai and H. Kojima (1982) 8th Symp. Ant. Met., NIPR, Tokyo. (4) Yanai, K. and H. Kojima (1982) Meteoritics (abs.) 17, 300. (5) Prinz, M. et al. (1980) LPS XI, 902-904. (6) Clayton, R. N. et al. (1983) LPS XIV, 124-125. (7) Wasson, J. T. et al. (1980) Z. Naturforsch 35a, 781-795. (8) Nehru, C. E. et al. (1983) PLPSC, JGR 18, B237-244. (9) Bunch, T. E. et al. (1970) Cont. Min. Pet. 25, 297-340. Founding: NASA NAG 9-32 (M. Prinz, P. I.).

Table 1. Modal analysis (vol.%) of Yamato primitive achondrites

	74357	791493	75274	8002	*IAB Avg (range)	*Winonaites Avg (range)
ol	68.8	43.1	26.0	25.6	27.1 (13.2-39.8)	32.5 (28.1-36.8)
opx	15.0	37.2	48.7	53.9	47.5 (34.6-65.4)	47.3 (40.4-54.3)
cpx	3.5	tr	0.2	2.5	5.6 (0.5-10.3)	4.2 (0.7- 7.4)
plag	-	1.6	3.4	11.7	19.0 (10.3-31.8)	15.1 (8.7-20.0)
phos	0.1	5.0	0.2	-	0.6 (0.1- 3.3)	0.5 (0.1- 1.5)
chromite	0.2	1.0	0.2	0.1	0.2 (0.1- 0.9)	0.4 (0.1- 0.9)
kamacite	9.6	9.0	19.6	6.0		
troilite	2.4	3.0	0.2	0.1		
schreib	0.4	0.1	1.5	0.1		
No. points	1500	900	600	1000	12 Meteorites	5 Meteorites
Area mm^2	86.7	37.3	10.8	27.0		

*Data from Prinz et al. (1). silicates only.

Table 2. Pyroxene compositions in Yamato primitive achondrites

	Y-74357		Y-791493		Y-75274		Y-8002	
	Opx	Cpx	Opx	Cpx	Opx	Cpx	Opx	Cpx
SiO_2	56.1	53.9	55.4	52.7	56.7	54.2	59.3	54.0
TiO_2	0.15	0.31	0.08	0.40	0.27	0.75	0.19	0.81
Al_2O_3	0.27	0.92	0.36	0.93	0.38	0.71	0.33	1.03
Cr_2O_3	0.43	1.25	0.35	1.37	0.47	0.74	0.46	0.77
FeO	9.1	4.1	8.5	2.68	2.67	0.90	2.60	0.74
MnO	0.52	0.41	0.53	0.37	0.48	0.30	0.34	0.26
MgO	31.4	17.6	32.9	18.8	37.1	19.9	36.3	19.5
CaO	1.28	20.5	1.22	21.8	1.85	22.5	1.36	23.0
Na_2O	0.06	0.50	0.04	0.58	0.04	0.56	0.04	0.50
Total	99.31	99.71	99.38	99.66	100.03	100.62	100.92	100.66
En	83.8	50.9	85.3	52.2	93.9	54.3	93.8	53.6
Fs	13.7	6.3	12.4	4.2	2.9	1.4	3.7	1.1
Wo	2.5	42.8	2.3	43.6	3.3	44.3	2.5	45.3

Table 3. Phosphates in three Yamato primitive achondrites

	Y-74357		Y-791493		Y-75274	Carlton
	M	A	M	A	FB	FB
SiO_2	0.41	0.42	0.05	0.15	0.78	0.26
Al_2O_3	0.03	0.08	0.03	0.05	0.02	0.02
FeO	1.2	0.86	1.12	1.20	1.7	1.9
MgO	4.0	0.39	3.9	0.31	33.1	33.2
CaO	46.5	54.5	45.8	54.2	7.9	5.8
Na_2O	2.73	0.26	2.88	0.25	5.7	7.3
P_2O_5	46.4	41.1	46.5	41.5	50.3	49.8
Cl		4.4		4.8		
F		0.8		0.5		
Subtotal	101.27	102.81	100.28	102.51	99.48	98.24
Less O =Cl,F	-	1.33	-	1.29	-	-
Total	101.27	101.48	100.28	101.22	99.48	98.26

M = merrillite; A = apatite (chlor); FB =farringtonite-brianite
*A IIICD iron with silicates, from (1).

Table 4. Metal and schreibersite from three Yamato primitive achondrites

	Y-74357		Y-791493		Y-75274/Y-8002	
	M	S	M	S	M	S
Fe	94.8	56.2-61.0	93.6	39.8-41.3	95.2	52.9-73.4
Ni	4.9	23.6-29.1	6.2	43.9-46.7	5.5	15.1-32.9
Co	0.17	---	0.23	---	0.31	---
P	0.10	15.0-15.3	0.08	14.7-15.3	0.11	11.3-15.3
Total	99.97		100.11		101.12	

M = metal; S = schreibersite; --- = below detection. Metal analyses have 0.5% variability in Ni.

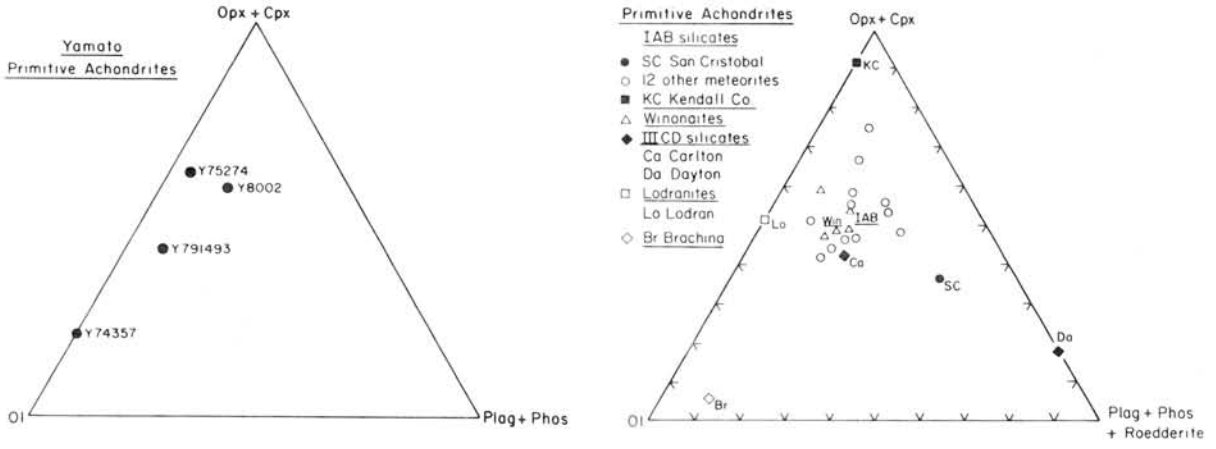

Figure 1. Modal data for four samples representing three Yamato primitive achondrites, compared with data from other primitive achondrites (1).

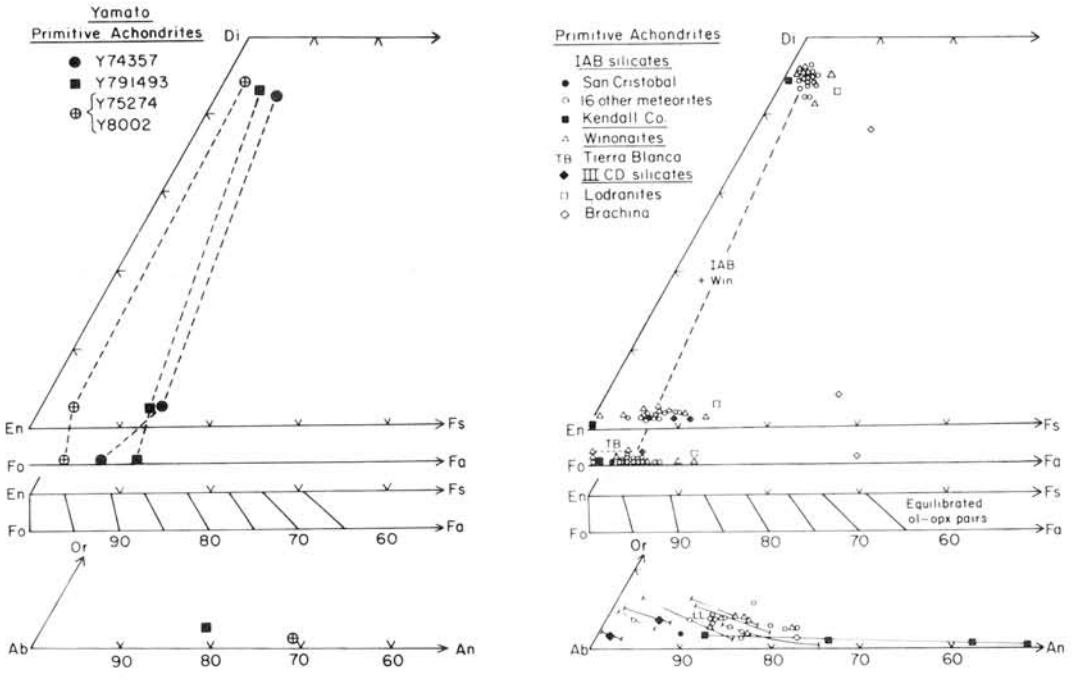

Figure 2. Mineralogical data for three Yamato primitive achondrites, compared with data from other primitive achondrites (1).

MATRIX MATERIAL IN TYPE 3 ORDINARY CHONDRITES - COMPOSITION AND RELATIONSHIP WITH CHONDRULES

Edward R.D. Scott, G. Jeffrey Taylor and Klaus Keil
Institute of Meteoritics, University of New Mexico, Albuquerque, NM 87131, USA

Matrix material in type 3 ordinary chondrites contains micron to submicron Fe-rich olivine, Fe-poor low-Ca pyroxene and amorphous material rich in Si, Al, Ca, Na and K [1,2]. It forms rims on chondrules, metal-sulfide aggregates, Al-rich inclusions and chondritic clasts, and lumps up to a millimeter in size, which may contain coarser silicates [3-5]. Individual rims and lumps are far too heterogeneous to be random mixtures of micron-sized grains. Broad-beam microprobe analyses show compositional variations which can be understood in terms of varying proportions of FeO-rich olivine and a mixture of feldspathic material rich in Si, Ca, Al, Na and K and olivine and low-Ca pyroxene with lower Fe/(Fe+Mg) ratios [5].

Metamorphism produces an inverse correlation between mean Fe/(Fe+Mg) of chondrite matrices and petrologic subtype [2]. However, a decrease in Al/Si with increasing subtype is unlikely to be metamorphic in origin. Instead, it probably reflects an overabundance of low-subtype LL chondrites, which have high Al/Si ratios, relative to H and L chondrites, which have low Al/Si ratios [5]. Similarly, high Na/Si and low Mg/Si ratios of LL matrices relative to H and L matrices probably reflect primary differences between groups. The proportion of feldspathic material in matrix could be affected by shock, but it seems probable that most compositional variations predate the formation of rims and lumps.

Evidence that matrix material was present when chondrules formed is provided by the presence of matrix lumps in chondrules [5], and plastic deformation of hot chondrules rimmed by matrix [6, 7]. Since chondrules are nebular, not planetary, products [e.g. 8, 9], matrix must be also. This is consistent with the relatively unfractionated composition of matrix relative to CI chondrites [10, 11]. Since chondrules formed by melting of preexisting solid material [see 12] and matrix is heterogeneous like chondrules, we must consider whether chondrules could have formed from matrix material. We have found a single chondrule that has an internal matrix lump and a matrix rim that are both virtually identical in composition to that of the chondrule [5]. However, most chondrules differ in composition from associated matrix rims and lumps. On average, mean matrix is somewhat enriched in Al, Mn, Na, K, and P relative to mean chondrules, even allowing for loss of metallic Fe,Ni and associated elements during chondrule formation.

We conclude that some chondrules formed from matrix material, but recognize that many chondrules could not form directly from our samples of matrix material. This may be due to fractionation processes occurring during the chondrule-forming process. In some regions, precursor materials were wholly or partly vaporized and then condensed forming Al-rich chondrules and inclusions [13]. Since there is no compositional hiatus between Al-rich and Mg,Fe-rich chondrules [13] (many barred olivine chondrules [14] appear to be intermediate in composition), it is probable that many Mg,Fe-rich chondrules were affected to some extent by these fractionation processes. Condensates and residues could have been added to unfractionated matrix

material. Collisions between partly molten chondrules and between chondrules and matrix may also have modified chondrule compositions. Thus the absence of an exact match between surviving matrix material and chondrules is understandable, even if matrix material were the only chondrule precursor material.

Matrices of C3 chondrites [15] tend to be more homogeneous and less fractionated relative to CI chondrites than matrices of ordinary chondrites. However, there are heterogeneous chondrule rims and matrix lumps in both kinds of type 3 chondrites [5], and iron-rich olivine is the major ingredient in ordinary and carbonaceous matrices. From these observations and similarities between chondrules and Ca,Al-rich chondrules and inclusions in ordinary and carbonaceous chondrites [11, 13], we conclude that matrices in both kinds of chondrites have related origins.

References: [1] Nagahara H. (1983) Meteoritics, in press. [2] Huss G.R. et al. (1981) Geochim. Cosmochim. Acta 45, 33-51. [3] Ikeda Y. et al. (1981) Mem. Nat. Inst. Polar Research Sp. Issue No. 17, 124-144. [4] Fujimaki H. et al. (1981) ibid. Sp. Issue No. 20, 161-174. [5] Scott E.R.D. et al. (1984) Geochim. Cosmochim. Acta, submitted. [6] Kurat G. (1982) at Conference On Chondrules and Their Origins, Lunar and Planetary Institute. [7] Hutchison R. et al. (1979) Nature 280, 116-119. [8] Taylor G.J. et al. (1983) In Chondrules and Their Origins (E.A. King ed.) pp. 262-278. [9] Grossman J.N. and Wasson J.T. (1983) In Chondrules and Their Origins (E.A. King ed.) pp. 81-121. [10] Taylor G.J. et al. (1984) Lunar and Planetary Science XV, in press. [11] Scott E.R.D. and Taylor G.J. (1983) J. Geophys. Res., 88 Suppl., B275-B286. [12]. King E.A. (1983) Editor, Chondrules and Their Origins, Lunar and Planetary Institute, Houston. [13] Bischoff A. and Keil K. (1983) Nature 303, 588-592; (1984) Geochim. Cosmochim. Acta, in press. [14] Lux G. et al. (1981) ibid. 45, 675-685. [15] McSween H.Y. and Richardson S.M. (1977) ibid. 41, 1145-1161.

ELECTRON AND ION PROBE DETERMINATIONS OF SOME ELEMENT PARTITIONS IN INDIVIDUAL CHONDRULES.

K. FREDRIKSSON, Dept. of Mineral Sciences, Smithsonian Institution, Washington, D.C., 20560, USA
S. SPECHT, Max Planck Institut für Chemie, D-6500 Mainz, Federal Republic of Germany

Individual chondrules from so-called "equilibrated" H, L and LL chondrites, i.e. of petrographic Grades 4 through 6 (7), have grossly variable amounts and ratios of Al/Ca/Ti, while bulk samples of all chondrites are nearly equal in these respects (Fredriksson, 1982, 1983; Fredriksson and Specht, in press). As an average, these chondrules also have an excess, 30 to 50 wt%, of CaO over bulk samples. Chondrules from Grade 3, "unequilibrated" (variable Fe/Mg), chondrites, however, have nearly constant Al/Ca/Ti.

This apparent paradox lead us to attempt ion probe determinations of some trace elements in a few of the previously analyzed chondrules which had been finely ground and pressed into pellets. As standards (also for resolving elemental peaks from molecular) we used powders of the silicate portion of Allegan (H5) chondrite, native and spiked with 20 and 100 ppm of some elements of interest, pelletized as the chondrules. Fig. 1 shows the calibration runs for Ba, V and Sc, relative to chosen "background peaks" (masses 47, 141), which appeared nearly constant in samples and standards in spite of being unidentified complex molecular peaks as revealed at high resolution (5000). The element peaks also showed molecular interferences at high resolution, ranging from 98 to 45% for ^{45}Sc (+0 and +100 ppm Ba, respectively).

Fig. 2 shows the increasing positive correlation of Ca with Sc and V and of Al with Sr and Ba from Grade 3 through Grade 4 to Grade 5. These results indicate that Ca resides in a pyroxene, Al in a feldspar, phase. Coupled with the negative correlation of Al-Ca and excess CaO in chondrules from "equilibrated" chondrites, the results also imply that chondrules formed in a closed system from a parent material, homogenous on a large scale but inhomogenous on the submillimeter scale, especially with regard to Al, Ca and Ti. In this respect the chondrules resemble the micro-irghizites (micro-tektites; Fredriksson and Glass, 1983). Furthermore, Grade 5 chondrites are not equilibrated (see also Rambaldi et al., 1981), and have no metamorphic relation to Grade 3 chondrites.

References: Fredriksson, K. (1982) Lunar and Planet. Sci. XIII, 233-234.
Fredriksson, K. (1983) In Chondrules and Their Origin, Lunar and Planetary Inst., Houston, TX, 44-52.
Fredriksson, K. and B.P. Glass (1983) Lunar and Planet. Sci. XIV, 209-210.
Fredriksson, K. and S. Specht (1984) Meteoritics (Abstr.), in press.
Rambaldi, E., B.J. Fredriksson, and K. Fredriksson (1981) Earth and Planet. Sci. Lett 56, 107-126.

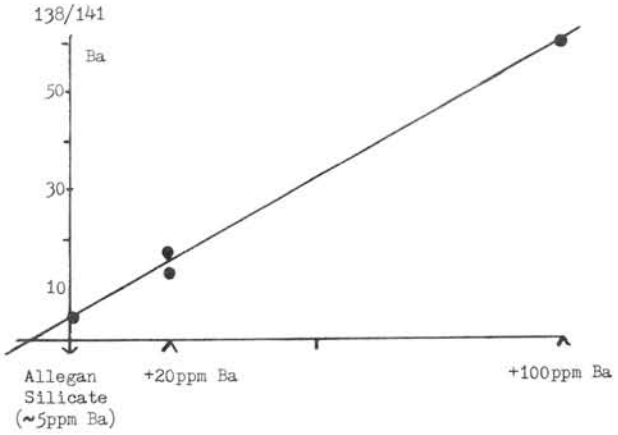

Fig. 1. Ion probe calibration runs (Cameca, IMS 3f, isotope program) of ^{138}Ba vs "background mass" 141 and ^{45}Sc, ^{51}V vs "background mass" 47.

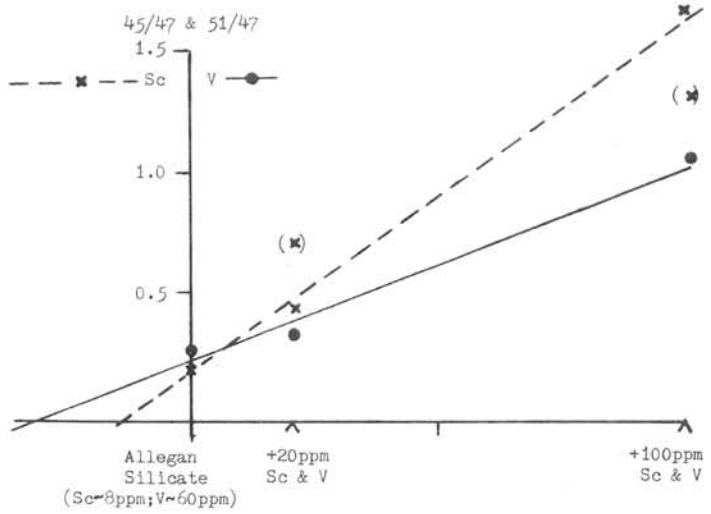

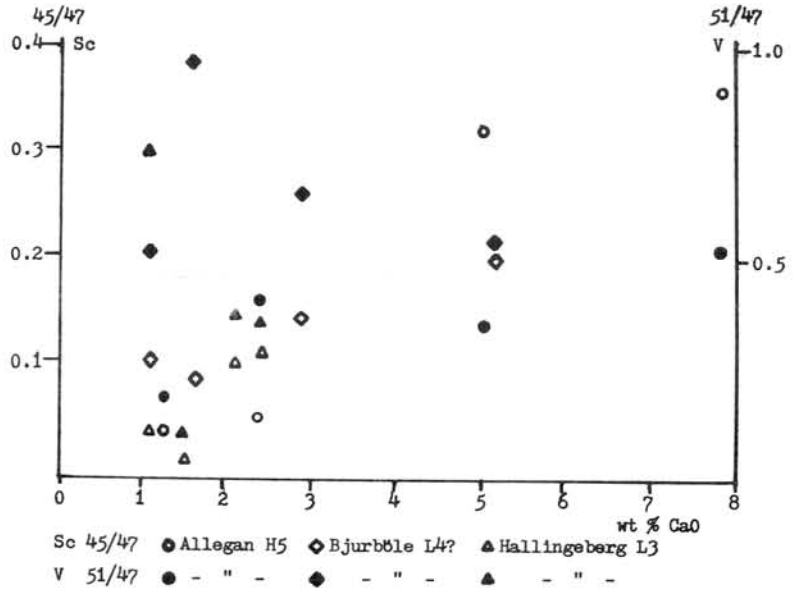

Fig. 2 Relative concentration of Sc, V and Sr, Ba in individual chondrules with extreme contents of Ca and Al, which are negatively correlated in Allegan, partially in Bjurböle.

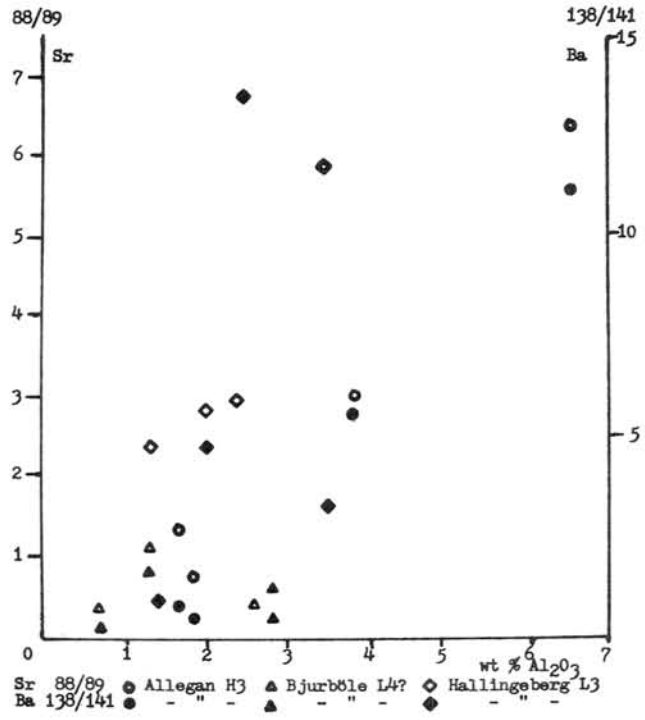

15－1

PETROLOGY OF THE Y-7308 HOWARDITE

Ikeda Y.* and Takeda H.**
*Dept. of Earth Sciences, Ibaraki Univ., Mito 310.
**Mineralogical Inst., Faculty of Science, Univ. of Tokyo, Tokyo 113.

The Yamato-7308 howardite includes many kinds of clasts, glass beads or fragments, and mineral fragments[1, 2]. Clasts are smaller than several millimeters in size and comprise diogenite clasts, eucrite clasts, and Hd-Fa-Trid-Pl clasts.

Diogenite clasts consist mainly of magnesian orthopyroxenes and their ratios of Mg/Mg+Fe are 76-68 atomic percents (Fig. 1).

Eucrite clasts are classified into three subtypes, hypersthene(Hyp)eucrites, inverted pigeonite(IPig)eucrites, and pigeonite(Pig)eucrites. Hyp-eucrite clasts consist mainly of plageoclase and orthopyroxene with minor high-Ca pyroxene, and the Mg/Mg+Fe ratios of orthopyroxene are 68-66 atomic percents(Fig.1). IPig-eucrite clasts consist mainly of plagioclase and inverted pigeonite and the Mg/Mg+Fe ratios of low-Ca pyroxene are 61-48 atomic percents. Pig-eucrite clasts consist mainly of plagioclase and pigeonite with high-Ca pyroxene lamallae, and the Mg/Mg +Fe ratios of low-Ca pyroxene are 54-29 atomic percents.

Hd-Fa-Trid-Pl clasts are holocrystalline rocks consisting of ferrous high-Ca clinopyroxene, ferrous olivine, tridymite, plagioclase, chromite, ilmenite, etc. The ferrous olivine shows Mg/Mg+Fe of 10-14 atomic percents and the ratios of the ferrous high-Ca clinopyroxene are 31-27 atomic percents (Fig. 1).

The pyroxenes in these clasts show continuous spectrum of Mg/Mg+Fe ratios as shown in Fig. 1. Pyroxenes and olivines which occur as mineral fragments in the matrix of the meteorite also show wide ranges of Mg/Mg+Fe ratios. The raitos of olivine fragments are 86 to 71 atomic percents, and those of low-Ca pyroxene of pyroxene fragments are 78 to less than 50 atomic percents. The latter range well coincides with the compositional range of low-Ca pyroxenes in diogenite and eucrite clasts, and the pyroxene fragments may have derived from these clasts by complete disaggregation.

The wide and continuous compositional ranges of low-Ca pyroxenes and olivines in the meteorite are considered to be produced mainly by fractional crystallization from a primary magnesian magma. The primary magma firstly crystallized magnesian olivine, which occurs as mineral fragments in the matrix. Secondly the magma crystallized magnesian orthopyroxene resulting in diogenites, and then combined plagioclase forming Hyp-eucrites. Next the magma crystallized magnesian pigeonite instead of orthopyroxene, resulting in IPig-eucrites. Further fractional crystallization produced ferrous magma which resulted in Pig-eucrites, and finally Hd-Fa-Trid-Pl rocks crystallized from the extremely-differentiated acidic magma.

The composition of plagioclases in Hyp-eucrite clasts is An_{96}-An_{89} and that of plagioclases in Hd-Fa-Trid-Pl clasts is An_{85}-An_{77}. This difference in plagioclase composition between

magnesian and ferrous differentiates is too small in comparison to terrestrial igneous complex, and may be explained by Na-loss during the crystallization of magma.

Minor amounts of Fe metals occur in these clasts and as mineral fragments in the matrix. Most of them are depleted in Ni and are considered to be formed from FeS and/or FeO components by the S-escape and/or reduction during the crystallization of magma above-stated.

[1] Yagi K, Lovering J.F., Shima M., and Okada A. (1978), Mem. Nat. Inst. Polar Resear., Specail Issue, 8, 121-141. [2] Nerue C.E., Delaney J.S., Prinz M., Weisberg M., and Takeda H. (1983), Lunar Planet. Sci., 14, 550-551.

Fig. 1. Chemical compositions of pyroxenes and olivines in atomic percents. Open triangles: orthopyroxenes in diogenite clasts, open squares: pyroxenes in Hyp-eucrite clasts, solid circles: pyroxenes in IPig-eucrite clasts, open hexagon: bulk composition of a pyroxene fragment consisting of pigeonite with augite lamellae, open circles: pyroxenes in Pig-eucrite clasts, and solid hexagons: high-Ca clinopyroxenes(upper hexagons) and olivines(lower hexagons) in Hd-Fa-Trid-Pl clasts. Dotted line is a presumed trend of orthopyroxenes and pigeonites crystallized from the primary magma (see text).

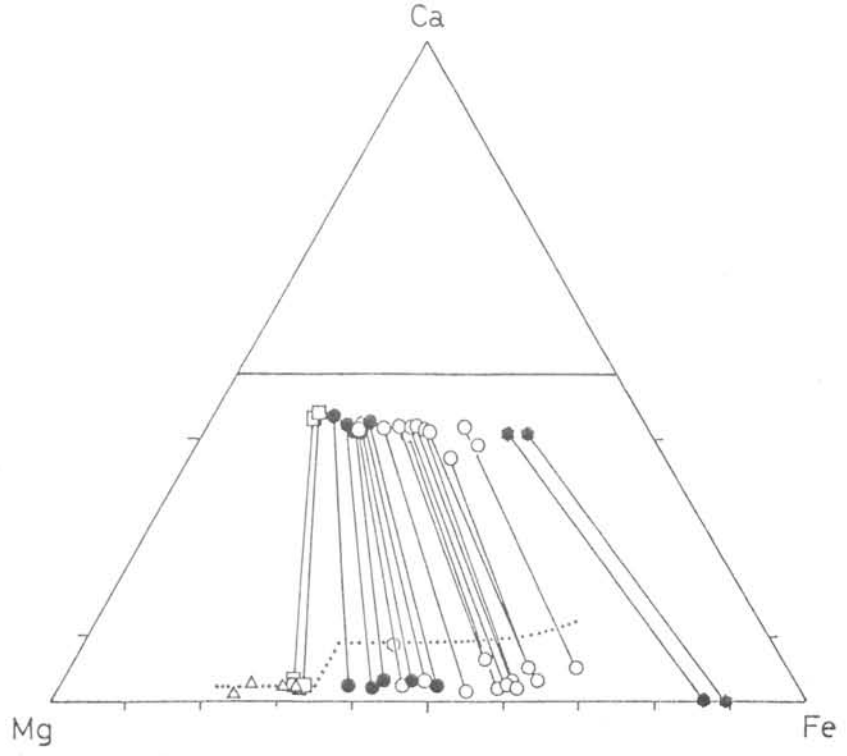

16－1

Classification of the some basaltic achondrites from the Yamato-79 meteorite collection including pigeonite cumulate eucrites, a new group

Jeremy S. Delaney[1], C. O'Neill[1], C.E. Nehru[1,2], M. Prinz[1], C.P. Stokes[1,2], K. Yanai[3] and H. Kojima[3]
(1) Amer. Museum. Nat. Hist., NY, NY 10024. (2) Brooklyn College (CUNY), Brooklyn, NY. (3) National Institute of Polar Reserach, Tokyo 173

Among the 1979 meteorite collection from Yamato Mountains many new basaltic achondrite specimens have been recognized. Fourteen new specimens and two older (1974) meteorites have been studied modally and petrographically to characterize and classify these samples. All basaltic achondrite subgroups are represented and several specimens are paired. Modes (using automated electron microprobe techniques: 1) are given in Table 1. These samples are discussed in groups corresponding to their classification.

1. Eucrites: Y-74356; Y-792510.

These two eucrites all fall within the modal range of typical eucrites (Table 1) but are texturally different. Y-74356 and Y-792510 are brecciated. (a) Y-74356 has been described elsewhere (2,3) and contains En41Wo4 to En31Wo42 pyroxene An91.6Or0.3 feldspar. Coexisting ilmenite contains 1.1% MgO. The pyroxene is finely exsolved pigeonite (En36Wo7) (2,3), homogeneous and varies in texture from poikilitic to subophitic in mafic clasts. No severe shock features are present. (b) Y-792510 is a lightly brecciated eucrite with coarse, well developed subophitic texture. Pyroxene is up to 5 mm long and feldspar is often 500-1000 μm long. Y-792510 contains En37Wo2 to En30Wo45 pyroxene with An87Or1.8 feldspar. Ilmenite contains 0.5% MgO. The inverted pigeonite of Y-792510 displays well developed "herring-bone" exsolution very similar to that in Moore County or Nagaria (3,4). The subsolidus history of this pyroxene may be summarized by sequence: $pigeonite_1$ - $pigeonite_2$ + $augite_1$ - orthopyroxene + $augite_2$. Augite lamellae (1-10μm) are cross cut by submicron augite lamellae. A few pyroxene grains have much more abundant augite lamellae near edges indicating that the original pigeonite was zoned with augite rims. Many pyroxene grains show fractures and mosaicism attributed to shock. Feldspar is generally coarse grained and lathy with little evidence of shock. Both pyroxene and feldspar have clouded patches presumably caused by subsolidus annealing (5).

2. Polymict Eucrites: Y-791186; Y-791960

(a) Y-791186 is a pyroxene-plagioclase breccia containing significantly less feldspar than the eucrites and most polymict eucrites (Table 1) and is dominated by mineral clasts. Several large pyroxene clasts appear to be unexsolved orthopyroxene, although shock features have obscured some optical details. In a few instances, this opx is intimately interfingered with similar pyroxene. This texture is often seen in magnesian orthopyroxenite clasts from howardites (7). Other pyroxene clasts are exsolved pigeonite similar to Juvinas-type pyroxene (1). This specimen is, therefore, polymict with respect to pyroxene textures. Compositionally, however, the pyroxene of Y-791186 has an almost constant Mg/(Fe+Mg) (En44-38Wo3 to En30Wo40) and is similar to the eucrites. This feature of textural diversity and compositional uniformity in a polymict breccia was previously described for the Elephant Moraine polymict eucrites (8) and is ascribed to metamorphism of a polymict breccia. Further study of the components present in this breccia is necessary before it may be fineally classified but the obvious eucrite

pyroxene and eucritic textures of mafic clasts suggest that this is a polymict eucrite. If, however, the orthopyroxenite component is recognized to be 10% vol. of this specimen, then it may be reclassified as a howardite following the nomenclature of (9). Feldspar ranges from An72 to An93 with most analyses falling between An89 and An91. (b) Y-791960 is a polymict eucrite very similar to the Yamato I suite of polymict eucrites (1). It is texturally very similar and is modally almost identical to the mean composition of this group (Table 1). It contains pyroxene of all the types discussed by (4), but in addition contains 1.5-2.0% (vol.) magnesian pyroxene (En72-77Wo2) similar to diogenitic pyroxene. Y-791960 is probably paired with the Yamato I suite of polymict eucrites. The presence of magnesian pyroxene, therefore, extends the range of compositions known in the Yamato polymict eucrites.

3. Howardites: Y-791074, 791208, 791492, 791573

These four howardite specimens all have similar modes (Table 1) and are more feldspathic than Y-7308, the first Yamato howardite (1). All contain olivine but with varying ranges of composition (Table 2). Pyroxene in all four ranges from magnesian orthopyroxene En78Wo2 to iron-rich eucritic pigeonites En30-40Wo5-10. Many of the more iron-rich pyroxenes are exsolved with En25-30Wo40-50 lamellae. In Y-791573 and Y-791492, rare En88Wo0.4 pyroxenes occur but orthopyroxene in the composition range En78-En72(Wo2-3) is the most abundant in all four sections. Y-791074 contains significantly more feldspar then the other three which have almost identical modes. It also contains more iron-rich olivine (Table 2). It is a coarse grained breccia with few lithic fragments. The fine matrix between pyroxene feldspar clasts is darker than in the others and may contian some glass. Y-791208, Y-791492 and Y-791573 are all very similar texturally and mineralogically. All contain orthopyroxene, pigeonite and feldspar mineral clasts in a fine-grained matrix as well as a variety of lithic clasts. Y-791208 differs from Y-791492 and Y-791573 as it has prominent lithic clasts that are very fine-grained, variolitic to spherulitic basalts with glassy interstices and some angular xenocrysts of both pyroxene and plagioclase. These clasts may represent an impact melt of the breccia but further study is required. Y-791208 has the largest range of olivine composition (Fo45-91) but the rarity of this mineral in howardites suggests that the smaller ranges of the other samples may be an artifact of sampling. Both the feldspar and pyroxene compositional ranges are comparable in all four specimens. In particular about half the pyroxene (analyzed during modal studies) in each sample falls within the range En78-En72. This similarity between the ranges of randomly sampled pyroxene suggests that all these specimens may be form a single howardite meteorite. Differences between their modal pyroxene/feldspar ratios and the Fe/Mg ratios of the olivine may be the result of localized heterogeneity. At present, Y-791208, 791492 and 791573 are all believed to be samples of a single howardite and are, therefore, paired. Y-791074 is the more feldspathic and also contains more Fe-rich mafic silicates. Y-791074 is, therefore, considered to be a separate meteorite, but the similarities of the abundance of Mg-rich pyroxene is all four specimens suggest that Y-791074 may also be paired with the others. The first Yamato howardite Y-7308 has a comparable pyroxene composition distribution to these samples so that despite modal differences all five specimens may be paired.

4. Pyroxene-rich samples

Seven specimens from the Y-79 collection are very pyorxene-rich but contain more feldspar than the true diogenite Y-74097 (or any other diogenite) (Table 1). Using textural criteria, these seven samples are paired

into three groups: (a) 791199; (b) 791200 + 791201; (c) 791000 + 791072 + 791073 + 791422. (a) Y-791199. The thin section studied contains two large, slightly shocked coarse pyroxenite clasts with an intervening band of breccia. These clasts appear to be of the same lithology and have pigeonite host compositions En66-64Wo2-5 with coarse exsolved blebs of En42Wo45 augite. Feldspar grains in these lithic clasts are variable from An83Or0.3 to An75Or2.7. The saml1 breccia band between the clasts contains, in addition to pyroxene similar to that in the lithic fragments, more clacic feldspar (An90Or0.4). Chromite in both lithologies which are similar. This specimen is, therefore, considered to be a monomict pigeonite-rich cumulate and is classified as a pigeonite cumulate eucrite. The only non-Antarctic pyroxene as its main pyroxene cumulate eucrite Binda (10) contains more feldspar but has orthopyroxene as its main pyroxene phase. This meteorite perhaps resembles Y-75032, another pigeonite-bearing meteorite presently classified as a diogenite (11). (b) Y-791200 and 791201 are very similar texturally despite their large modal differences. Both have pigeonite of variable composition set in a glassy matrix, and appear to represent a pigeonite-rich lithology that has suffered some brecciation and melting (pyroxene in glassy material is more iron-rich than in clasts). The most magnesian pyroxene is En69Wo2 in 791200 with minor iron enrichment toward clast edges. Y-791201 is slightly more iron-rich haveing pyroxene cores of En66Wo2. In both samples pyroxene compositions vary significantly and variation of exsolution style (blebby vs lamellae) suggest that these samples may be polymict. The amount of iron-rich pyroxene increases as the melt fraction increases. Both samples contain feldspar that ranges from An93 to An89 and differs dramatically from that in Y-791199. The feldspar of Y-791201 is variably shocked and in a few cases is either maskelynite or devitrified maskelynite. The modal composition, together with the textures and compositions of the pyroxene and the feldspar suggest that these two samples are probably paired and sample another pigeonite-cumulate eucrite. (c) Y-791000, 791072, 791073, 791422 These four specimens are texturally very similar and have a distinctive appearance. All contain abundant, large heavily shocked exsolved pigeonite clasts and less common shocked feldspar in a very dark glassy matrix. Because of the coarse grain size (up to 3 mm long pigeonite) the major modal difference between 791073 and the others (Table 1) is not significant. This difference is caused by the presence of large feldspar clasts and abundant glass in the small area of 791073 studied. Small differences in mean pyroxene composition may be detected from specimen to specimen (Table 2) but all samples have overlapping ranges. Much of the variation of Fe/(Fe+Mg) appears to be the result of reaction between the pigeonite clasts and the more iron-rich surrounding matrix. Y-791073 contains more feldspathic and glassy material and has the most iron-rich pyroxenes. Prior to the generation of the glass matrix all the pyroxene in these samples was probably about En69. Most of the pyroxene is partly mosaicized and is badly deformed by shock, but exsolved blebs of augite are present and the pyroxene appears to have been pigeonite originally. These specimens, therefore, sample a pigeonite-rich lithology distinct from the hyperstherne dominated diogenites despite the modal similarity. These samples may be classified as diogenites, if the definition of a diogenite is relaxed to include pigeonite, but would be better classified as pigeonite-cumulate eucrites.

Discusstion The suite of 16 specimens samples (9-10) meteorites that show all the diversity of the entire basaltic achondrite suite. The recognition

of three very different eucrites increases the similarity ot the Antarctic meteorite collections to the collections from elsewhere since eucrites are more abundant than polymict eucrites. The total number of polymict eucrites from Antarctica is still, however, a special feature of the Antarctic collections. The new Yamato howardite(s) are comparable to previously known howardites. The pigeonite-rich specimens are, however, unique. The seven specimens studied appear to represent three meteorites that are distinct from diogenites as they contain pigeonite rather than orthopyroxene, but they are also less feldspathic than the diogenites and the cumulate eucrites (cf, 11) and are, therefore, of great significance and are assigned to a new subgroup of basaltic achondrites, the piogenite-cumulate-eucrites.

REFERENCES: (1) Delaney et al. (1983) MNIPRSI 30, 202. (2) Takeda (1979) Icarus 40, 455. (3) Takeda et al. (1981) PLPSC 14, JGR 88 Supplement, B245. (5) Harlow and Klimentidis (1980) PLPSC 11, 1131. (6) Delaney et al. (1983) LPS XIV. (7) Nehru et al. (1981) LPS XII, 765. (8) Delaney et al. (1982) PLPSC 13, JGR 87 Supplement, A339. (9) Delaney et al. (1983a,b) Meteoritics 18, (a)103, (b)247. (10) Garcia, Prinz (1978) Meteoritics 13, 473. (11) Takeda, Mori (1981) Meteoritics 16, 390. Acknowledgements: NASA founding NAG 9-31 (M. Prinz, P.I.).

Table 1. Modes of new Yamato basaltic achondrites
in order of decreasing feldspar content

	792510	74356	791960	791201	791186	791074	791492	791073	791573
	E	E	PE	CE[a]	PE?	H	H[b]	D[c]	H[b]
olivine	-	-	0.1	-	-	1.65	2.5	-	5.1
orthopyroxene	27.8	8.5	15.7	43.6	34.2	38.2	49.0	44.5	52.8
pigeonite	11.2	40.9	32.6	8.2	12.8	25.4	17.0	12.4	14.5
augite	12.0	5.7	9.2	10.0	13.1	5.8	5.8	13.2	4.9
feldspar	43.2	42.9	38.7	36.4	32.3	25.5	23.2	21.5	19.7
silica	4.1	1.1	2.7	0.9	6.5	2.0	1.3	6.3	1.2
ilmenite	1.1	0.8	0.3	0.1	0.5	tr	0.2	-	0.5
chromite	0.2	0.2	0.1	0.3	0.3	1.1	0.5	0.5	0.9
phosphate	0.1	-	tr	tr	-	-	-	-	0.4
troilite	0.4	tr	0.7	0.4	0.3	0.3	0.5	1.0	0.1
kamacite	-	-	-	-	-	-	-	-	-
Area mm^2	50.8	47.6	67.9	64.4	42.0	22.8	52.2	12.6	55.8
# points	909	898	1017	759	923	972	930	579	934

	791208	791200	791072	791199	791422	791000	74097	Polymict	Eucrite	Means
	H[b]	CE[a]	CE[c]	CE	CE[c]	CE[c]	D	Y	EET	ALH
olivine	3.3	-	-	-	-	-		0.7	-	tr
orthopyroxene	53.2	65.0	65.3	79.0	61.9	65.7	96.7	8.2	24.4	12.1
pigeonite	17.3	15.5	15.8	8.1	29.0	26.7	-	34.4	23.3	27.1
augite	4.1	6.5	5.1	5.3	4.0	3.7	-	12.4	7.8	13.1
feldspar	19.5	10.4	5.7	4.9	4.2	2.7	0.1	38.8	40.8	43.0
silica	1.2	0.9	5.6	1.4	-	0.9	0.7	3.5	3.7	3.6
ilmenite	0.1	tr	0.2	-	-	-	-	0.8	0.7	0.5
chromite	0.7	1.12	0.3	0.5	0.4	0.2	1.1	0.2	0.1	0.2
phosphate	tr	-	0.3	0.1	-	-	-	0.2	-	0.1
troilte	0.6	0.1	1.5	0.3	0.1	0.2	1.6	0.5	0.1	0.1
kamacite	tr	-	0.2	-	-	-	-	-	tr	0.1
Area mm^2	118.6	72.7	26	46.3	17.8	96.2	85.2	-	-	-
# points	1012	762	584	968	558	752	554	-	-	-

Notes for Table 1: I E=eucrite; PE=polymict eucrite; CE=cumulate eucrite; H=howardite; D=diogenite.

II a,b,c,d superscripts identify sections paired provisionally on the basis of modal, mineralogical and textural data.

III Use of "pigeonite" includes both true pigeonite and orthopyroxene-clinopyroxene overlaps and, hence, represent a systematic overestimate of piogenite abundance.

Table 2. Summary of mineral composition ranges in Yamato achondrites

Specimen	Low Ca-pyx max. En/Wo	Low Ca-pyx min. En/Wo	High Ca-pyx max. En/Wo	High Ca-pyx min. En/Wo	Feldspar max. An/Or	Feldspar min. An/Or	Feldspar Mean An/Or	Olivine Fe
	eucrites							
74356	41/4	-	31/42	-	95/.2	89/.4	91/.3	none
792510	37/2	-	30/45	-	89/.4	83/1.2	87/.6	none
	polymict eucrites							
791186	43/3	38/3	31/44	-	94	72/2.5	90	none
791960	77/2	30/5	40/35	27/40				none
	howardites							
791074	80/1	35/4	35/40	25/40	93	80		45-72
791208	85/1	38/2	42/43	34/43	93	70		45-91
791492	88/.4	35/4			93	77		74-91
791573	87/1	34/9	43/44	29/41	93	77		63-91
	pyroxene-rich achondrites							
791199	66/3	62/2	42/45	-	90/.5	75/2.5	84	none
791200	69/2	58/3	42/45	-	93	88	91	none
791201	66/2	45/2			93	86	91	none
791000	69/2	57.2			91/.4	86/.4	89/.4	
791072	66/2	62/2			91	86	88?	
791073	65/2	55/4			91	81	89	
791422	65/2	59/5			92	89	90?	
	diogenite							
74097					91?	89?	?	

LUNAR METEORITE IN JAPANESE COLLECTION OF THE YAMATO METEORITES

K. Yanai and H. Kojima
National Institute of Polar Research, Tokyo 173

Yamato-791197 has been classified as an anorthositic breccia. This specimen is nearly complate stone, 25.4 grams and covered with a thick fusion crust which is dusty grey color. The interior consists large amount of angular clasts in a black matrix. The clasts show in color from grey to white and their size are under 4mm, however most of clasts are smaller than 1 mm.

The section of the specimen shows numerous clasts in brown matrix. There are two type clasts (polymineral and monomineral) in the section. Most of larger clasts are mainly polymineralic which are composed of most plagioclase with minor pyroxene and olivine, and plagioclase-pyroxene. The smaller clasts are individual mineral fragments of most plagioclase and some pyroxenes and minor of olivine. In the rare case the specimen contains small glass spherule. The clasts show a variety of texture including diabasic, bsaltic and granulitic, and most of them have been shocked more or less.

Microprobe analyses show that feldspar ranges from An97 to 98.2 with most analysis following between An95.5 and An97.5, and they are containing 0.6% (maximum) of Or component; pyroxene and olivine is variable in composition, pyroxene: Wo1.7-54.8, En5.9-83.1, Fs9.0-58.9 and olivine, Fo13.6-82.1 were analyzed. MnO content of the both pyroxene and olivine are lower than theirs of the all achondrites, but they are very similar to the some of lunar rock, especially anorthositic breccia.

This specimen shows a brecciated texture of numerous lithic fragments, which is common occurrences in the most polymict eucrites and howardites, but it is different from eucrites and howardites in most respects of mineralogically, chemically and others.

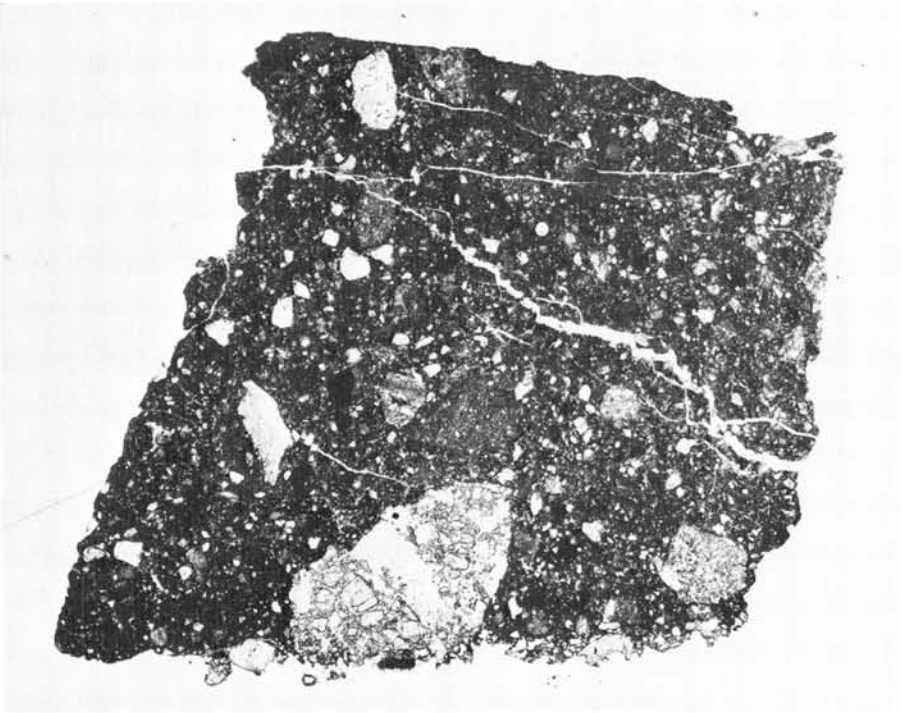

Fig. 1. Photomicrograph of thin section of Y-791197. Width 7 mm

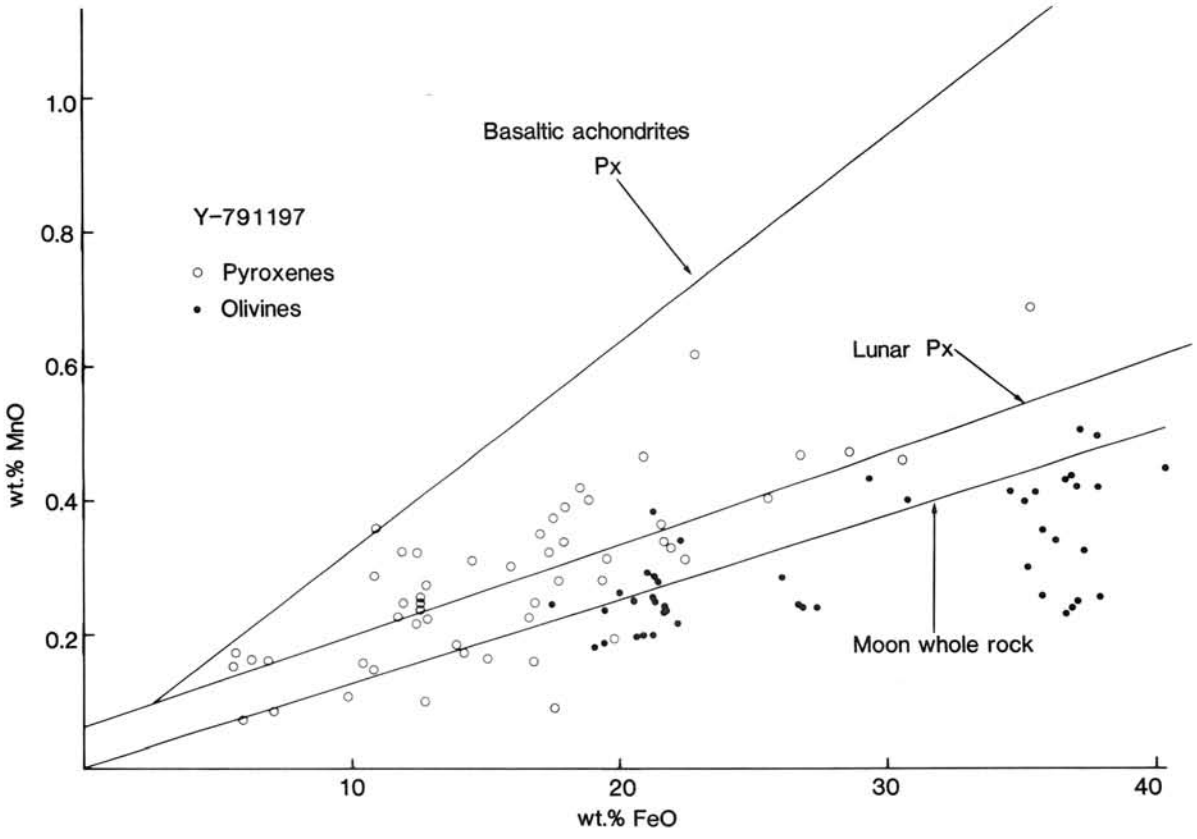

Fig. 2. Olivines and pyroxenes from Yamato-791197 have MnO/FeO ratios appropriate for lunar rocks, much lower than MnO/FeO ratios of basaltic achondrites

18－1

CHEMICAL COMPOSITIONS OF MATRICES AND CHONDRULE-RIMS OF UNEQUILIBRATED ORDINARY CHONDRITES

Satoshi MATSUNAMI:
Geological Institute, University of Tokyo, Hongo, Tokyo 113.

The matrices and chondrule-rims of eight unequilibrated ordinary chondrites, Semarkona (LL3), Krymka (L3), Sharps (H3), Chainpur (LL3), Tieschitz(H3), ALH-77214 (L or LL3), Mezo Madaras (L3) and ALH-77216 (L3), have been investigated in detail with the scanning electron microscope. The analyses were made by a broad area EDS technique, using a Link System Model 860 energy dispersive spectrometer equipped to a JEOL-T200.

It is shown that the matrix and chondrule-rim materials of UOCs studied here are characterized by lower Mg/Si, Ca/Si, Ca/Al ratios, higher FeO/(FeO+MgO) ratio and larger variations in Al/Si, Na/Si, K/Si ratios than bulk meteorites. These features in chemical composition suggest some implications in the condensation and fractionation processes in the cooling solar nebula.

(1) Implications in condensation process.--- Inspections of the CIPW norms of average compositions of matrix and chondrule-rim in UOCs studied suggest that differences between these average chemical compositions of matrix materials and bulk compositions of chondrules from UOCs and meteorite samples might have been attributed to different degrees of reactions among pyroxene, plagioclase, Fe and gas phase to form Fa, Ab, and Ne components in the cooling solar nebula.

(2) Implications in fractionation processes of refractory lithophile elements.--- Particularly, chemical compositions of matrices and chondrule-rims of Semarkona chondrite have been compared in detail with those of 29 chondrules obtained by Grossman and Wasson (1983). These comparisons reveal that the precursor materials of chondrules in Semarkona might be mixtures composed mainly of the refractory, olivine-rich, FeO-free component (Grossman and Wasson, 1983) and the non-refractory, low Mg/Si, Al/Si, Ca/Si, high Ca/Al, FeO-rich COMPONENT X (this work). In Semarkona, several chondrule-rims are enriched in COMPONENT X. On the other hand, compositional variations of matrices and chondrule-rims of Semarkona may be explained by the mixing of COMPONENT X and the Al-enriched (high Al/Si), sodic plagioclase-like component in various ratios. Relationships among the refractory component, COMPONENT X and the Al-enriched, sodic plagioclase-like component are schematically illustrated in Fig. 1. There might have been a fractionation process of these refractories (Mg, Al, Ca) between chondrules and matrix materials in the solar nebula at medium to low temperatures.

It is also worth noting that COMPONENT X is located on the low-(Mg, Al, Ca)/Si-side extension of the trend defined by bulk compositions of enstatite, ordinary and CI chondrites (1, 2) (E-O Line in Fig. 1). The COMPONENT X may represent the "latest

stage condensate" and the "end-product" by high temperature fractionation of refractory lithophile elements (3, 4, 5). The non-refractory component such as COMPONENT X in Semarkona might have had an important role as a linkage between the precursor materials of chondrules and matrix, chondrule-rim materials to the genesis of chondritic materials of UOCs.

The author thanks Dr. B. Mason of the Smithsonian Institution for providing the meteorite samples and Drs. K. Yokoyama and Y. Saito of the National Science Museum for permitting him to use scanning electron microscope.

References: (1) Grossman, J. N. and Wasson, J. T. (1983): GCA, 47, 759-771. (2) Kerridge, J. F. (1979): Proc. 10th Lunar Sci. Conf., 989-996. (3) Larimer, J. W. and Anders, E. (1970): GCA, 34, 367-387. (4) Ganapathy, R. and Anders, E. (1974): Proc. 5th Lunar Conf., 1181-1206. (5) Larimer, J. W. (1979): Icarus, 40, 446-454.

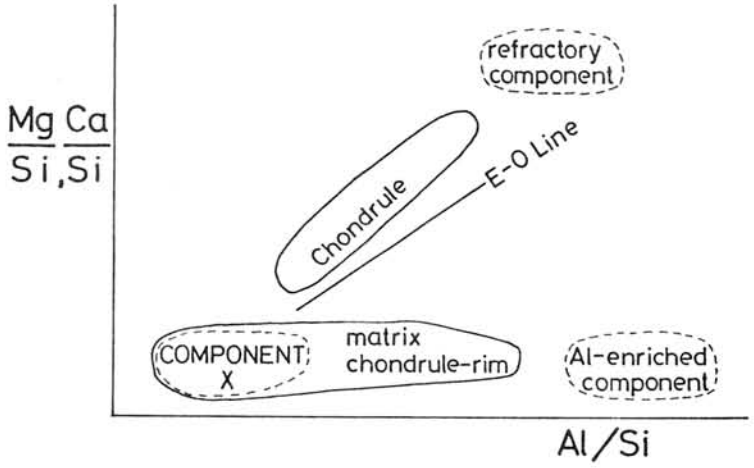

Fig. 1 Schematic relationships among three components of Semarkona chondrite (the refractory component (Grossman and Wasson, 1983), the non-refractory, Al-depleted COMPONENT X and the Al-enriched, sodic plagioclase-like component (this work)), chondrule compositions (Grossman and Wasson, 1983) and matrix, chondrule-rim compositions (this work).

19－1

COARSE-GRAINED LITHIC FRAGMENTS IN UNEQUILIBRATED ORDINARY CHONDRITES

Kimura M.
Earth Sciences, Ibaraki University, Mito 310.

Unequilibrated ordinary chondrites comprise various constituent units such as chondrules, matrix, and so on. Coarse-grained lithic fragments (CGF hereafter) is an unique constituent unit in them, although CGF's are poor in amount in 4 LL3, 3 L3, and 4 H3 chondrites studied here. CGF's are nearly holocrystalline and their size distribution resembles those of chondrules. Anhedral Mg-rich olivine and pyroxene, up to 0.8mm in size, are dominant in CGF's, as well as Mg-rich chondrules. Normative olivine to pyroxene ratios vary widely in both units (Fig.1). The range of atomic Mg/Mg+Fe ratios of CGF's agrees with that of Mg-rich chondrules, especially IP-chondrules defined by Ikeda (1980). The chemical compositions of spinels in CGF's resemble those in IP-chondrules.

On the contrary, CGF's have the following features different from those of chondrules: 1)Allotriomorphic-granular texture, 2)homogeneous olivine and orthopyroxene in chemical composition, 3)absence of clinoenstatite, 4)depletion of plagioclase and diopside components from bulk composition (Figs. 2 and 3), and 5)chemical compositions of normative plagioclase in CGF's are richer in anorthite component than those in chondrules.

Thus, CGF's closely relate to Mg-rich chondrules, especially IP-type, and it seems that CGF's are equivalent to Mg-rich chondrules depleted in some components. However, they evidently underwent different thermal history from chondrules. It is evident that CGF's are not fragments of equilibrated chondrites, because plagioclase component is depleted in CGF's and chemical compositions of olivine and pyroxene are different from those in equilibrated chondrites.

Depletion of plagioclase and diopside components, and chemical compositions of normative plagioclase in CGF's suggest that the precursor materials of CGF's were heated above about 1200°C and melted to lose these componet. However, since the ranges of atomic Mg/Mg+Fe ratios and normative olivine to pyroxene ratios of CGF's agree with Mg-rich chondrules, the degree of partial melting was not so high. At any rate, such a thermal history of CGF's can explain the other characteristic features of them such as texture, homogeneous compositions of minerals, and the presence of orthopyroxene. It is probable that the precursor materisls of CGF's were partially melted to fractionate some components and cooled slowly. We can suppose that such a thermal history of these materials occurred in some planetesimals. These planetesimals later fragmented to form CGF's, and they mixed with chondrules, and so on, thoroughly, until all constituent materials of ordinary chondrites were finally consolidated in a parent body.

Fig.1. Plotting of normative pyroxene (Px)-olivine (Ol)-feldspar (F) for bulk compositions of CGF's (left) and chondrules in ALH-77249 (L3) (right).
Fig.2. Distribution of normative F/F+Ol+Px ratios in CGF's (square, triangle, and circle) and chondrules (CL) in ALH-77249. Average ratios of them are shown.
Fig.3. Distribution of normative Di/Di+Hy+Ol ratios in CGF's and chondrules.

Fig. 1

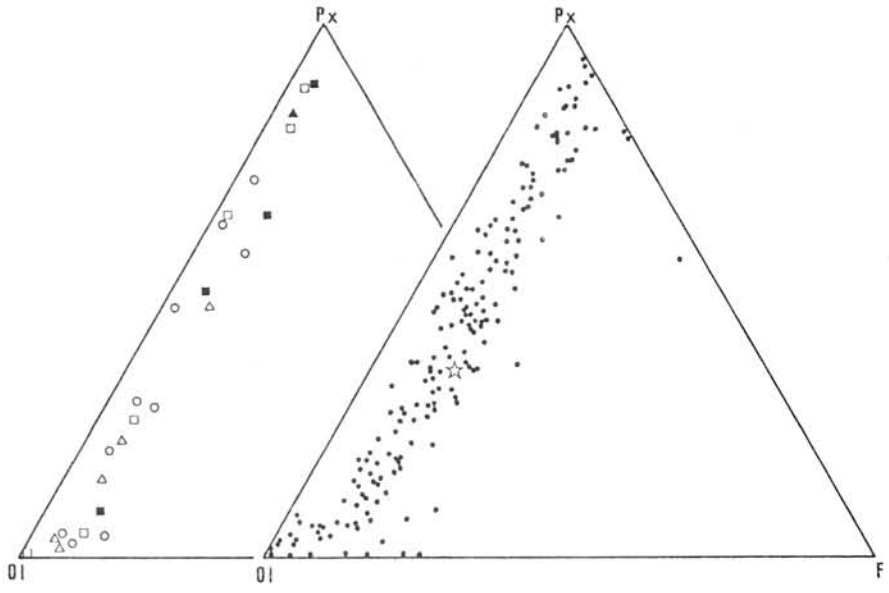

Fig. 2

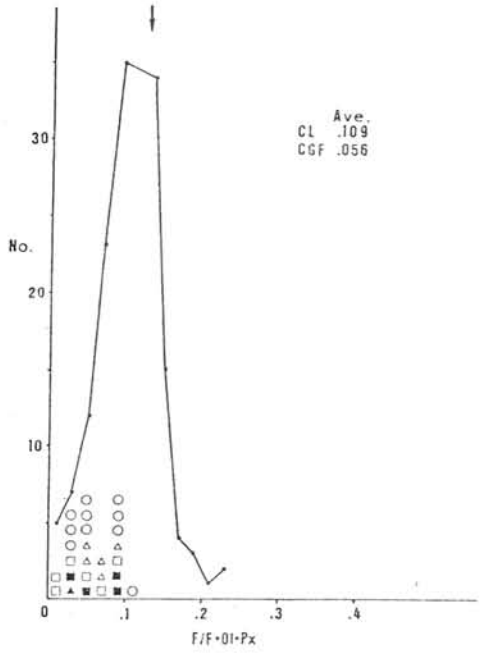

Fig. 3

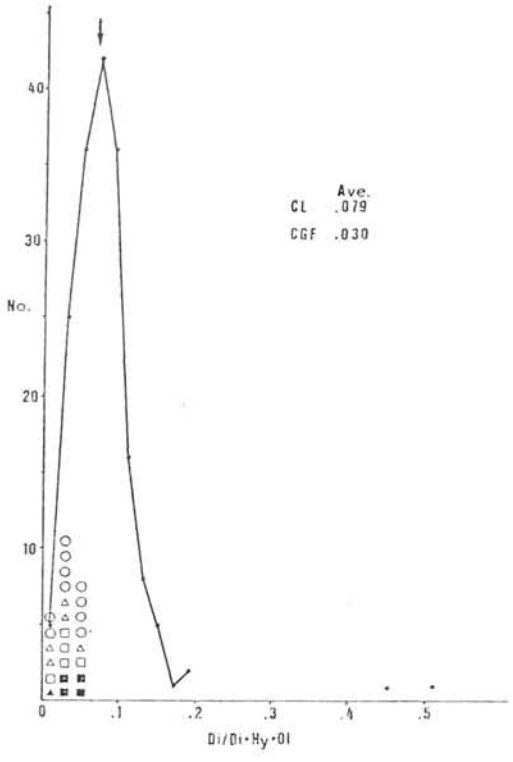

ANALYTICAL ELECTRON MICROSCOPY OF A CHONDRULE (L3:ALH-77015) INCLUDING RELICT OLIVINE

Watanabe, S., Kitamura, M. and Morimoto, N.
Dept. Geol. & Mineral., Fac. Science, Kyoto Univ.,
Sakyo, Kyoto, 606

Relict olivine grains, found for the first time by Nagahara (1981) in ALH-77015(L3), suggest existence of solid olivine grains before the formation of chodrules. Fine textures of relict grains must give information on the conditions during and before the formation of chondrules. A chondrule including olivine grains with dusty core and clear rim in ALH-77015 (L3) has been examined by analytical electron microscopy (AEM) in this study. The chondrule has rather irregular shape and consists mainly of olivine, pyroxene and opaque minerals.

Olivine : Dusty looking of the core of olivine is due to fine inclusions of chromite (Fig.1). Abundance of chromite is about 1 μm^{-2}. AEM analysis of olivine avoiding the effect of chromite shows the reverse and normal Fe-Mg zoning in the core and rim, respectively. This is consistent with previous results by Nagahara (1981) and Rambaldi (1981), and suggests that the dusty core of olivine is relict.

Figure 2 is a dark field electron micrograph (g=222) near the boundary between the core and rim of an olivine. The dislocation density of the core ($\sim 10^{9}$ cm^{-2}) is extremely higher than that of the rim ($\sim 2 \times 10^{8}$ cm^{-2}). Ashworth and Barbar (1975) reported that shock deformed olivine in some chondrites has dislocation density of $10^{8} \sim 10^{9}$ cm^{-2}. The fact that only the core has high dislocation density can be explained as, i) dislocation texture was inherited from the preexisting olivine, which had suffered as severe shearing as olivine in the sheared nodule of kimberlite, or ii) intensitive shock deformation, probably during shock melting, has caused the dislocation texture.

Pyroxene : Orthopyroxene and clinoenstatite coexist in this chondrule. A pyroxene grain consists of three parts : orthopyroxene core is mantled by clinoenstatite of approximately the same composition, and the outest rim is augite. Augite is slightly Ca-zoned, and its Ca-poor part shows spinodal decomposition texture of augite and pigeonite. This assembladge, orthopyroxene and rapidly cooled phases, is unlikely to have crystallized from melt through a monotonic cooling, and suggests the existence of relict orthopyroxene.

[REFERENCES]

Nagahara, H. (1981) : Nature, 292, 135-136
Rambaldi, E.R. (1981) : Nature, 293, 558-561
Ashworth, J.R. and Barbar, D.J. (1975) : Earth Planet.Sci.Lett., 27,43-50

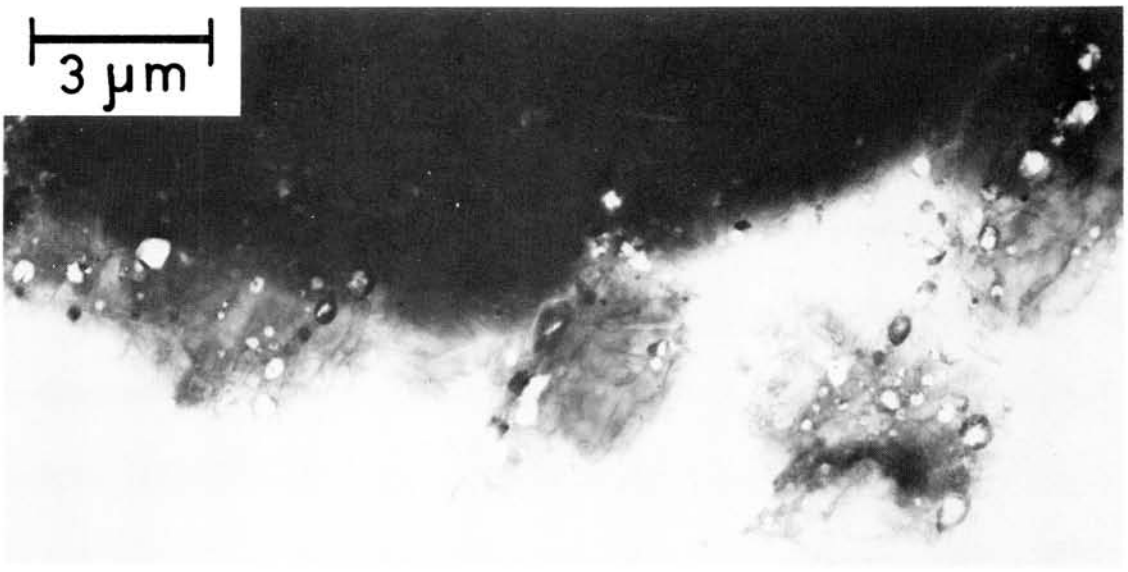

Fig.1 Electron micrograph of the core of olivine. fine chromite inclusions and holes around them because of preferential ion-thinning can be observed.

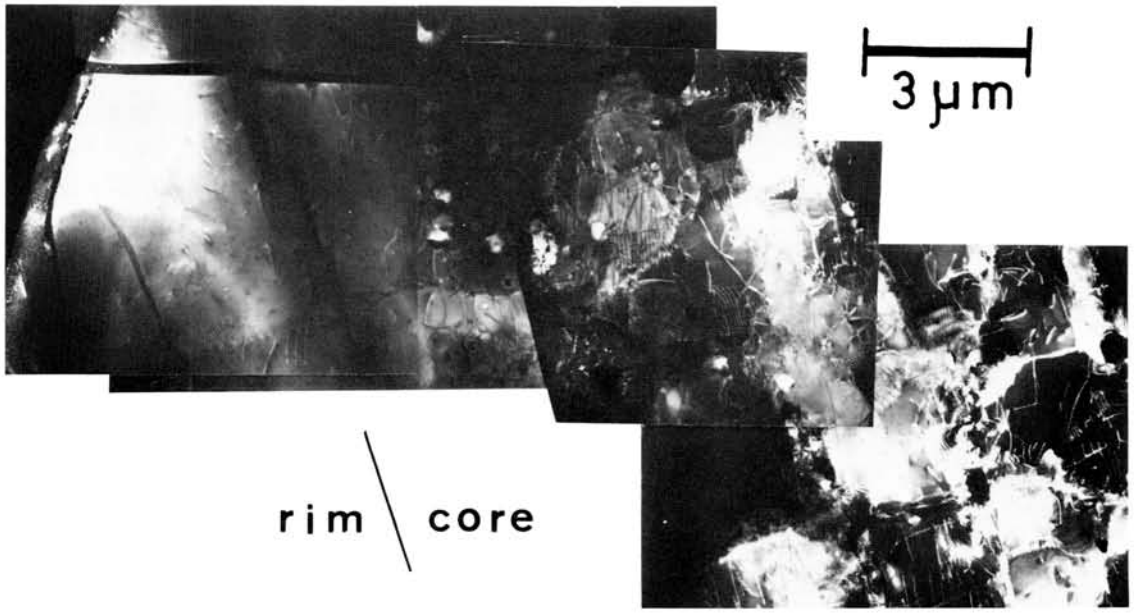

Fig.2 Dark-field electron micrograph (g=222) around the boundary between the core and rim of olivine. The dislocation density of the core is extremingly high.

THERMAL HISTORY OF 'RELICT PYROXENE' IN THE ALLENDE METEORITE

Kitamura, M., Isobe, H., Watanabe, S. and Morimoto, N.

Department of Geology and Mineralogy, Faculty of Science
Kyoto University, Sakyo, Kyoto, 606, Japan

Olivine crystals in chondrules of L3 type chondrite have 'relict olivine' in their core regions (Nagahara, 1981; Rambaldi, 1981). Existence of the 'relict mineral' gives information of the state of the precusor and formation of the chondrules. In the present study, the 'relict pyroxenes' and 'relict olivine', surrounded by rapidly crystallized pyroxenes, have been found by analytical electron microscopy (AEM).

The chondrule consisting mainly of olivine, pyroxene and iron sulfides was studied, where the equigranular olivine grains are in the central portion of the chondrule, while the pyroxene grains in the outer portion. The pyroxene grains are homogeneous clinoenstatite with (100) twin under an opitcal microscope. However, thin Ca-rich margins were found around a few clinoenstatite grains by electron probe micro-analysis (EPMA). One of the grains was ion-thinned and studied by AEM.

Most of the grain (region A) shows three different textures; the core is clinoenstatite, the mantle is pigeonite with exsolved augite and the marginal is the mixture of pigeonite and augite formed by the spinodal decomposition with about 18 nm periodicity (Figure 1). The composition of the region A is Fe-poor ($Fs_{\sim 1}$) but changes in the Ca component from Ca-free at the core through $Wo_{\sim 10}$ at the mantle to $Wo_{\sim 30}$ at the rim. A small part of the grain (region B), surrounded by the region A, shows different composition and structure. This region consists of olivine and clinoenstatite with augite lamellae ~0.1 μm thick(Figure 2). The compositions of olivine, clinoenstatite and augite are Fo_{30}, $Fs_{\sim 5}Wo_{\sim 3}$ and $Fs_{\sim 10}Wo_{\sim 30}$, respectively. The composition of olivine is also richer in Fe than that ($Fo_{\sim 6}$) of most olivines in the chondrules. The compositions of the pyroxenes are richer in Fe than those of the region A. Since augite can exsolve only from pigeonite ($Wo_{\sim 15}$ - $Wo_{\sim 25}$) or orthopyroxene ($Wo_{\sim 1}$ - $Wo_{\sim 5}$), the clinoenstatite in the region B must have been transformed from orthopyroxene with the augite lamellae.

The decomposition texture in the region A indicates the almost same cooling rate of 10^{1}~10^{-1}°C/hr as that of the pyroxenes in L3 chondrite (Kitamura et al., 1983). However, the region B records much slower cooling rate than that of the region A, because the exsolution lamella of augite in the region B is thicker than those in the region A. If the region B was formed after the decomposition of the region A, the decomposition texture of the region A must have been coarsened to that of the region B. Therefore, the region B indicates the 'relict pyroxene and olivine', which must have once been kept in the 'grand-parent body' of the chondrite for a time enough to exsolve the augite.

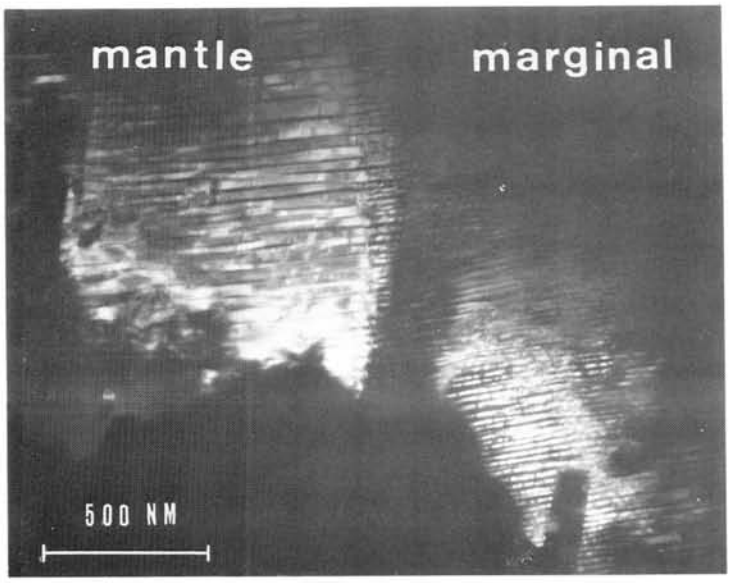

Figure 1. Dark field electron micrograph of the mantle and marginal of the region A. Pigeonite is in bright, while augite in dark. In the mantle, exsolution lamellae of augite in pigeonite are observed. The spinodal decomposition of augite and pigeonite in the marginal has the periodicity of about 18 nm.

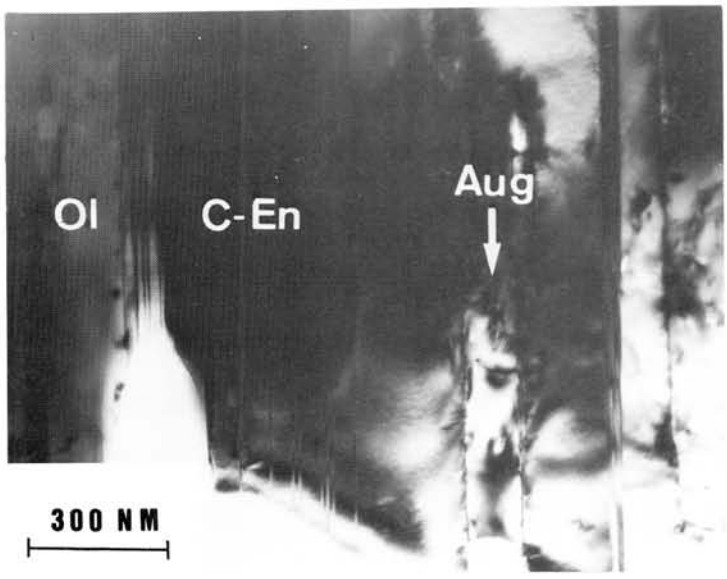

Figure 2. Electron micrograph of the region B consisting of olivine (Ol) and clinoenstatite (C-En) with augite lamella (Aug).

[REFERENCES]

Nagahara, H. (1981) : Nature, 292, 135-136.
Rambaldi, E.R. (1981) : Nature, 293, 558-561.
Kitamura,M., Yasuda,M., Watanabe,S., Morimoto,N.(1983) : Earth & Planetary Science Letters, 63, 189-201.

22－1

AN ANALYTICAL TRANSMISSION ELECTRON MICROSCOPIC STUDY OF SHOCK-PRODUCED VEINS IN THE TENHAM CHONDRITE

Hiroshi Mori and Hiroshi Takeda

Mineralogical Institute, University of Tokyo, Hongo 7-3-1, Tokyo 113, JAPAN

An analytical transmission electron microscope (ATEM) study was conducted to determine the chemical compositions of shock-produced high-pressure minerals (i.e. ringwoodite and majorite) in the Tenham chondrite. The meteorite is an equilibrated olivine-hypersthene chondrite (L6) with a network of thin black veins (Binns ,1967). The black veins contain subrounded mineral fragments and black vein matrix.

TEM observations of the subrounded mineral fragments which have the olivine composition and are replaced by an isotropic phase revealed that they are composed of polycrystalline aggregates of submicron sized faulted spinel (Price et al.,1979 : Madon and Poirier,1980). They reported a fine interstitial glassy phase within the fine scale polycrystalline aggregates. We performed X-ray microchemical analyses of submicron sized spinel crystals (Fig. 1) by ATEM and confirmed that they have a chemical composition of $(Mg_{0.76}Fe_{0.24})_2SiO_4$, which indicates an isochemical transformation.

Majorite, the garnet form of $(Mg,Fe)SiO_3$ is known to have two types of occurrence in the Tenham chondrite. One is as an isotropic phase which replaced orthopyroxene xenocrysts enclosed in the shock vein. The other is as fine equant isotropic crystals in a darker matrix, which includes composite droplets of troilite, kamacite and taenite (Price et al.,1979). We determined the chemical composition of the garnet phases which occur as fine equant crystals (Fig.2) in the black vein matrix (type II). The composition showed significant deviation from original orthopyroxene ($Wo_{1.4}En_{79.4}Fs_{19.2}$). The majorite has a low Fe/(Mg + Fe) value of 0.10 and contains larger amounts of Al_2O_3 (up to 5.5 wt%), Cr_2O_3, CaO and Na_2O. Probably the equant majorite grains are quench crystals from fused vein materials produced by shock melting of a multiphase assemblage containing olivine, pyroxene, plagioclase, chromite, troilite, kamacite and taenite. We could not obtain a chemical composition of the type I majorite which may have been produced by isochemical transformation because of rare crystals of an optically isotropic material with the orthopyroxene composition.

We thank Dr. B. Mason for the Tenham chondrite sample.

Fig. 1 Electron micrograph of one crystal from a polycrystalline aggregate of ringwoodite, γ-$(Mg_{0.76},Fe_{0.24})_2SiO_4$. Stacking faults are prominent within the crystal. (magnification, x 143000)

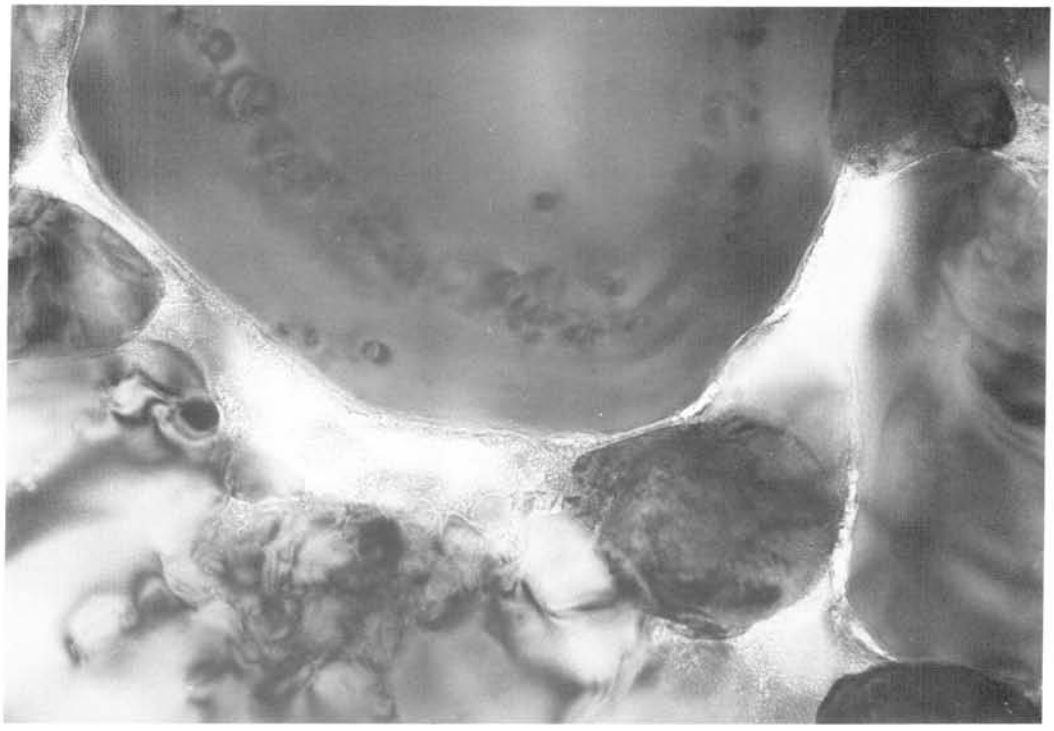

Fig. 2 Electron micrograph of majorite crystals with an interstitial glassy phase. (magnification , x 65000)

COMPOSITION AND STRUCTURAL SUBSTITUTION OF METEORITIC PLAGIOCLASES

Yasunori Miúra and Takeshi Tomisaka

Dept. Mineralogical Sciences and Geol., Fac. of Science
Yamaguchi University, Yamaguchi 753, Japan

Small amounts of iron, magnesium and Na (and/or Ca) vacancy are found in meteoritic plagioclases, and significant departures (up to 9 mole %) from ideal feldspar stoichiometry are observed. Seven end-members are used in this study,where six end-members are used already in lunar plagioclases; that is, $KAlSi_3O_8$ (Or), $NaAlSi_3O_8$ (Ab), $CaAl_2Si_2O_8$ (An), $(Fe,Mg)Al_2Si_2O_8$, $Ca(Fe,Mg)Si_3O_8$, $[\ ]Si_4O_8$ and $M(MT)_4O_8$, where [ ] means Na and/or Ca vacancy, M=K,Na,Ca, and T=Al,Si,Fe,Mg. The samples analyzed by electron microprobe are Y-75135,93 (L5-4), ALHA769,75 (L6), Holbrook (L6), Y-74640,81 (H6), Y-75258,97 (LL6) and Allende (CV3) chondrites, and Juvinas eucrites. Some data previously reported are recalculated for reference in this study;that is, Adams Co. (H5, Fodor et al., 1980), Naragh (H6, Adib & Lious, 1979) and Atlanta chondrites (EL6, Rubin, 1983), EETA79006 eucrites (Simon et al., 1982), ALHA77302 and ALHA76005 eucrites (Simon & Papike, 1983).

The preliminary results are obtained as follows:

1. Total amounts of end-members except Or, Ab and An in chondrites show increase with Ab content; i.e., 9.0 mole% in CV3 Allende, 6.2 mole% in L6, 6.0 mole% in E6, 3.5 mole% in H6 and 2.1 mole% LL6. The similar tendency observed in eucrites; that is, 5.7 mole% in Juvinas, 3.2 mole% in ALHA77302, 2.7 mole% in ALHA 77006 and 2.6 mole% in EETA79006.
2. The amounts of cation vacancy are significantly increased with Ab content.
3. The amounts of $CaAl_2Si_2O_8$ are decreased from the usual An content up to 9 mole%.
4. Cell dimensions of plagioclase in Juvinas eucrites are considerably smaller than those of An_{80} plagioclase.
5. Small amounts of excess M cations (i.e., $M(MT)_4O_8$) are observed only in exsolved regions of Juvinas plagioclase.

Reference:

Adib, D. and J.G. Lious (1979): Meteoritics, 14,257-272.
Fodor, R.V. et al. (1980): Meteoritics, 15,41-62.
Rubin, A.E. (1983): Meteoritics, 18, 113-121.
Simon, S.B. et al. (1982): Meteoritics, 17, 1498-162.
Simon, S.B. and J.J. Papike (1983): Meteoritics, 18, 35-50.

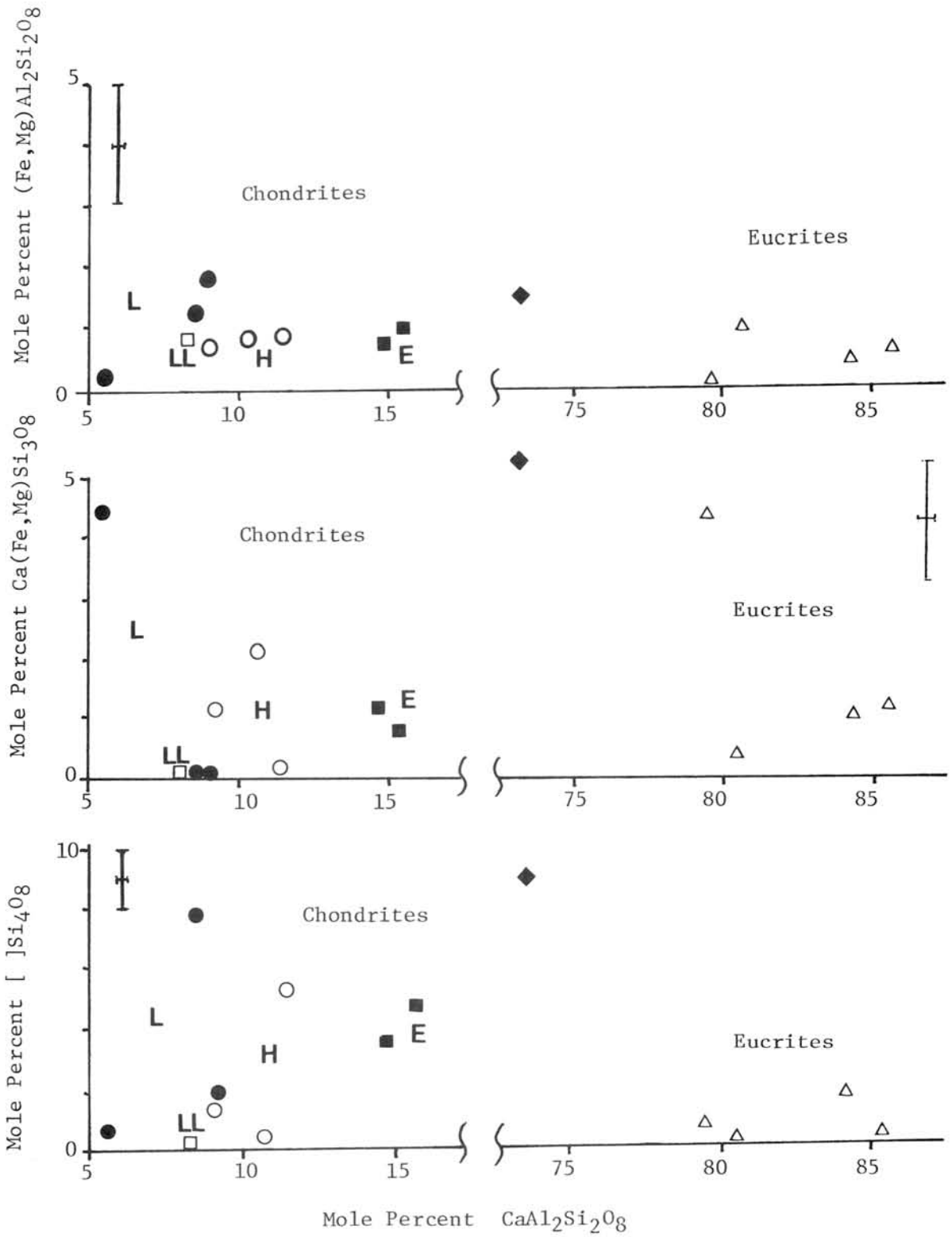

Fig. 1. Variations in $(Fe,Mg)Al_2Si_2O_8$, $Ca(Fe,Mg)Si_3O_8$ and $[\ ]Si_4O_8$ as a function of $CaAl_2Si_2O_8$ for meteoritic plagioclases. ●: L-chondrites; □: LL-chondrites; ○:H-chondrites; ■:E-chondrites;◆:Juvinas;△:eucrites.

Ni, Fe AND Co VARIATION PATTERNS OF TWELVE ANTARCTIC CHONDRITES

Smith, D.G.W.[1], Launspach S.[1] and Miúra, Y.[2]
1 Department of Geology, University of Alberta, Edmonton, Alta., CANADA, T6G 2E3.
2 Department of Mineralogical Sciences and Geology, Faculty of Science
Yamaguchi University, 1677-1, Yoshida, Yamaguchi 753, JAPAN

The variations in concentrations of Ni, Fe and Co in the metal phases of twelve different antarctic chondrites have been investigated by electron microprobe techniques similar to those described by Smith and Launspach (1983). Modifications were made, however, in order to minimise a tendency to sample preferentially taenite grains which are characteristically smaller than the associated kamacite. The results of these analyses are summarised in Table 1 and Figure 1.

Table 1: Sample numbers, group & petrologic type and average metal compositions

sample numbers	group & Type	average metal compositions			
		no. pts.	Ni	Fe	Co
Y74640.81-3	H6	375	12.41	87.17	0.42
Y74647.95-3	H5-6	725	14.21	85.39	0.40
ALH76865-2	H6	318	9.80	89.75	0.45
ALH77288.64-2	H6	362	9.22	90.32	0.46
Y74190.72-3	L6	450	13.00	86.28	0.72
Y74362.84-3	L6	530	13.03	86.26	0.71
Y75102.74	L6	256	14.72	84.54	0.74
Y75115.91-2	L(?)	162	21.46	77.96	0.59
ALH76975.85-3	L6	355	14.72	84.61	0.67
ALH77214.93-1	L(?)	79	18.80	80.52	0.68
Y74646.93	LL5-6	170	29.29	69.43	1.28
ALH77307.85	C3	93	13.67	85.82	0.51

The H-group chondrites all exhibit similar and rather simple patterns with concentrations corresponding to major amounts of kamacite and lesser amounts of taenite and tetrataenite. Co shows little scatter and its concentration in kamacite is centred around 0.5%. These results are very similar to those reported previously for Kielpa (H5) and Nuevo Mercurio (H5) (Smith, 1980; Miúra et al., 1984). They are consistent with originally homogeneous kamacite and taenite phases having acquired a limited amount of inhomogeneity by diffusion processes during cooling from high temperatures and/or during long-term re-heating to low temperatures with the conversion of the most Ni-rich regions to tetrataenite by further limited local diffusion. Taenite of the H-group samples lies in a composition range from about 28-42 wt.% Ni and is centred around the middle of that range. The Co content of this taenite shows very little scatter, ranging from about 0.25% down to zero, with an average value around 0.1%.

L-group chondrites show significantly higher Co values in the kamacite and a wider range of Ni values in this phase. There is also some evidence of a bimodal clustering of the Co concentrations in kamacite (e.g., #Y74362.84-3). Kamacite is still the dominant metal phase but less so than in H-group samples. There is a great range of taenite compositions, not only in Ni values but also in the Co concentrations for a

given Ni value. The degree of scatter varies from meteorite to meteorite and is most extreme in the case of #Y75102.74 in which Ni ranges from 19% up to 50% and Co from 0.1% to more than 1%. Two L-group samples show a cluster of Ni-Co values between kamacite and taenite, which may be martensite compositions, now possibly represented by plessitic intergrowths. It is most improbable that these compositional variations reflect simply the random sampling of diffusion profiles across kamacite/taenite and taenite/tetrataenite boundaries. Rather they suggest that the metal phases mat never have been represented by homogeneous kamacite and taenite, but may be collections of assorted grains of diverse origins.

The one LL-group sample shows a wide range of Ni and Co values but also some tendency towards a multimodal distribution of Ni values. The Co concentrations for both kamacite (2%-3%) and taenite (0.2%-2.0%) are very much higher that the corresponding values in H and L groups and show great variations for a given Ni value. Only two points with Ni>50 wt.% were measured, but if these do indeed correspond to tetrataenite, they also have unusually high Co contents.

The C3 chondrite investigated shows a reversal of the trend seen in the other chondrites: low-Ni kamacite is associated with low Co (0.2%-0.5%) and the high-Ni phase with high Co (1.3%-2.0%). The average Ni content of the kamacite (4-5%) is distinctly lower than in other chondrites. The high-Ni phase in this chondrite is very similar in composition to the high-Ni phase in Allende, and may be awaruite. If these Fe,Ni phases were formed in equilibrium with one another, the coexistence would indicate a temperature of formation of $<\sim 340^{\circ}C$ (Huemann & Karsten, 1963) and, since tetrataenite does not appear to be present, $>\sim 300^{\circ}C$ (Clarke & Scott, 1980).

Two of the chondrite samples received for investigation Y75115.91-2 and ALH77214.93-1, had not been classified as to group and petrologic type. The Ni-Co patterns (Figure 1) suggest that both may be members of the L group. However, in both of them, the overall average Ni appears to be anomalously high and the Co low. Also, the kamacite in ALH77214.93-1 shows a distinctly lower Ni content than other L group samples.

It is difficult to envisage how the compositional variations seen in the metal phases of L6 and LL5-6 samples could survive thermal events that are held to have brought about substantial homogeneity amongst the refractory silicates and produced the degree of recrystallisation that characterises the higher petrologic types. Clearly, however, the evidence afforded by metal compositions must be accommodated by satisfactory models for the thermal histories of chondritic meteorites.

REFERENCES:

CLARKE, R.S. Jr., et al. (1971): Smithsonian Contrib. Earth Sci., 5, 1-53.
CLARKE, R.S. Jr., & SCOTT, E.R.D. (1980): American Mineralogist, 65, 624-631.
HEUMANN, T. & KARSTEN, G. (1963): Arch. Eisenhuettenw., 34, 781-785.
MIURA, Y. et al. (1984): Proc. 8th Symp. Antarctic meteorites, N.I.P.R., (in press).
SMITH, D.G.W. (1980): Canadian Mineralogist, 18, 433-442.
SMITH, D.G.W. & LAUNSPACH, S. (1983): Microbeam Analysis - 1983, 47-50, San Franscico Press.

Figure 1: Ni-Co plots for the 12 chondrites investigated. Note that in the interest of conciseness, the following data points have been omitted: Y75102.74 - Ni 7%, Co 2.2%; Y75115.91-2 - Ni 8%, Co 1.5%; Y74190.72-3 - Ni 8%, Co 1.8% & Ni 13%, Co 1.45%. Note also the change of scale for Co in Y74646.93 - the only LL group chondrite.

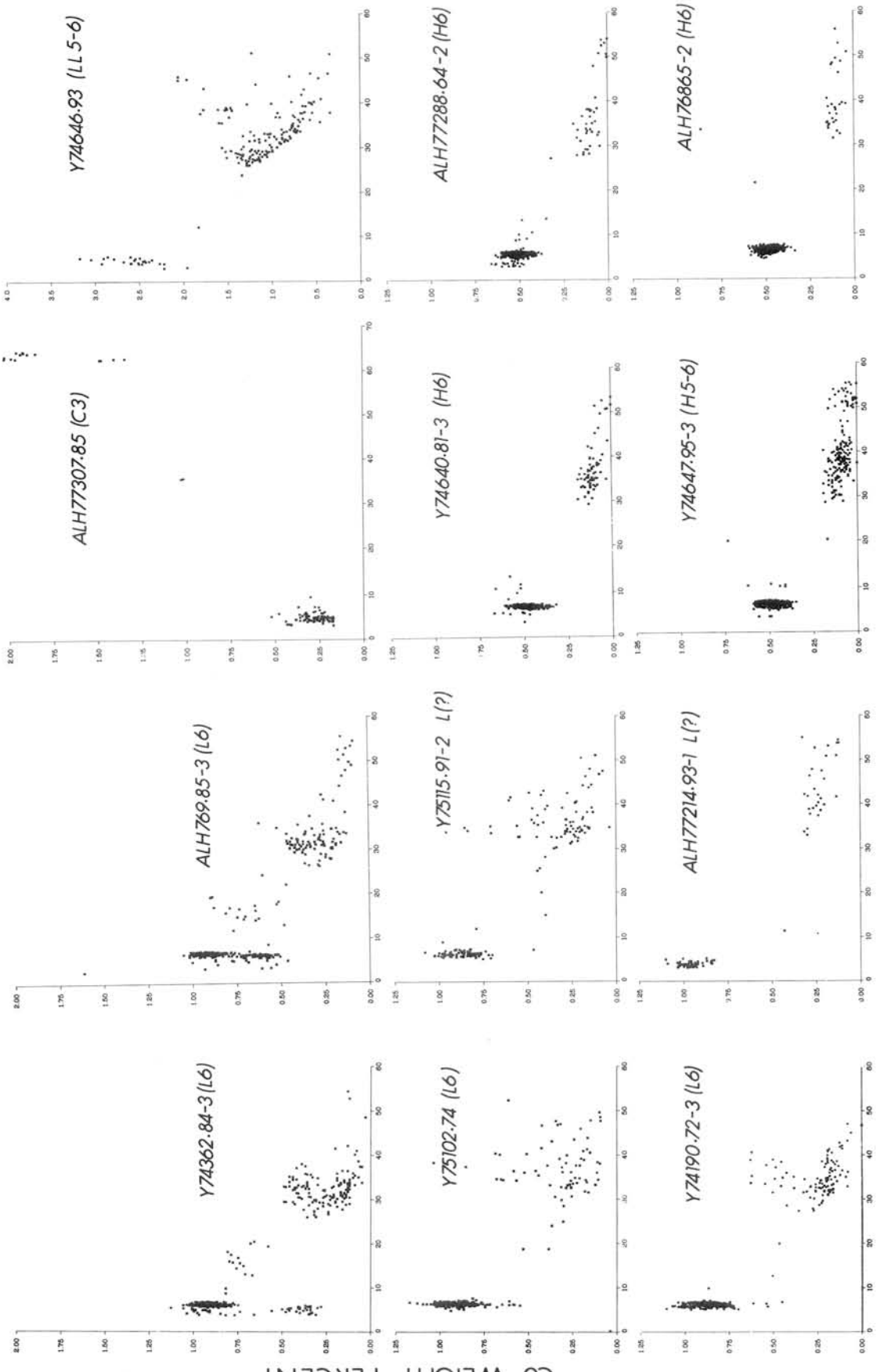
Y74646.93 (LL5-6)
ALH77288.64-2 (H6)
ALH76865-2 (H6)
ALH77307.85 (C3)
Y74640.81-3 (H6)
Y74647.95-3 (H5-6)
ALH769.85-3 (L6)
Y75115.91-2 L(?)
ALH77214.93-1 L(?)
Y74362.84-3 (L6)
Y75102.74 (L6)
Y74190.72-3 (L6)
Co WEIGHT PERCENT
Ni WEIGHT PERCENT

FIGURE 1

Friday, March 23, 1984

0945 - 1745 Presentation, Auditorium

Mineralogical characterization of matrix materials in carbonaceous chondrite Yamato-793321 and Belgica-7904 by HREM

Akai, J
Faculty of Science, Niigata University,950-21 Niigata, Japan

Matrix materials of carbonaceous chondrite containing large amount of phyllosilicate are very difficult to be identified and characterized. Their characterization is one of the most urgent and significant challenges in the study of carbonaceous chondrites to elucidate their origin. Recent high resolution electron microscopic (HREM) studies of the phyllosilicate shed light on the character of these materials (Mackinnon & Buseck,1979; Akai, 1979,1980,1982;Barber,1981). The matrix materials in Y-793321 and B-7904 were examined mainly by HREM.

General description (Textural relations)

Both specimens of Y-793321 and B-7904 supplied at first have fusion crusts. Dispersed throughout the matrix are chondrules, fragments of chondrules, irregular form inclusions (CAI?) and isolated or aggregated grains of olivine and/or pyroxenes (Y-793321 & B-7904). The ratio of these chondrules and grains etc to the matrix is slightly higher than that of Murchison or Y-74662 ,or is approximately equal (Y-793321 , B-7904 respectively). Under the microscope,slight prefered orientation of elengated olivine and pyroxene grains , and matrix materials was observed (B-7904 & Y-793321) (Fig.1). Olivines and Ca-poor pyroxenes are abundent phase, occurring as chondrules, isolated or aggregated grains (Y-793221 & B-7904). Olivine grains in both specimens have either composition near Fo_{100} or Fe-rich one with variable amounts. Pyroxene grains are also almost Fe-free type En_{100} or Fe-rich. Ca-rich pyroxenes occur as small grains along the inner wall (rim) of the irregular inclusions (CAI?) (Y-793321). The compositions of these materials are listed in Table 1.

Phyllosilicate occurrences and compositions

Phyllosilicates in Y-793321 and B-7904 are found in two different occurrences. 1) Phyllosilicates as matrix materials. Most of the phyllosilicate are present as the matrix phase. 2) Phyllosilicates filling irregular inclusions or occurring adjacent to olivine or pyroxene grain aggregate are rarely found. These may be derived by alteration . Observation by EM reveals that many small (submicron) grains are contained in the matrix of Y-793321 and B-7904. Then the compositions of the pure phyllosilicates cannot be obtained by EPMA The results of EPMA analyses are shown in Table 1. The compositions of the matrix are similar to those in other CM2 chondrites (Fuchs et al.,1973; McSween and Richardson,1977, Bunch and Change,1980, Akai, 1980,1982). Phyllosilicates coating chondrules and olivine or pyroxene grains were found. The compositions of the matrix near the fusion crusts showed slightly higher Fe contents than the other parts.

HREM,EM and AEM investigations

In the polished thin sections of Y-793321 and B-7904, the available portions as far apart as possible from the fusion crust were those 4~5 mm apart from the fusion crust. The results of HREM investigations of matrix phases of various portions in Y-793321 and B-7904 indicatd that all the phyllosilicates did not always show clear lattice resolutions but have defect structure in (001) layer structures (Y-793321, Fig.2). At the present time, the author could not confirm whether this defect structures arised from heating at the time of meteorite fall or from other phenomena prior to the fall.

However, the original shapes and textures seem to be preserved unchanged. Submicron-size grains of olivine and pyroxenes are widely distributed in the matrix of Y-793321 and B-7904 (Fig.3).They are usually not so angular but sometimes very rounded shapes. Complex surface patterns (poly ring halo -like) were sometimes found on the olivine or pyroxene grains (Fig.4 ,Y-79 3321). These patterns are similar to those found on plagioclase surface which suffered slight weathering on the earth (Tazaki,1977). These textural relations suggest the possibility that these mineral grains altered to phyllosilicates.

Phyllosilicates can be largely grouped into 3 types in shapes and crystallinity. These classifications can be evidently found especially on the specimen of Y-793321. The one is thick platy phyllosilicate (type I). The second one is very poorly crystalized type with only a few～several phyllosilicate layers in thickness(type II).The matrix phyllosilicates are mostly composed of these two types. The third one is tubular type (Fig.5). The shape of this type is very characteristic and it may be intermediate in crystallinity. AEM investigation indicated that the composition of the type I platy phyllosilicate is very Fe rich one . The three types (especially type I and II) are very different in their shapes and crystallinity. Then, these features suggest the possibility of different origins of these phyllosilicates.

Considering overall features observed to date, we can assume the possible scenario of phyllosilicate formation . A part of phyllosilicate, at least, may be formed by alteration of olivine or pyroxene grains by the reaction with aqueous or gasseous phase. Another phyllosilicates may be formed in different conditions and/or different places. Then they were mixed with other component minerals , inclusions and chondrules. The places where phyllosilicates were formed may not be restricted to some parent body but may also be solar nebula . These phyllosilicate and other minerals formed in different conditions may be mixed and accreted onto parent body (or meteorite) with prefered orientation. Then these possibilities don't reject further speculation that much more older materials from interstellar dusts may also be inducted .

References

Akai,J(1979) 23 Ann.Meet.Clay Sci. Soc .Japan Abstract,69
------(1980) Mem Nat. Inst.Poar Res. sp. Iss. 17 ,299-310
Barber,D.J.(1981) Geochem Cosmochem.Acta,45,945-970
Bunch ,T.E. and Chang S.(1980) Geochem. Cosmochem.Acta,44,1543-1577
Fuchs,L.H.,Olsen,E. and Jensen,K.J. (1973) Smithon. Contrib. Earth Sci.10,1-39
Mackinnon,D.R. and Buseck,P.R.(1979) Nature,280,219-220
McSween,H.R.Jr and Richardson S.M.(1977) Geochem.Cosmochem.Acta,41,1145-1161
Tazaki,K (1977MS) Ph.D. Thesis of Tokyo Kyoiku Univ.

Table 1 Major element composition (Y-793321 & B-7904)

	Matrix of Y-793321		Matrix of B-7904		Y-793321			
	Aver.value(10)	fusion cr.	Aver.Value(10)	fus.cr.	Diop.	Oliv	Oliv	Ca-poor pyrox
SiO_2	28.9 %	24.6	30.6	26.5	48.5	41.8	32.3	60.2
TiO_2	0.05	0.07	0.11	0.07	0.2	0.06	0.03	0.06
Al_2O_3	2.7	1.6	2.47	2.25	7.4	0.07	0.02	0.29
Cr_2O_3	0.74	0.31	0.57	0.47	0.2	1.04	0.4	0.74
FeO	38.5	51.4	31.8	46.8	0.2	1.41	45.3	1.07
MnO	0.26	0.13	0.27	0.35	0.02	0.35	0.41	0.05
MgO	14.4	14.2	18.1	17.3	16.4	54.7	22.06	37.1
CaO	0.79	0.36	1.65	0.78	26.4	0.22	0.18	0.57
Na_2O	0.91	0.41	0.57	0.46	0.04	0.02	0.04	0.0
K_2O	0.06	0.0	0.03	0.0	0.01	0.0	0.0	0.02
Total	87.3	93.1	86.2	94.9	99.37	99.67	100.74	100.1

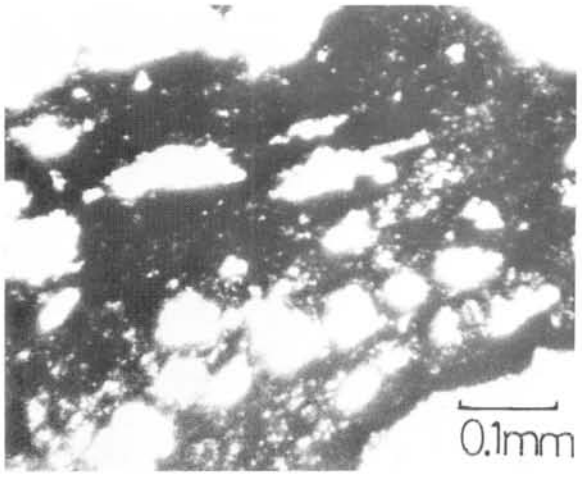

Fig.1 Optical micrograph of B-7904

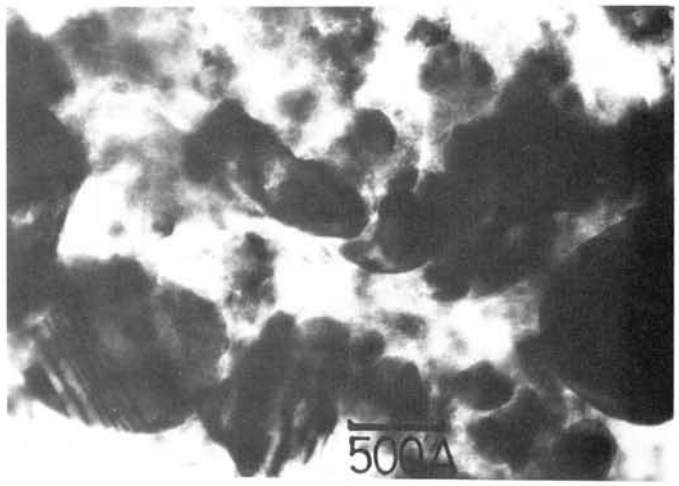

Fig.3 Electron Micrograph of matrix texture in B-7904 indicating the presence of grains with rounded shapes.

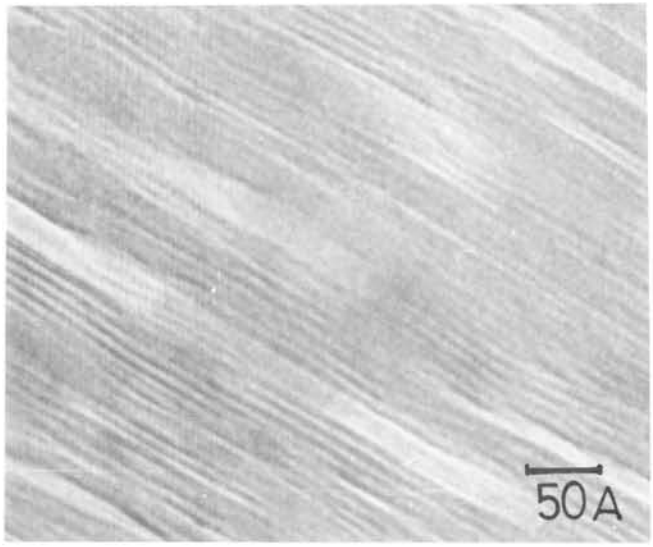

Fig.2 High Resolution Electron Micro graph of phyllosilicate in Y-79 3321 showing defect structure.

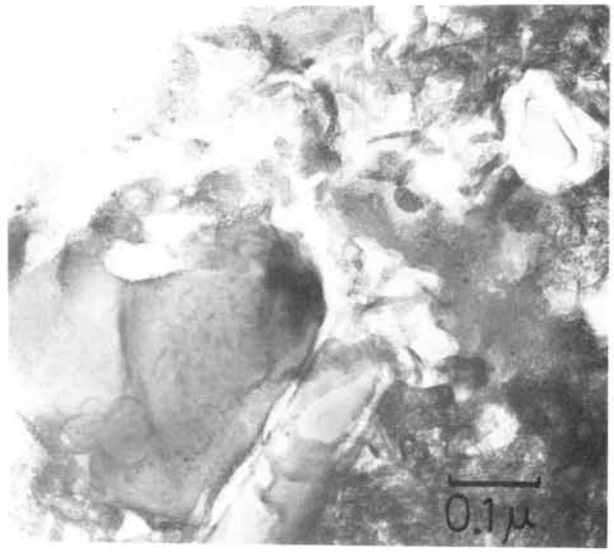

Fig.4 Electron Micrpgraph of olivine grains in Y-793321 having halo -like patterns.

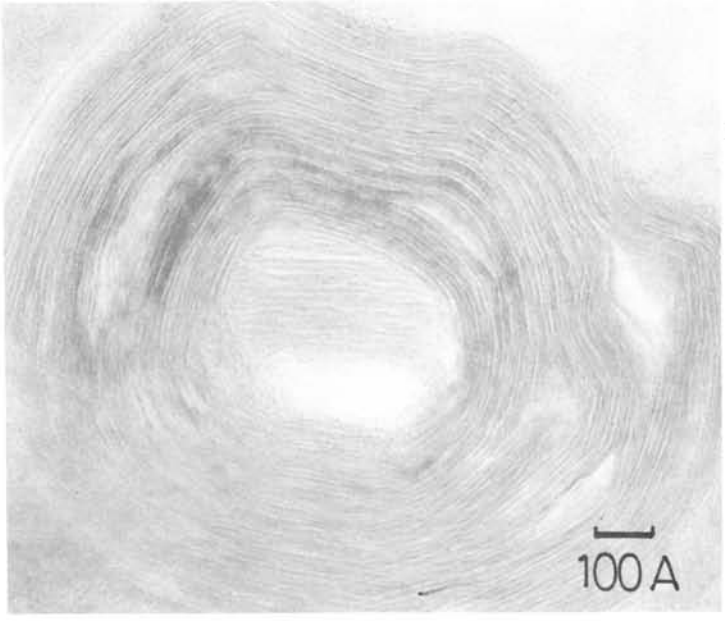

Fig.5 High Resolution Electron micrograph of tubular form phyllosilicate in the matrix of Y-793321.

26

High Resolution Electron Microscopy of Pyroxenes from Jilin and Shuangyang Chondrites

Meng Yanxi and Zhang Shuyuan
Department of Geology, Peking University, Beijing, China

Pyroxenes in Jilin and Shuangyang chondrites (H5) are mainly composed of Ca-poor pyroxenes. High resolution electron microscopy study shows these Ca-poor pyroxenes contain coherent, intimate intergrowthes of orthohombic and monoclinic bronzite. The intergrowthes are of parallel (100) planes. Although these pyroxenes are indentified as orthohombic, the emerging frequency of monoclinic parts is so high that the selected-area electron diffrection patterns contains remarkable streaks parallet to a*. The widths of the clinohombic regions are integer times of 9Å. According to P. R. Buseck et al. (1975), this indicated the complete history of these Ca-poor pyroxenes from Jilin and Shuangyang chondrites, included: precipitation of protobronzite at temperatures above 1000°C; rapid inversion to clinobronzite; sluggish inversion to bronzite in the stability field of orthopyroxenes. As a result the relationship between the Ca-poor pyroxenes in H3 and H4 chondrites (mainly monoclinic) and those in H5 chondrites (orthohombic) is promulgated, and this seems to be direct evidence supporting metamorphism pattern of chondrites.

ON THE ORIGIN OF PALLASITE

Eiichi TAKAHASHI

Institute for Thermal Spring Research, Okayama University,
Misasa, Tottori-ken, 682-02, JAPAN

Pallasite is a unique stony-iron meteorite composed dominantly of olivine and Fe-Ni metal (Mason, 1962). Cooling rate of the rock based on its very well developed Widmanstatten patterns indicates that the rock was originally formed in an interior of relatively large parent body (or bodies) that has 200 to 500 km radius (Wood, 1978; Matsui et al.,1980). The maximum experienced temperature of the rock must be higher than the metal/sulfide eutectic temperature (1270 deg.K.) and the duration of such high temperature stage must not have been longer than 5×10^3 years (Ohtani, 1983).

From its unique mineral paragenesis, pallasite is often considered to represent the core/mantle boundary of its parent planet. A tough question follows, however, that why the metal and olivine which are very different in density reside together? Considering the frequent appearance of pallasite compared with the iron-meteorites and the Ca-poor achondrites, it is difficult to assume that the rock was derived only from a thin boundary layer between the silicate-mantle and the iron-core.

During the melting studies of chondrites by the present authors, it has been cleared that olivine is the liquidus phase in at least L, LL, and C chondrites at pressures less than 5 kbar. In the temperature range above the silicate solidus, the metal-sulfide eutectic melts form numerous isolated globules (liquid droplets) surrounded by silicates.

Different from the current belief, gravitational settling of the metal/sulfide liquid droplets from the residual olivine crystals did not take place in the above melting study of chondrites. On the contrary, the silicate partial melts were segregated from the metal-olivine residues within short experimental runs.

A series of experiments have been carried out at 1600 deg.c. and 5 kbar (above the melting point of Fe but below that of olivine), in order to test the critical conditions for the metal/olivine separation with mixtures of pure Fe and San-Carlos olivine (Fo=90). No gravitational separation was observed for the mixtures of Fe/oliv=0.1 to 0.5 in volume ratio for up to 24 hours run durations.

The unique mineral assemblage of pallasite is able to explain as a residue of partial melting of a chondritic source material. In order to form the olivine/metal residue, however, a melting temperature higher than about 1400 deg.c. is necessary and the expected degree of partial melting is greater than some 50 percent. The separation of the metal and olivine, however, did not take place probably because of the relatively small metal to olivine ratio in the residues.

29－1

IRON HYDRIDE AND ORIGIN OF THE EARTH; CAN E-CHONDRITE MAKE THE EARTH?

Suzuki T., Akimoto S. and Fukai Y.*

Institute for Solid State Physics, University of Tokyo, Minato-ku, Tokyo 106
*Department of Physics, Chuo University, Bunkyo-ku, Tokyo 112

It has been generally accepted that the density of the earth's outer core is smaller by several percent than that of pure iron under corresponding pressure - temperature conditions. To explain this density deficit, dissolution of some lighter elements, such as S, O, and Si, into iron have been discussed. Recent experiments[1)2)] demonstrated that a considerable amount of hydrogen can be dissolved in iron at high pressures and temperatures, in contrast to the fact that hydrogen is scarcely dissolved in iron at normal condition. Hence, Fukai and Akimoto[3)] proposed that hydroden should be one of the most probable candidates for the lighter element in the earth's core. Further, they considered that the only possible source of hydrogen in the core should be the water in the primordial material of earth, and showed experimentally that iron and water actually react at high pressures and temperatures, to yield iron hydride and iron oxide. They argued that the produced iron hydride should melt and sink to form the earth's core, and that the produced iron oxide was dissolved in the silicate phases to form the earth's mantle. Since the source of water in the proto-earth might be the hydrous minerals in the primordial material, in the present study, we investigated the direct reaction of iron and hydrous minerals at high pressures and temperatures.

A tetrahedral-anvil type of apparatus was used in the present high pressure experiments. An intimate mixture of iron, talc and brucite was used as starting materials. A Pt-tube was used as a sample container and simultaneously as a heating element. Temperature was measured with a Pt/Pt-13%Rh thermocouple. The specimens were held at around 5 GPa and temperature ranging from 1000° to 1200° for 20 to 60 min and quenched isobarically. The recovered specimens were examined by Debye - Sherrer X-ray diffraction technique and under petrographic microscope.

Results of the present experiments are summarized in Table 1. In all the run products, FeO containing olivine and pyroxene were identified. The existence of FeO in the silicate phases indicate that the following reactions have taken place. First, talc and brucite were dehydrated to form the non-hydrous silicate and water. Then, in the second stage, water and iron react to form iron hydride and iron oxide;

$$(2/x+1)Fe + H_2O \rightarrow (2/x)FeH_x + FeO.$$

Iron hydride thus produced at high pressures is unstable at normal conditions and decomposes into iron and hydrogen. Hence we can not observe iron hydride

Table 1. Conditions and results of high-pressure and high-temperature experiments.

Run no.	Starting materials	Pres. (GPa)	Temp. (°C)	Time (min)	Run products
1	5Fe+Ta+Br	5.3	1000	60	Fe+Ol(Fa50±10)+Px(Fs15±10)
2	5Fe+Ta+2Br	5.2	1000	60	Fe+Ol(Fa55±10)+(Px)
3	5Fe+Ta+2Br	5.3	1200	20	Fe(melt)+Ol(Fa50±10)+(Px)

Abbreviations: Ta; talc, Br; brucite, Ol; olivine, Px; pyroxene, Fa; fayalite, Fs; ferrosilite.

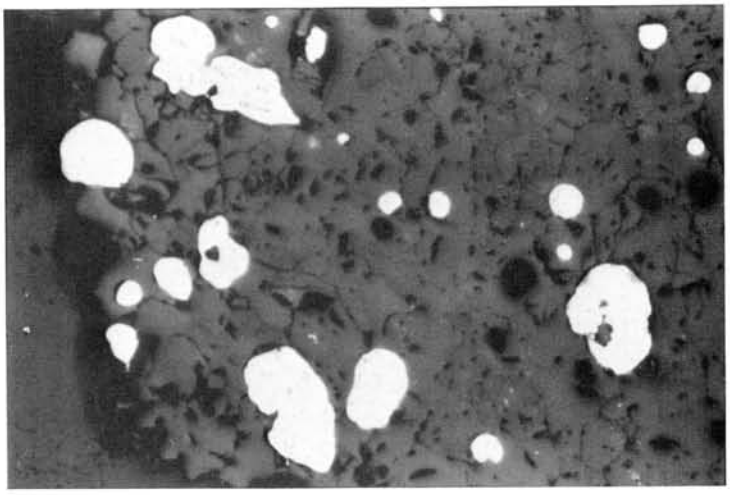

Figure 1. Photomicrograph of the recovered specimen run no.3 (under reflected light). A number of "balls of iron" are seen. Dark matrix is mainly composed of olivine. Range of view is 0.5 mm wide.

in the quenched specimen. The FeO produced in this reaction then reacts with silicate to form olivine and pyroxene.

An interesting feature was observed in run no. 3. As shown in Figure 1, a number of "spherical balls of iron" were identified under microscope. This suggests that the metallic phase was in liquid state at 1200°C. Since the melting temperature of iron at this pressure is about 1700°C[4], the melting temperature of iron may be decreased by about 500 K by possible dissolution of hydrogen or oxygen. Preliminary microprobe analysis revealed that this "ball of iron" is almost pure iron and oxygen was scarcely dissolved. Therefore, the remarkable decrease of the melting temperature of iron must be attributed to the dissolution of hydrogen, and almost all amounts of FeO, which was produced by the reaction of iron and water, enter into the silicate phases.

These experimental results indicate that if iron and hydrous minerals coexisted in the proto earth, iron hydride and FeO containing silicates were produced, and iron hydride should melt and sink to form the proto core. If the primordial material contained 1~2 wt% of water, it is sufficient to make a nessesory amount of FeO in the actual mantle. Therefore, FeO content of the primordial material may be very small. Since the oxygen isotope ratio of E-chondrite shows the fractionation trend very similar to that of the earth and moon[5], it has been expected that E-chondrite may hold the key to solve the probrem relating to the origin of the earth and moon. E-chondrite, however, scarcely contains water, and we can not expect the iron water reaction to occur in the primordial material solely composed of E-chondrite. But if water was supplied from some other materials, the reaction of iron and water could occur and provide FeO to the silicate phase. Indeed, Fukai[6] was shown that, by starting from the 9:1 mixture of E- and Cl-chondrite like materials, and considering the iron water reaction that followed, it is possible to establish a consistent picture of the evolution process of the earth.

REFERENCE

1)Antonov V.E. et al.: Script. Met., 16 203 (1982).
2)Fukai Y. et al.: Jpn. J. Appl. Phys., 21 L318 (1982).
3)Fukai Y. and Akimoto S.: Proc. Japan Acad., 59 SerB 158 (1983).
4)Strong H.M. et al.: Met. Trans., 4 2657 (1973).
5)Clayton R.N. et al.: Earth Planet. Sci. Lett., 30 10 (1976).
6)Fukai Y.: Nature in press. (1984).

30

ORIGIN OF THE MOON

Kiyoshi Nakazawa and Chushiro Hayashi

Geophysical Institute, University of Tokyo
*)Department of physics, Kyoto University

We propose a new scenario of the lunar origin, which is a natural extension of planetary formation processes studied so far by us. According to these studies, the Earth grew up in a gaseous solar nebula and, hence, the terrestrial Hill sphere was filled by a gas forming a dense primordial atmosphere. In the later stages, this atmosphere as well as the solar nebula was dissipated gradually, owing to strong activities of the early-Sun in a T Tauri stage.

We study a series of dynamical processes where a slightly unbound planetesimal is trapped within the terrestrial Hill sphere, under the above-mentioned circumstances that the gas density of the primordial atmosphere is gradually decreasing. It is clear that two conditions must be satisfied for the lunar origin: first, an unbound planetesimal entering the Hill sphere has to dissipate its kinetic energy and comes into a bound orbit before it escapes from the Hill sphere and, second, the bound planetesimal never falls onto the surface of the Earth.

The first condition is studied by calculating the orbital motion of a planetesimal in the Hill sphere, which is affected both by soalr gravity and by atmospheric gas drag. The results show that an unbound planetesimal with the lunar mass or less can be trapped in the Hill sphere with a high probability, if it enters the Hill sphere at stages before the atmospheric density is decreased to about 1/50 of the initial value.

In order to study of the second condition, the orbital change of the trapped proto-Moon is calculated under the perturbations of gas drag as well as tide. The results show that the trapped proto-Moon can survive as a satellite without falling onto the Earth if it enters the Hill sphere at stages after the density of the escaping atmosphere is decreased to about 1/5 of the initial. This condition is consistent with the trapping (first) condition.

CHEMICAL COMPOSITIONS OF YAMATO POLYMICT ACHONDRITES

Fukuoka, T. and Suzuki, E.

Department of Chemistry, Gakushuin University, Mejiro, Toshima-ku Tokyo 171.

More than 5,000 specimens of meteorites were collected on the Antarctic ice field by both Japan and U.S. teams since 1969. These collections include a large number of polymict eucrites which are typical achondrites in Antarctic meteorite collection. Most of the specimens probably fell on the ice field as meteorite shower.

In this study, in order to know the number of meteorite showers for polymict eucrites and howardited in the region of Yamato Mountains from the chemical features, the abundances of more than 20 elements in 17 samples of matrices from 1 howardite and 7 polymict eucrites have been determined by instrumental neutron activation analysis (INAA). The matrix samples were provided from National Institute of Polar Research of Japan. The samples were purified with the exclusion of small chips of clasts to eliminate chemical effect from those prior to INAA under a binocular type microscope.

The preliminary results for major chemical abundances are shown in Table 1. The chemical composition of Y790727 howardite differ from those of polymict eucrites (Table 1). In order to check the chemical homogeneity of a meteorite, the differences of chemical compositions of matrices from distant site of single meteorite will be discussed, including minor and trace chemical compositions. The comparisons of the chemical compositions of differect meteorite will be carried out subsequently to discuss the number of meteorite showers.

Table 1 Major chemical abundances in the matrices of Yamato polymict achondrites by INAA.

Sample	Wt	TiO_2	Al_2O_3	MgO	CaO	Na_2O	MnO	K	V
	mg	%	%	%	%	%	%	ppm	ppm
Y74159-103	82	0.80	10.5	9.0	11.7	0.46	0.54	450	55
Y74159-104	88	0.82	10.4	7.9	9.4	0.49	0.58	340	70
Y74159-105	92	0.51	10.6	9.2	9.5	0.46	0.59	560	74
Y790006-91	73	0.58	10.3	8.4	9.5	0.47	0.58	350	63
Y790007-97	64	0.42	-	11.5	9.2	0.50	0.58	610	91
Y790007-98	53	0.41	-	9.3	9.1	0.45	0.57	780	-
Y790007-99	52	0.42	10.1	11.4	10.0	0.45	0.57	510	66
Y790020-94	66	0.60	10.7	9.6	10.1	0.44	0.59	410	68
Y790020-95	91	0.71	11.5	10.7	9.6	0.41	0.55	420	76
Y790020-97	78	0.58	11.1	8.5	9.8	0.45	0.55	510	77
Y790113-91	77	0.70	9.9	8.6	8.4	0.47	0.59	540	76
Y790122-93	78	0.84	11.4	7.8	10.0	0.53	0.55	610	42
Y790122-94	69	0.65	11.2	9.7	9.2	0.54	0.57	370	54
Y790122-95	84	0.77	10.4	8.3	10.1	0.49	0.54	570	59
Y790727-92	75	0.48	6.4	17.5	5.0	0.26	0.54	260	96
Y790727-93	97	0.51	5.9	16.7	5.5	0.24	0.54	420	112
Y791186-91	57	0.80	10.6	8.2	9.7	0.49	0.56	520	57
Errors (%)*		10-22	1-5	3-12	3-7	1	1	10-33	4-17

* Errors for INAA are due to counting statistics.

Chemical studies on distribution of germanium and gallium in Antarctic iron meteorites

Takesi Nagata,[1] Akimasa Masuda,[2] Isamu Taguchi[3] and Yoshiaki Ono[4]

1) National Institute of Polar Research, 2) Faculty of Science, The University of Tokyo, 3) R & D Laboratories-I, Nippon Steel Corporation, 4) Electron Optics Technical and Engineering Division, JEOL LTD

I. Introduction

It is well known that some iron meteorites show high concentrations of Ge and Ga. To our best knowledge, however, a paper on the states of existence of Ge and Ga in iron meteorites is not found. We try to study segregations of Ge and Ga in this second paper of our chemical studies.[1]

II. Experimental

The Antarctic iron meteorites, mainly ALH-77263, ALH-77289 and Y-791076 were polished and analyzed by CMA[2] (Computer aided Micro Analyzer). CMA is a newly developed scanning-type analyzer which is based on the same analytical principle as EPMA. A large area sample up to 10cm square can be quantitatively analyzed in a short time. The data were fully processed and displayed on a color displayer. Up to 5 elements are simultaneously analyzed. The six elements, Ge, Ga, Ni, Co, P and S, of the above samples were analyzed using an analytical unit spot (pixel) of 4 x 4 μm and a measuring time of 0.15 sec per one spot.

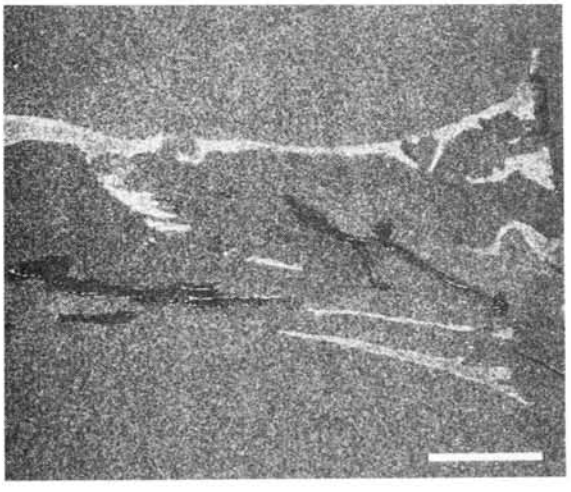

Fig.1 Distribution of Ge in ALH-77263 studied by CMA (original in colors): Analytical unit spot, 4 x 4 μm; Measured area, 1.7 x 2 mm; Scale bar, 400 μm.

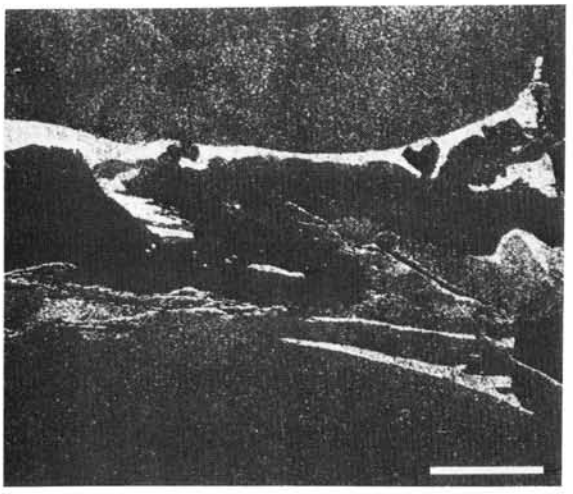

Fig.2 Distribution of Ga in ALH-77263, studied by CMA (original in colors): Analytical unit spot, 4 x 4 μm; Measured area, 1.7 x 2 mm; Scale bar, 400 μm.

III. Results

(1) Figs. 1 to 3 show the distributions of Ge, Ga and Ni, respectively, in ALH-77263 (Ni: 6.78%, Co: 0.47%, P: 0.20%, Ge: 0.0409, Ga: 0.0099), studied by CMA. Table 1 shows the results of quantitative analysis of ALH 77263 by CMA. Seven analyzed spots (cf. Table 1) are marked in Fig. 3. Figs. 1 to 3 reveal that Ge and Ga are almost the same in distribution and much related with Ni distribution. Table 1 also shows the above-mentioned similarity, investigated by spot analysis. No.1 and 2 are the spots where Ge, Ga and Ni are in lower concentrations. Contractingly, No.3 and 4 show that Ge and Ga concentrations are higher in taenite of high Ni concentration. However, Figs. 1 and 3 reveal that taenite does not always contain higher concentrations of Ge and Ga. At the spots, No.5 and 6, phosphide is located and the Ge and Ga concentrations are lower. At the spots No.7, sulphide is found and the concentrations of the two elements are lower.

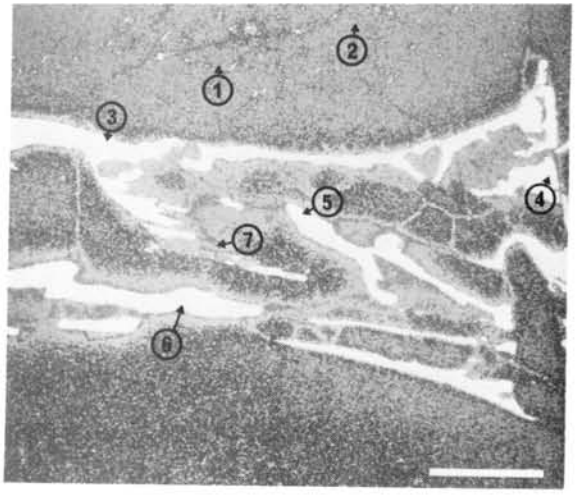

Fig.3 Distribution of Ni in ALH-77263, studied by CMA (original in colors): Analytical unit spot, 4 x 4 μm; Measured area; 1.7 x 2 mm; Scale bar, 400 μm

(2) Chemical studies were also conducted on ALH-77289; Y-791076 and the other Antarctic iron meteorites. The similar tendencies of Ge and Ga segregation were found in ALH-77289. However, the similar tendencies were not found in Y-791076 and the others because of the low concentration of the two elements.

Table 1 Quantitative analysis of the spots marked in Fig. 3

(wt. %)

No.	Ge	Ga	Ni	Co	P	S	Fe
1	0.046	<0.002	6.89	0.366	0.068	<0.002	92.63
2	0.041	0.012	6.48	0.405	0.107	<0.002	92.95
3	0.079	0.065	34.68	0.090	0.011	<0.002	65.08
4	0.093	0.043	34.86	0.067	0.005	<0.002	64.93
5	0.002	<0.002	33.52	0.113	15.71	0.002	50.65
6	0.006	0.008	33.86	0.085	15.85	0.002	50.18
7	<0.001	<0.002	0.63	0.046	0.005	30.92	68.39

References

1) T. Nagata, A. Masuda and I. Taguchi: Memory of National Institute of Polar Research, Special Issue, No.30 (in press)
2) I. Taguchi, H. Hamada and M. Kama: Lecture at the Annual Meeting of Japan Institute of Metals (November, 1981)

UNUSUAL METAL PHASES IN THE TUXTUAC LL CHONDRITE

Mireille Christophe Michel-Levy, Michel Bourot-Denise
Laboratoire Minéralogie-Cristallographie associé au CNRS - Paris VI
Jacques Danon, Rosa B.Scorzelli, Isabel Souza-Azevedo
Centro Brasileiro de Pesquisas Fisicas, Rio de Janeiro

The Tuxtuac stone is a LL5 chondrite presenting well delineated chondrules which evolved in a gaseous medium. This is indicated by the great abundance of intra and intercrystalline voids that can be observed as irregular vugs, bubble-like holes or negative crystals. The metal phases showing unexpected features have been carefully investigated.

The Mössbauer spectrum of the separated metal fraction of Tuxtuac is unusual when compared with those of other chondrites[1]. It indicates the presence of at least two Ni-Fe alloy phases, a major one ($\sim$ 85%) corresponding to a Ni rich taenite ($\sim$ 40%) and a smaller proportion ($\sim$ 15%) of the Fe-Ni 50-50 ordered phase (tetrataenite). These proportions of taenite and tetrataenite roughly correspond to those optically observed in polished sections of the chondrite.

Scanning electron microscopy and microprobe analysis show the presence of a major Ni phase with 38% Ni associated to a 50% Ni phase in smaller proportions. The phases are not intermixed but form regions with dimensions up to hundred of microns, as is illustrated in figure 1.

The X-Ray diffraction of the metal phase yield, rather unexpectedly, a single parameter for both phases, with value $a_o = 3.589 \pm 0.001$ Å. This is smaller than the value corresponding to a 38% Ni taenite ($a_o = 3.596 \pm 0.001$Å) and larger than that of tetrataenite ($a_o = 3.582 \pm 0.001$ Å).

The existence of a 38% disordered Ni-Fe alloy with tetrataenite has been assumed to occur in the cloudy zone of some zoned taenites.[2] . However, in the case of Tuxtuac, both phases are present as large domains, a fact which remains unexplained at present.

1 - J. Danon, R.B.Scorzelli, I.Souza Azevedo, M.Christophe-Michel-Levy, Nature, 281, 469 (1979).

2 - J.F.Albertson, J.M.Knudsen, N.O.Roy-Poulsen, L.Vistisen, Phys.Scripta 22, 171 (1980)

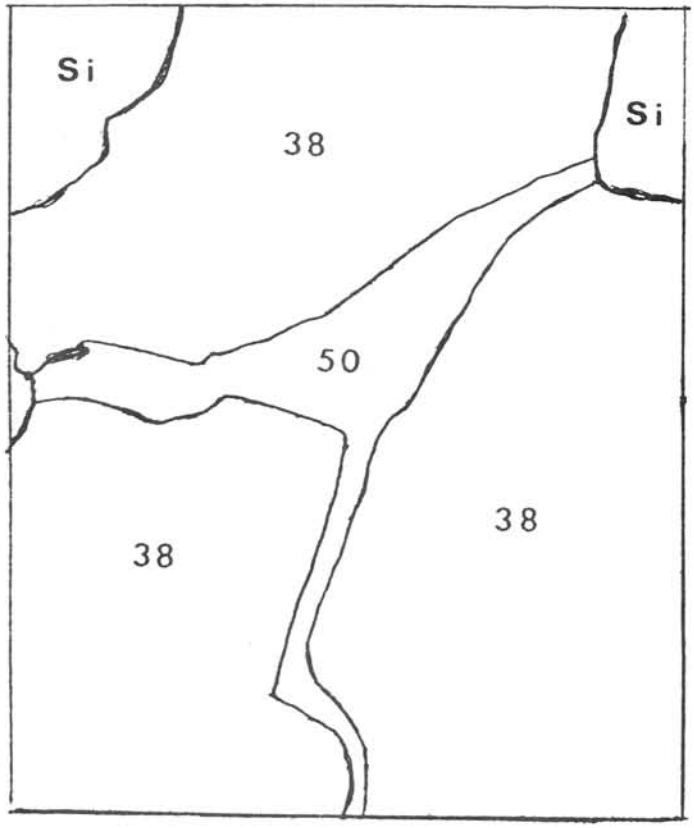

X5000

Fig. 1

34－1

Precise determination of REE, Ba, Sr, Rb, K, Ca and Mg abundances in the individual chondrules of H-chondrites

Y.Nishikawa[#], N.Nakamura[#] and R.Hutchison[@]

Department of Earth Sciences, Faculty of Science Kobe University

@ Department of Mineralogy, British Musium

In order to examine the distribution of trace elements in H-chondrites, we have determined the concentrations of trace, minor and major elements in 27 chondrules and 4 matrices from 3 chondrites (Tieschitz (H3), Jilin (H4), Allegan (H5)) whose metamorphic grades are different, together with the analysis of trace elements in the whole rock of Antarctic H-chondrites (Y-74371, -74155, -74492 and -790986).

Trace elements (REE, Ba, Sr, (K) and Rb) and some major elements (Ca and Mg) were analysed precisely by I.D. methods. On the other hand the abundances of 12 major and minor elements were determined by EPMA.

The results are shown Fig.1(a),(b),(c), Fig.2 and Table 1. Based on the chondrite-normalized REE patterns, all the chondrules are divided into 3 groups (group A,B,C): group A has a relatively high REE abundance with no fractionation as already noticed by Gooding et al. (1980), group B has a light-REE depleted pattern with a gradual increase toward heavy-REE and group C has a downward concave pattern with a remarkable positive Eu anomaly (Fig.1(a),(b),(c)).

Tieschitz (H3) has only group A chondrules. On the contrary Allegan (H5) has group B,C chondrules. All three groups are found in Jilin (H4). Because REE is expected to be redistributed among the constituent minerals of equilibrated chondrules (type 4,5), it is important to investigate the relationship between REE and the mineral compositions in chondrules. For this purpose the normative mineral compositions are shown in Table 1.

REE patterns of group B,C chondrules are qualitatively explainable assuming the solid/liquid partition coefficients of

minerals if REE is redistributed among the constituent minerals under the equilibrium condition. Moreover, the clear correlation between Sm and Ca (Fig.2), and the normative mineral compositions observed in group B,C (Table 1) suggest that REE patterns of these groups are mainly controlled by Clinopyroxenes (Nishikawa and Nakamura, 1983). But REE patterns of group A chondrules in Jilin and Tieschitz can't be explained from the normative mineral compositions. It is worth noting that the Sm-Ca trend of Jilin group A is distinctly different from the group B,C correlation line, even from group A of Tieschitz.

REE in group B,C chondrules is considered to have been lossed from chondrules to matrix as a result of the thermal metamorphism, but such an effect is not seen for group A of Jilin. The group A chondrules of Jilin are considered to keep some primitive features but to have been subject to more or less thermal effects.

It is remarkable that all the Tieschitz chondrules analysed follow a steep Sm-Ca correlation line. Furthermore, interestingly the data of Sm and Ca from Allende (C3) chondrules are plotted on this line. In view of the fact that REE enriched chondrules (2,3,4) have higher contents of Ca, Al and Ti, it may be possible that these chondrules contain similar, high REE-carried component(s), though further detailed examinations would be required.

References

Gooding J.L., Keil K., Fukuoka T. and Schmitt R.A.
Earth Planet. Sci. Lett. 50, 171-180, 1980

Nishikawa Y. and Nakamura N.
Abstract (in Japanese) presented at the Annual Meeting of the Geochemical Society of Japan, 41-42, 1983

Fig.1(a)

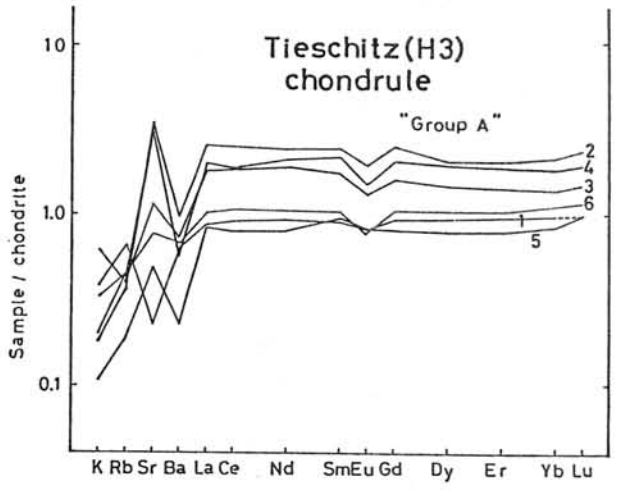

Fig.1(b)

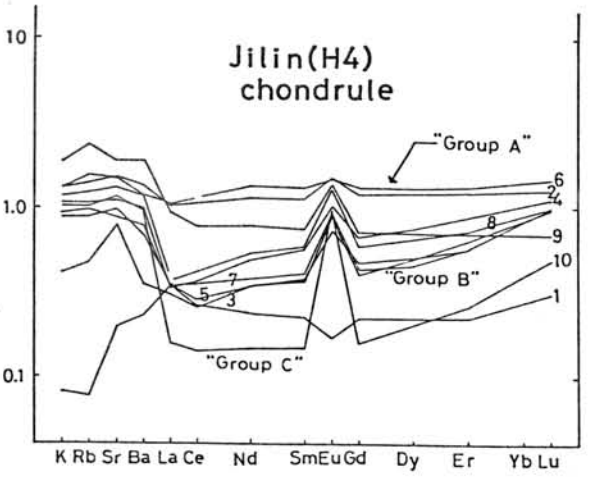

Fig.1(c)

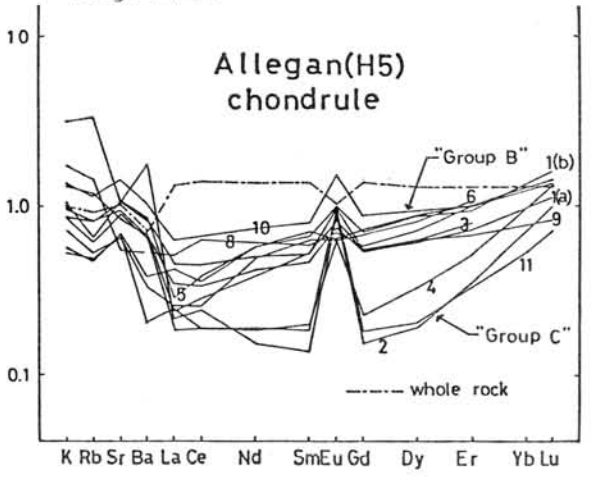

Fig.2

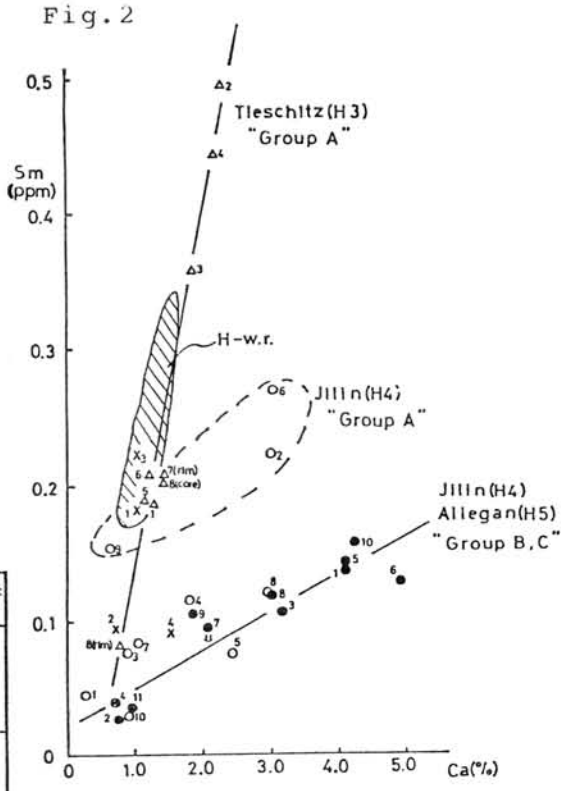

Table 1

REE pattern - Mineral comp.(Norm)

	type 3	type 4	type 5	Σ Di#
Group A	Ol, Opx Cpx,(Pl)$	Ol, Opx Cpx, Pl		No
Group B		Ol, Opx Cpx, Pl		O.K
Group C		Ol, Opx (Cpx)@, Pl		O.K

$: calculated only as norm. mineral

@: less abundant compared to Group B

#: an index whether REE patterns are explained by the conbination of the partition coefficients of constituent minerals or not

Neutron Activation Analysis of Rare Earth Elements for Some Meteorites including Antarctic Meteorites

Mitsuru Ebihara

Dept. of Chemistry, Gunma University, Maebashi, Gunma 371

Ten of the rare earth elements (REE) (La, Ce, Nd, Sm, Eu, Gd, Tb, Tm, Yb and Lu) were measured for 10-50 mg of meteorite samples by radiochemical neutron activation analysis.

Meteorite specimens, along with REE composite standard prepared from individual REE reagent, Gd standard and Eu monitor were irradiated in a flux of 3.5 x 10E13 $n/cm^2/sec$ for 6 to 265 hours at the Japan Atomic Energy Research Institute. After an appropriate cooling interval, meteorite samples were fused with sodium peroxide and sodium hydroxide in Zr crucibles. REE were precipitated as a hydroxide form with other elements such as Sc and Fe. Hydroxide precipitates were dissolved in a minimum amount of conc. HBr and loaded onto cation exchange column resin (sieved Dowex 50W-X8, 200-400 mesh resin) which had been conditioned with 6.5 M HBr. All of the REE (>99%) were eluted with the first ten column volumes of 6.5 M HBr, whereas most of the Sc (>95%) stayed on resin bed. The REE eluents were dried on a hot plate. REE were separated from Fe by adding HF. REE fluorides were dissolved in conc. nitric acid and boric acid and REE were finally precipitated as REE oxalates. Chemical yields were determined by reactivation of the precipitate of REE oxalate. The details of chemical procedure will be seen elsewhere.

A part of the results are listed in Table 1 and their Cl-normalized patterns are illustrated in Fig. 1. Entirely flat patterns are observed for three enstatite chondrites studied here. The REE abundances in the Indarch chondrite are somewhat lower than those for the other two chondrites, which seem to be in good coinsidence with the relatively low abundance of Ca in this meteorite.

Table 1. REE abundances in three enstatite chondrites (in ppm).

Meteorite	La	Ce	Nd	Sm	Eu	Gd	Tb	Tm	Yb	Lu
Abee	0.285	0.863	0.588	0.206	0.068	0.292	0.046	0.031	0.209	0.033
Indarch	0.198	0.503	0.403	0.138	0.046	0.188	0.026	0.023	0.145	0.023
Qingzhen	0.273	0.740	0.578	0.186	0.063	0.239	0.037	0.031	0.194	0.031

Fig. 1. Cl-normalized REE patterns for three enstatite chondrites.

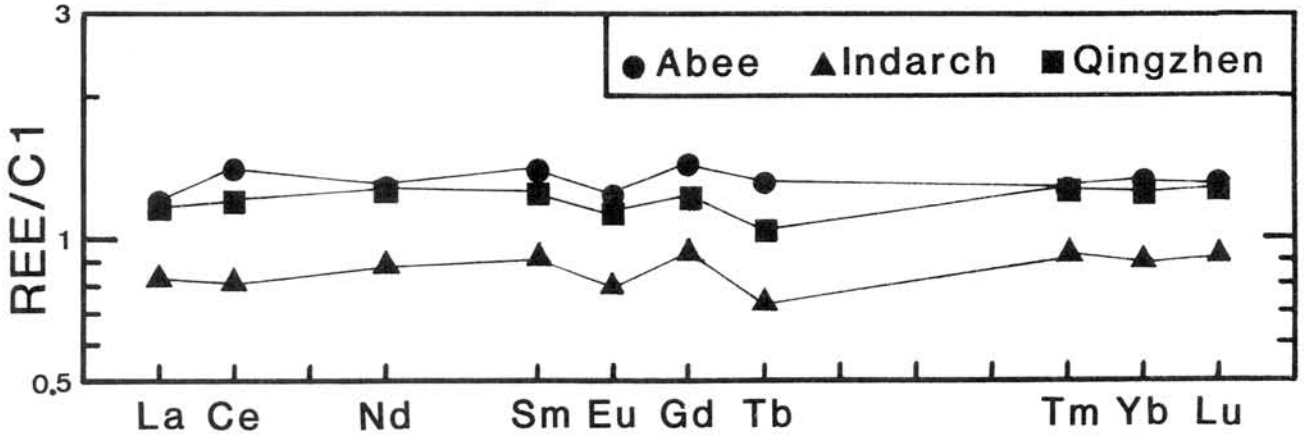

Studies of REE Abundances and Major Element Composistions of KAPOETA, JUVINAS and RODA Achondrites

Akimasa MASUDA, Kazuya TAKAHASHI and Hiroshi SHIMIZU
Department of Chemistry, The University of Tokyo

We determined REE abundances and major element compositions in mineral separates of Kapoeta (howardite), Juvinas (eucrite) and Roda (diogenite). Further we compared mineral fractions each other. The mineral separation was carried out with heavy liquids (bromoform and methylene iodide). Concentrations of major elements were determined by electron probe micro analyzer for each grain in each mineral fraction and REE were measured by mass spectrometric isotope dilution method.

For the fractions corresponding to plagioclase ($d<3.1$), their REE patterns and major element compositions are in good agreement between Kapoeta and Juvinas (Fig. 1). Therefore the plagioclase in Kapoeta can be regarded as originally identical with that in Juvinas. Fig. 2 shows the major element compositions of the fractions corresponding to pyroxene ($d>3.3$). As shown in Fig.2, there are two groups of pyroxenes in Kapoeta, group (A) with Juvinas-like compositions and group (B) corresponding to orthopyroxene.The group (B) has a wide range in composition, while the pyroxene in most diogenites (except Y-75032) has a narrow range in chemical composition ($Mg_{72-76}Fe_{22-26}$). So there is little similarity between the group (B) and diogenites.

Fig. 3 shows the REE patterns of these fractions comprising pyroxene, in Kapoeta and Juvinas. The group (A) (see Fig. 2) in Kapoeta is assumed to have an equivalent REE pattern to the sum of the pyroxene fractions in Juvinas. On this assumption, it is possible to calculate the REE pattern corresponding to the group (B) in Kapoeta from the consideration of the relative amount (presumably, 1.6 to 2.4) of pyroxene to plagioclase.

Fig. 4 shows the range of the REE patterns corresponding to the group (B) calculated by the above assumption and the REE patterns of Roda (bulk and pyroxene fraction). This estimated pattern seems to be similar to Roda, but major element compositions of group (B) are different from pyroxenes in Roda and other diogenites studied thus far. In spite of their narrow composition range, the diogenites are known to show the strikingly wide REE variation for absolute concentration and for

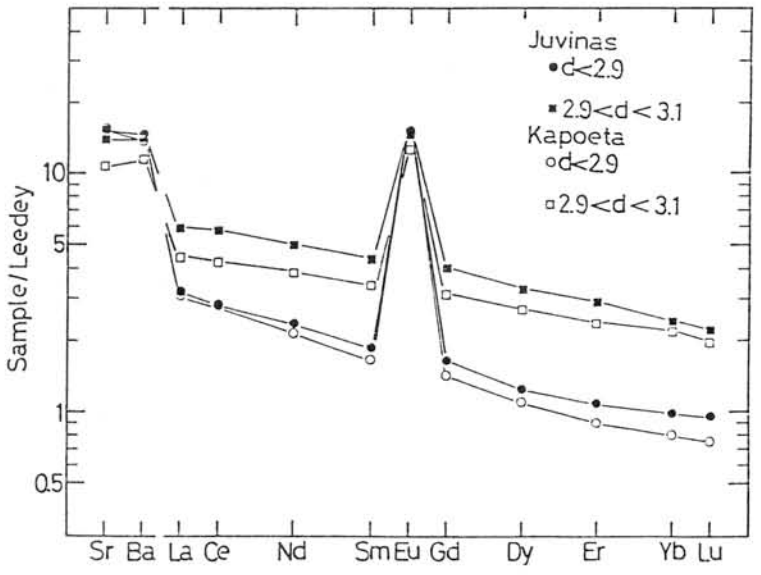

Fig. 1. The REE patterns of the fractions corresponding to plagioclase.

mutual abundance ratio. Then the group (B) composed of orthopyroxene in Kapoeta seems to be different from the known diogenites, based on the comparison of their REE patterns and major element compositions.

On the other hand, there is a clast composed of orthopyroxene in Kapoeta. Major element composition of this clast is uniform ($Mg_{74}Fe_{24}$) and close to the diogenites. Further the REE pattern of this clast is similar to one of the typical diogenites, specifically the Johnstown meteorite.

From these observations and estimations, we might conclude as follows:

(1) Kapoeta cannot be interpreted as a simple mixture of eucrite and diogenite, and group(B) in Kapoeta suggests the existence of the material intermediate between eucrite and diogenite, which might suggest the existence of originally howarditic layer.

(2) Diogenitic clasts are found as a rather minor ingredient in Kapoeta and perhaps they are essentially different from the group (B) (see Figs. 2 and 4) in Kapoeta.

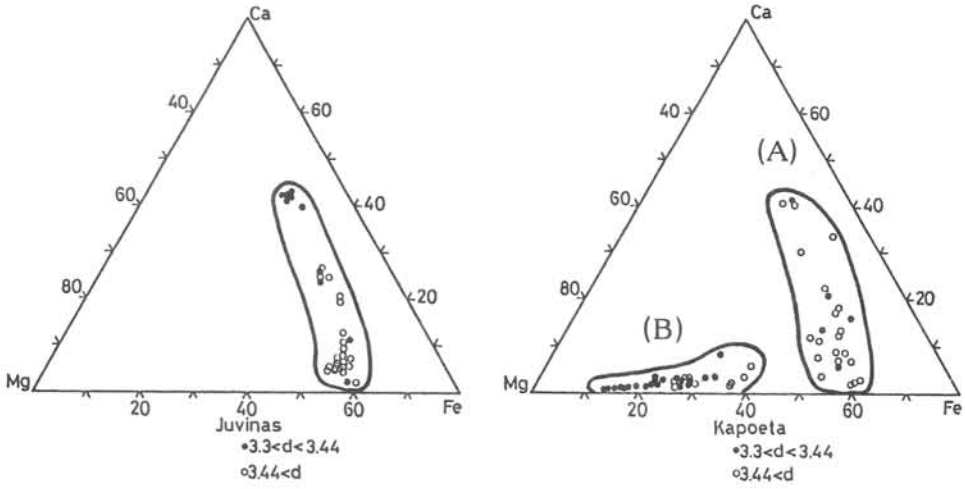

Fig. 2. The major element compositions of the fractions corresponding to pyroxene in Kapoeta and Juvinas.

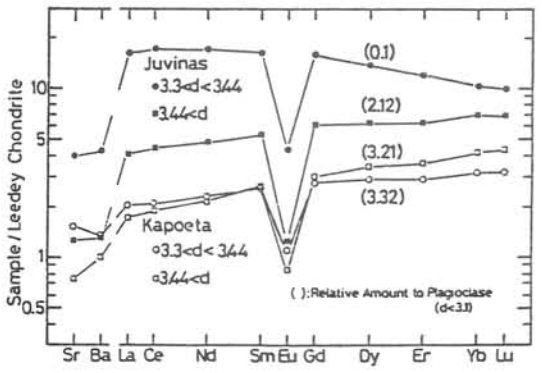

Fig. 3. The REE pattern of the fractions corresponding to pyroxene.

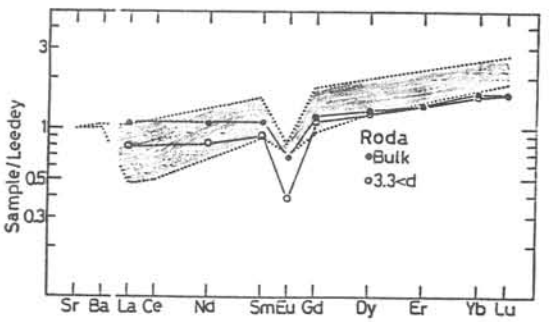

Fig. 4. The estimated range of the REE patterns corresponding to the group (B) (shaded) and Roda

AMINO ACIDS, CARBON AND SULFUR ABUNDANCES IN ANTARCTIC CARBONACEOUS CONDRITES

E. K. Gibson, Jr.*, J. R. Cronin**, R. K. Kotra***, T. R. Primas**, C. B. Moore**
* SN4/NASA JSC, Houston, TX 70058
** Dept. of Chemistry, Arizona State University, Tempe, AZ 85281
*** LEMSCO, NASA-JSC, Houston, TX 77058

Carbonaceous chondrites are the only natural source of prebiotic molecules available for study. The first unambiguous evidence for amino acids of extraterrestrial origins was obtained for the Murchison CM carbonaceous chondrite. Until the recovery of the meteorites from Antarctica, the number of available carbonaceous chondrites for study was small. The relatively cold, dry and sterile environment of the Antarctic may have been a fairly protective environment for the storage of the fragile carbonaceous chondrites. Gibson and Andrawes (1980) showed that the abundances of carbon and sulfur for numerous Antarctic meteorites have not been significantly altered by weathering processes operating in the Antarctic specimens prior to recovery. The purpose of this contribution is to report on the recent total carbon and sulfur abundances along with amino acid measurements made on three carbonaceous chondrites recovered in the Yamato and Belgica Mountains of Antarctica by Japanese expeditions.

The three samples (Y-793321, Y-791824, and B-7904) have been classified as CM carbonaceous chondrites by examination of hand specimens and thin sections by H. McSween (1983, oral communication) and Yanai (1982). The specimens had been handled in a clean manner since time of collection. Samples were processed in the JSC Curatorial Facility by Yanai prior to allocation. Total carbon and suflur abundances were carried out using the procedures of Moore et al. (1970) and Gibson and Moore (1974). Amino acids were analyzed using the ion-exchange chromatographic methodology described previously by Cronin and Hare (1977). Total carbon and sulfur abundances for the three samples are given in Table. 1.

Table 1

Sample Number	Carbon, wt.%	Sulfur, wt.%
Y-791824	1.390 ±0.010	3.531 ±0.052
Y-793321	1.780 ±0.030	3.623 ±0.032
B-7904	0.972 ±0.010	5.037 ±0.015

The carbon abundances for the Y-791824 and Y-793321 chondrites are similar to values observed for other CM chondrites from Antarctica (Gibson and Andrawes, 1980) but the B-7904 CM chondrite is depleted in carbon relative to other CM chondrites previously measured. The carbon abundances for the B-7904 chondrite are more similar to C3 chondrites. The sulfur abundances for the Y-791824 and Y-793321 chondrites are similar to values measured for CM chondries (Gibson and Andrawes, 1980), but the sulfur abundances for the B-7904 samples (5.037%) are like those found for C1 carbonaceous chondrites. The petrographic examination of this sample

indicates that a higher proportion of matrix is present than in most chondrites of this type. Perhaps we are noting one of the more unusual CM chondrites because its carbon and sulfur abundances are certainly not typical of other CM members of this group of carbonaceous chondrites.

Amino acid analyses of the three carbonaceous chondrites were carried out with acid hydrolyzed water extracts. The surprising general result was that, in contrast with earlier analyses, only trace amounts of amino acids were found. The results are unusual in that the three samples were very friable, intensely black materials, and appeared to be typical CM chondrites. CM chondrites have consistently been found to contain amino acids, even in the case of specimens with terrestrial ages exceeding 100 years (Cronin and Pizzarello, 1983) and in other Antarctic CM chondrites with greater terrestrial ages (Kotra, 1981; Cronin et al, 1979). Sample Y-791824 contains glycine at a concentration of about 2 nmole g^{-1} and alanine and α-aminoisobutyric acid at <1 nmole g^{-1}. The Murchison meteorite contains these amino acids at about 50 to 100 times these concentrations. Earlier analyses of the Antarctic CM meteorites Yamato 74662 and Alan Hills 77306 indicated that they contained 4-20 times the amounts here for the same amino acides. The ion exchange chromatograms also contained a rather large peak with a retention time about that of E-amino caproic acid. This identity needs to be confirmed by mass spectrometry. The B-7094 CM chondrite did not have indigenous amino acids at the concentration levels (less than 1 nmole g^{-1}), similar to the results obrained for Alan Hills-77307, type C3 (Kotra, 1981). Typical C3 chondrites usually contain only a trace amount of the indigenous amino acids.

From the analytical results, is it possible to say that the CM condrites from the Yamato and Belgica region have experienced liquid water prior to collection and analysis? CM chondrites are porous, and soluble organic compounds might well be leached under such circumstances. The total carbon values (1.4, 1.6 and 0.9%) are low and consistent with this possibility. Assuming a soluble organic compound content of 30 percent of total carbon (70% of typical CM chondrites carbon is insoluble) allows the calculation of an original total carbon content of about 1.9, 2.3 and 1.2%, values within the normal range for CM chondrites. However, it must be clearly stated that the number of quantitative organic analyses on CM meteorites is small and conclusions with regard to water activity may be premature. The Mighei (total carbon 2.5-2.6%) contains about 40 nmoles g^{-1} total amino acids which is comparable to the Alan Hills-77306 (C= 1.3%) and Nogoya (C= less than 1%). Other water soluble organic molecules such as carboxylic acids have to be studied.

Thus, the total carbon, sulfur, and amino acid analyses of three more Antarctic carbonaceous meteorites have provided some surprising results. Exposure to liquid water in the Antarctic could conceivably explain the observed depletions. A more exciting possibility is that we may be looking at a subgroup of the CM type meteorites. More light may be shed on this possibility if other chemical and petrologic data are viewed together with the data discussed here.

References:
Cronin J. R. and Hare, P. E. (1977) Anal. Biochem. 81, 151.
Cronin J. R. and Pizzarello S. (1983) Adv. Space Res. 3, 5-18.
Cronin J. R. et al. (1979) Science 206, 335-337.
Gibson E. K. Jr. and Andrawes F. F. (1980) Proc. 11th Lunar Planet Sci. Conf. 1223-1234.
Gibson E. K. Jr. and Moore G. W. (1974) Proc 5th Lunar Sci. Conf. 823-837.
Kotra R. K. (1981) Ph. D. Dissertation, Univ. of Maryland.
Moore C. B. et al. (1970) Proc. Apollo 11 Lunar Sci. Conf. 1375-1382.
Yanai, K. (1982) Meteorite News. 1, 26 pages. National Instit. of Polar Res. Tokyo.

SEARCH FOR AMINO ACIDS INDIGENOUS TO THE YAMATO-793321 AND BELGICA-7904 CARBONACEOUS CHONDRITES

SHIMOYAMA, A. and HARADA, K.
Department of Chemistry, University of Tsukuba
Sakura-mura, Ibaraki 305

We have examined for amino acids of the exterior and interior samples of C2 carbonaceous chondrites, the Yamato-793321 and the Belgica 7904. These samples were pulverized and refluxed with water for the extraction of amino acids and their precursors. The water extracts were hydrolyzed and processed further for analyses by an amino acid analyzer and by a gas chromatograph.

Amino acids found from the hydrolyzed water extracts of the two chondrites were aspartic acid, serine, glycine, alanine and β-alanine, and their quantities were very small as determined by the amino acid analyzer. The two most abundant amino acids are serine and glycine, each amounting ca. 300 pico moles per gram chondrite sample. Although these abundances are about three times more than those found in the procedural blank, it is not clear whether the amounts standing over the blank are of indigenous amino acids. However, the presence of β-alanine, though very minor(ca. 50 pico moles per gram sample), indicates that this amino acid is indigenous, since β-alanine is non-proteinaceous and that the compound was not detected in the procedural blank.

Attempts were made using the gas chromatograph to examine the optical isomers of the amino acids found from the water extracts. Minor peaks were observed at the retention times of D,L-alanine, D,L-valine and D,L-aspartic acid beside glycine for the Yamato-793321 samples. Also were found very small peaks at L-alanine and glycine for the Belgica-7904 samples. No conclusive evidence was obtained as to indigenous nature of the amino acids from peaks on the chromatograms.

Carbon analysis showed averages of 1.66% for the exterior and 1.69% for the interior samples of the Yamato-793321, and of 1.13 % for the exterior and 0.88% for the interior samples of the Belgica-7904. The Yamato-74662 has 1.51% carbon(Gibson and Yanai, 1979) which is about same as those for the Yamato-793321. However, the content of amino acids of the Yamato-793321 is about 100 times less than that reported for the Yamato-74662(Shimoyama et al., 1979). Further, the abundances of amino acids of those two C2 chondrites are less than, or nearly same as, that reported for the C3 ALHA-77307(Moore et al., 1981). We have no answer to the present finding that the two C2 carbonaceous chondrites contain such small quantities of amino acids. On the other hand, from the comparative examination of the exterior and interior samples, we found that the terrestrial contamination of amino acids to the two carbonaceous chondrites are at most at the level of subnamo moles, which is probably the lowest detection level of amino acids from this kind of samples.

STUDIES ON ORGANIC COMPONENTS IN CARBONACEOUS CHONDRITES, ALLENDE, ALH-77307, AND Y-74662, BY DIRECT PYROLYSIS

Murae, T., Masuda, A., and Takahashi, T.
Department of Chemistry, Faculty of Science, University of Tokyo, Bunkyo-ku, Tokyo 113

The organic components of a carbonaceous chondrite Allende (C3) and two Antarctic carbonaceous chondrites Y-74662 (C2) and ALH-77307 (C3) have been investigated by direct pyrolysis using Curie point pyrolyser (Japan Analytical Industry Co., LTD: Model JHP-2) connected to GC (Shimazu 7A-PF, column: 25m x 0.2 mm i.d. open tubular fused silica column, wall coated with silicone OV-101, detector: FID) or GC-MS (JEOL JMS-D300 equippted JMA-2000 mass data analysis system: the same column as for GC was inserted into ionization chamber directly).

Fig. 1 shows the outline of the system used for the analysis. A powdered sample of a meteorite wrapped with pyrofoil was placed in the pyrolysis system and heated at 160 ^{o}C for 20 min in the stream of nitrogen (GC) or hellium (GC-MS) befor pyrolysis in order to remove the volatile compounds which might be adsorbed on the surface of the meteorite in terrestrial enviroment and the gas was exhausted through a valve situated at the connector between the carrier line and the column. Pyrolysis was done for 3 sec (it has been cofirmed that 3 sec is enough for complete pylolysis) and in 1 sec after pyrolysis the exhaust valve was closed in order to introduce the pyrolized products into the analyzing column.

Pyrolysis was carried out at various temperature and some of the results were shown in fig. 2. The most effective pyrolysing temperature was about 700 ^{o}C for all meteorites. As can be seen in fig. 3, the results of pyrolysis are reproduceable at the same pyrolysing temperature.

The results of pyrolysis showed that (1) each of three meteorites has the different chromatographic pattern (fig. 4), (2) ALH-77307 produces very few compounds which have middle or high boiling tempera-ture and most of the products are very volatile, (3) compared with Y-74662, three times amount is necessary for Allende to yield similar chromatographic intensity and this fact seems to reflect the contents of carbonaceous compounds, and (4) according to mass chromatographic analyses and inspection of the mass spectrum of each peak, the main components of the pyrolysis products of Allende and Y-74662 are extremely different and in contrast with Allende which produces aliphatic hydrocarbons mainly, Y-74662 affords aromatic compounds as main components excepting naphtalene which was observed as an intense peak in all cases (fig.5 and 6).

Although precise investigations on the results of the pyrolyses are under way, on the bases of the above findings we consider that the processes responsible for carbonaceous compound formation in the solar nebula are different among these three carbonaceous chondrites, a fact which might reflect the difference in the physico-chemical conditions in the solar nebula.

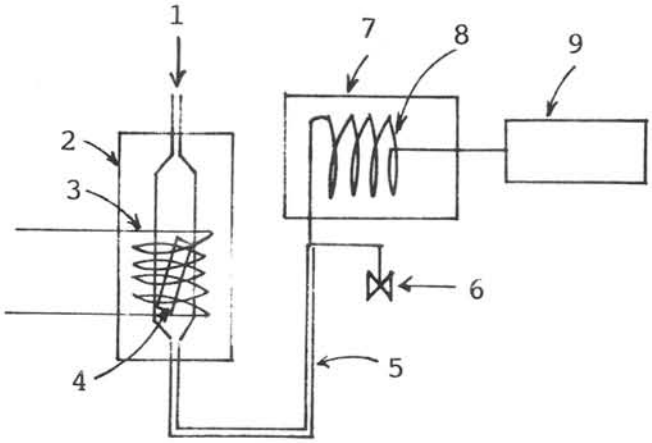

Fig. 1. Outline of the system of the pyrolysis.
1;Carrier gas
2;Oven for preheating
3;High frequency coil
4;Curie point pyrofoil
5;Carrier line, heated at 220 °C
6;Exhaust valve
7;GC oven
8;Capillary column
9;Detector (FID for GC, mass spectrometer for GC-MS)

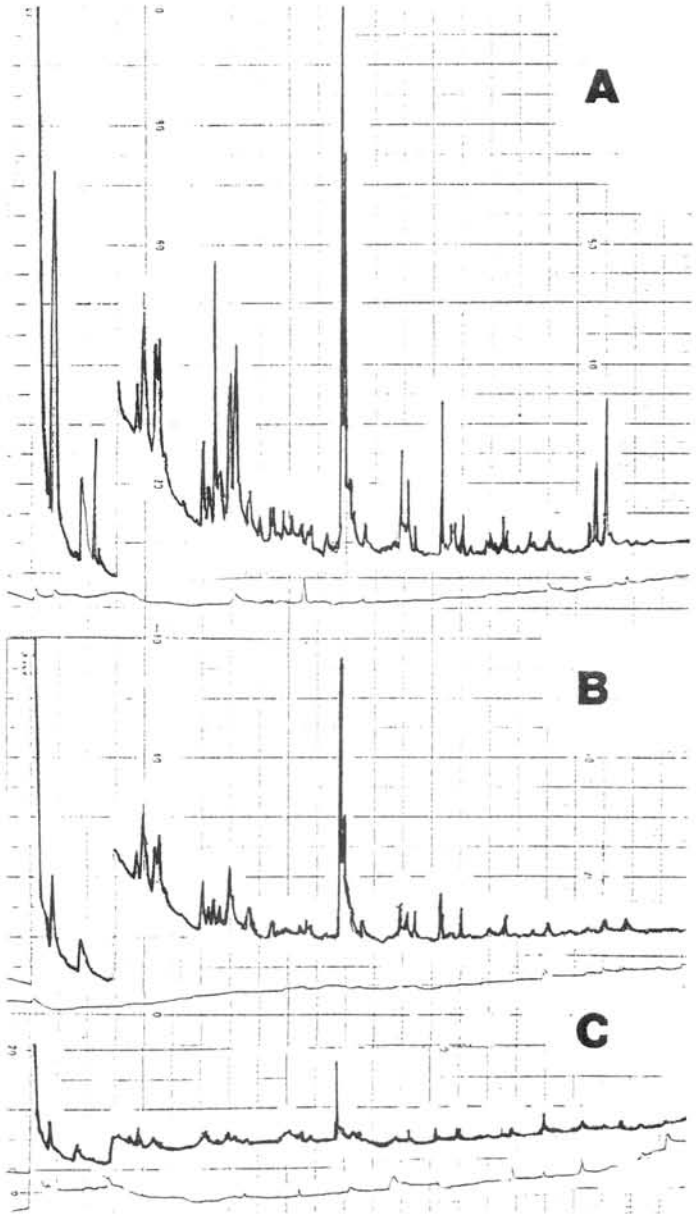

Fig. 2. GC chromatogram of products obtained by pyrolysis of Y-74662 on different pyrolysing temperature. Amount of meteorite (5 mg) and sensitivity of FID are the same for each run.
A:670 °C
B:500 °C
C:386 °C
Column temperature was 50 °C for initial 8 min and then elevated to 220 °C at the rate of 4°C/min for all of chromatogram.

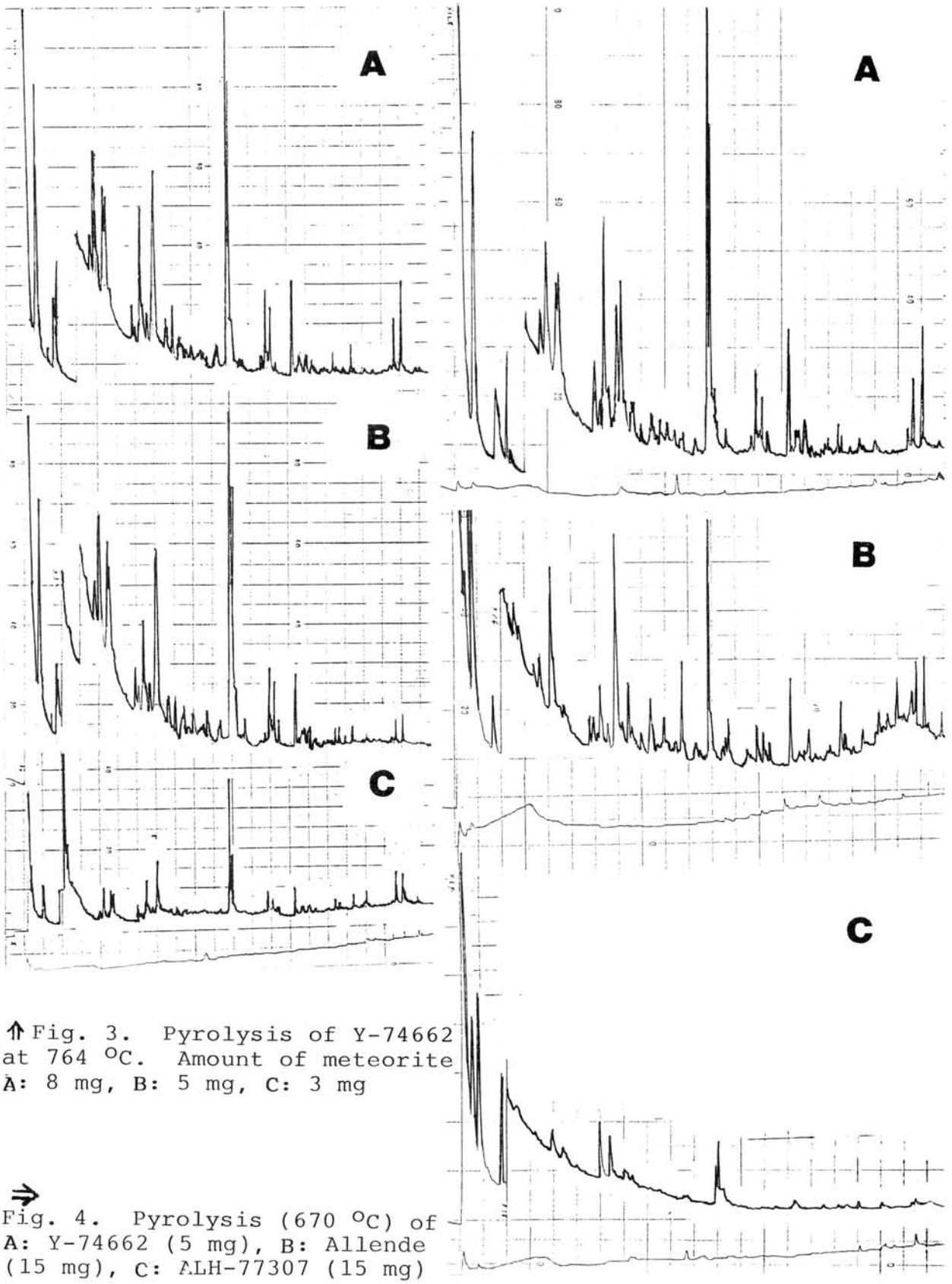

⇑ Fig. 3. Pyrolysis of Y-74662 at 764 °C. Amount of meteorite A: 8 mg, B: 5 mg, C: 3 mg

⇒ Fig. 4. Pyrolysis (670 °C) of A: Y-74662 (5 mg), B: Allende (15 mg), C: ALH-77307 (15 mg)

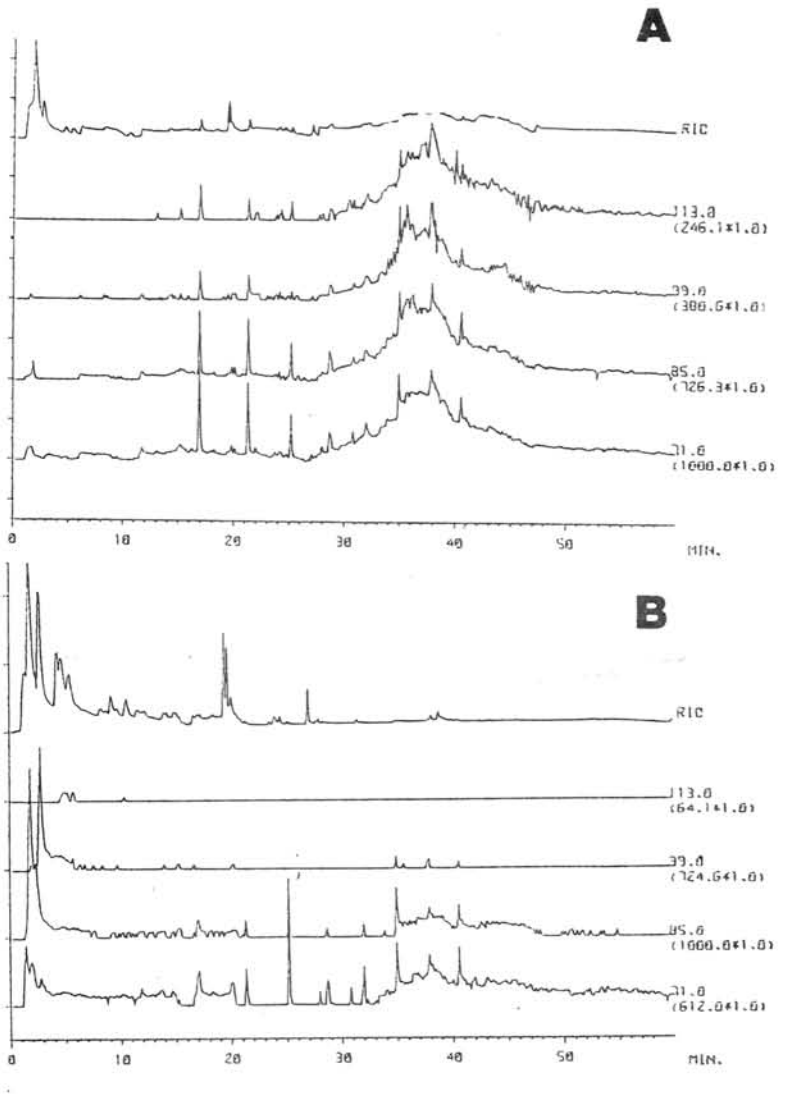

Fig. 5. Mass chromatogram monitored by the ions at m/z 71, 85, 99, and 113 (typical fragment ions for aliphatic hydrocarbons) of the pyrolysis products of
A::Allende
B:Y-74662

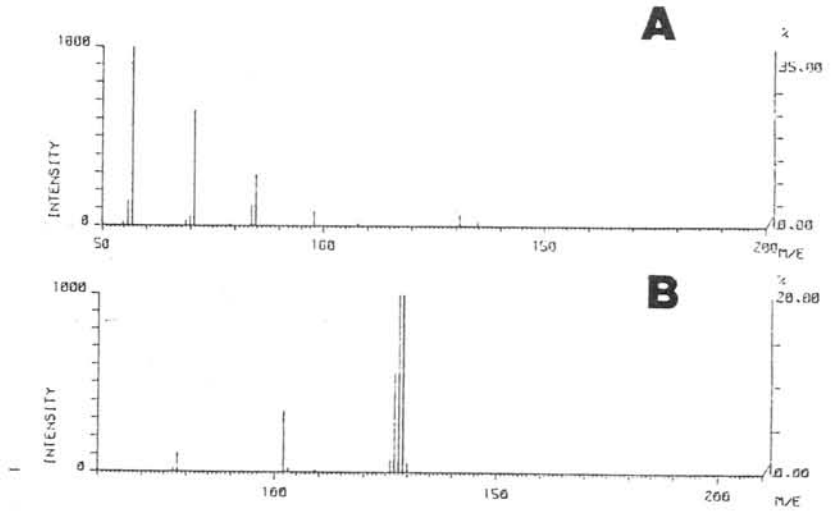

Fig. 6. Typical examples of mass spectra of main products obtained by pyrolysis of
A:Allende
B:Y-74662

OXYGEN ISOTOPES IN YAMATO METEORITES

Clayton, R.N.,* Mayeda, T.K.* and Yanai, K.**

*University of Chicago, Chicago, IL 60637. **National Institute for Polar Research, Tokyo 133.

The Antarctic meteorites greatly expand the possibility of discovery of new meteorite types and of increasing the number of examples of rare types. Oxygen isotopic abundances have proven useful in discriminating between different classes, and in recognizing interrelationships between classes. Special caution is necessary in applying oxygen isotope studies to Antarctic samples, however, because the ice is very strongly depleted in the heavy isotopes, so that even a few percent of oxygen contributed by weathering products can seriously perturb the original composition. Isotopic analyses of seven Yamato meteorites are given in Table 1.

The three lodranites have isotopic compositions similar to earlier analyses of Lodran, but displaced to lower $\delta^{18}O$ and $\delta^{17}O$, perhaps due to the presence of isotopically light weathering products. A search for relationships between lodranites and other meteorite types reveals two possible connections: (1) the lodranites fall on a slope-1/2 fractionation line which passes through the ureilites, and (2) the lodranites fall within a band of data points determined by analysis of various components of the CR chondrites, Renazzo and Al Rais. Oxygen isotopic analysis of Y790112 confirms its classification in the CR group.

Sample Y790981, a ureilite, has an isotopic composition displaced from other ureilites by about 2‰ in ^{18}O. This corresponds to about 8% contamination by weathering products. This meteorite was assigned a degree of weathering of B.

Sample Y790269 shows a rather severe effect of Antarctic weathering. Its $\delta^{18}O$ is shifted by 3-4‰, corresponding to 10-15% contamination. Its weathering classification is C.

Sample Y75097 has a typical unweathered L chondrite composition. An achondrite inclusion within this meteorite has a composition which does not correspond to any achondritic meteorites, but does fall within the range of H chondrites. This may be the first example of H-material included within an L chondrite.

TABLE 1.

OXYGEN ISOTOPIC COMPOSITIONS OF YAMATO METEORITES

Sample	Type	$\delta^{18}O$	$\delta^{17}O$
Y74357,93	lodranite	1.49	-0.45
		1.54	-0.40
		+1.52	-0.42
Y75274,91	lodranite	2.39	-0.08
		2.52	+0.23
		+2.45	+0.08
Y791493,93	lodranite	1.33	-0.18
		1.05	-0.39
		1.19	-0.28
Y790112,93	CR	2.22	-0.55
		2.55	-0.09
Y790981	ureilite	5.41	2.41
Y790269,91	H4	-0.08	+0.50
		+1.43	+1.24
Y75097,93	L6	4.61	3.63
		4.45	3.48
		4.53	3.56
Y75097,111	inclusion	4.48	3.04
		4.60	3.06
		4.54	3.05

41－1

Rb-Sr systematics and trace element abundance studies of the Antarctic LL-chondrites.

O.Okano[1], N.Nakamura[1),2)], K.Misawa[2)], H.Honma[3)] and H.Goto[4)]

1) Dept. of Sci. of Material Differentiation, The Graduate School of Sci. and Tech., Kobe Univ., Nada, Kobe, 657
2) Dept. of Earth Sci., Faculty of Sci., Kobe Univ.
3) Inst. for Thermal Spring Research, Okayama Univ., Misasa, Tottori-ken, 682-02
4) College of Liberal Arts, Kobe Univ.

Recently, Sato et al. (1982) reported the Antarctic LL-chondrites with unusual, petrological features induced by a impact-melting. In order to clarify age and trace-element chemical characteristics of these meteorites, we have initiated Rb-Sr isotopic and trace element abundance studies of the usual and shock-melted LL-chondrites from the Antarctica. So far analyses for whole rocks of three Antarctic (Y-74646(LL6-5), Y-75258(LL6) and Y-790964(LL6)) and non-Antarctic (Soko Banja) chondrites have been performed as a preliminary work.

In Fig.1, all four LL-chondrites show normal, flat REE abundance patterns when normalized to average ordinary chondrite. But the Y-790964, which is subjected to shock-melting , appears to have the somewhat high REE abundances with a slight fractionation, and to be systematically higher than those by Fukuoka and Ikeda(1983) for the same chondrite. Sr abundances in these chondrites are quite constant. On the other hand, Rb and K abundances are mostly variable.

In Fig.2, the Rb-Sr evolution diagram for whole rocks is shown. It is worth noting that the data points of three normal LL-chondrites (Y-74646, Y-75258 and Soko Banja) are plotted on a reference line of the 4.55 b.y.-age calculated from the Allende initial (Gray et al.,1973), which suggests that the Rb-Sr system of these chondrites were not disturbed by later events such as terrestrial weathering. Results obtained for these three LL-chondrites are consistent with previous works (e.g. Gopalan and Wetherill,1969; Minster and Allègre,1981). On the other hand, data point of Y-790964 deviates completely from the 4.55 b.y. reference line. The calculated model age is 3.74 b.y.. This young model age may not have a direct physical meaning but suggests that the Rb-Sr system of this chondrite has been reset or disturbed by younger (than 3.74 b.y.) event such as impact-melting on LL-chondrite parent body or less possibly terrestrial weathering. In order to clarify this problem, Rb-Sr isotopic and trace element analyses for mineral separates of Y-790964 and for whole rocks of other Antarctic LL-chondrites are in progress.

References

Fukuoka,T. and Ikeda,K. (1983) Papers presented to the eighth symposium on Antarctic meteorites, 17-19 Feb. 1983
Gopalan,K. and Wetherill,G.W. (1969) J. Geophys. Res., 74, 4349-4358.
Gray,C.M., Papanastassiou,D.A. and Wasserburg,G.J. (1973) Icarus, 20, 213-239.

Minster,J.F. and Allègre,C.J. (1981) Earth Planet. Sci. Lett., 56, 89-106.
Sato,G., Takeda,H., Yanai,K. and Kojima,H. (1982) Papers presented to the seventh symposium on Antarctic meteorites, 19-20 Feb. 1982

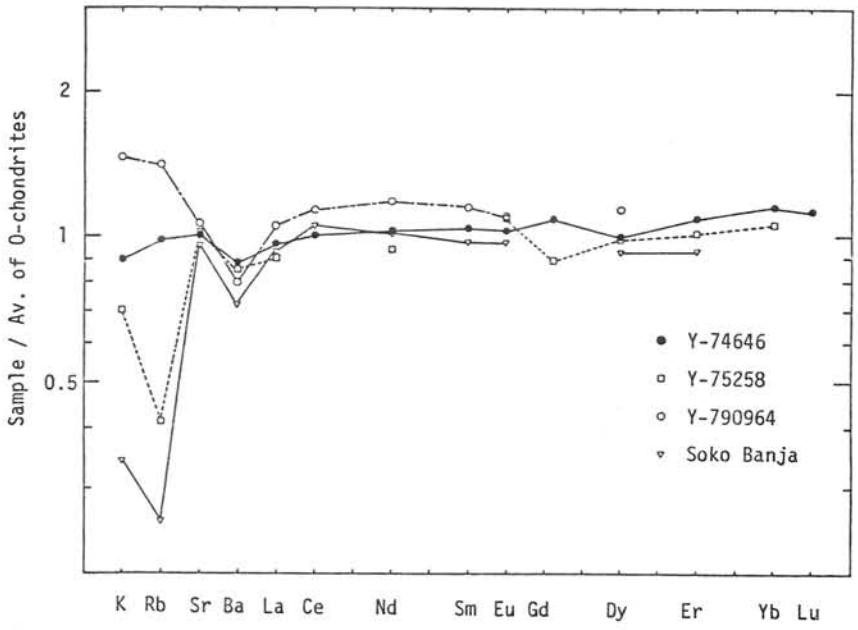

Fig. 1. Chondrite-normalized REE patterns of LL-chondrites.

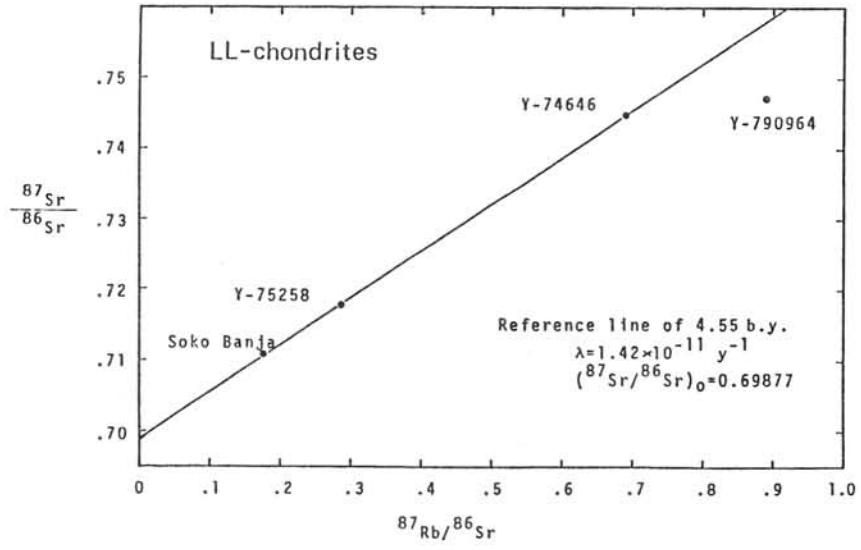

Fig. 2. $^{87}Rb/^{86}Sr$ vs. $^{87}Sr/^{86}Sr$ diagram for whole rock from LL-chondrites.

42－1

ANOMALOUS $^{3}He/^{4}He$ RATIO IN PACIFIC OCEAN SEDIMENTS —— EVIDENCE FOR METEORITE DEBRIS OR COSMIC DUST FALLOUT ?

Ozima, M., Takayanagi, M., Zashu, S. and Amari, S.
Geophysical Institute, University of Tokyo, Tokyo 113

36 sediments cored at 10 sites in the central to western Pacific ocean were studied for $^{3}He/^{4}He$ ratio. About 100 m.g. of sediment samples was used for the mass spectrometry, where $^{3}He/^{4}He$ ratio was measured with a double collector mass spectrometer with resolution of 600. The $^{3}He/^{4}He$ ratio range from 10^{-7} to more than 1×10^{-4}, the majority being higher than 10^{-5}. No clear relation between the geographical location and the $^{3}He/^{4}He$ ratio is apparent. The $^{3}He/^{4}He$ ratio is generally higher for the lower level in a sediment core and there is a positive correlation between the $^{3}He/^{4}He$ ratio and the ^{3}He content.

Since $^{3}He/^{4}He$ ratios so far measured in common terrestrial materials are less than 5×10^{-5} (1) and ^{3}He production in natural environments is very likely to be insignificant (2), it seems to be imperative to assume contamination of some extra-terrestrial materials in the sediments in order to account for the observed high $^{3}He/^{4}He$ ratio. For example, if Brownlee particles (3) which are enormously enriched in the He content ($\sim 10^{-2}$ cm^{3} STP/g) are responsible to the anomalous $^{3}He/^{4}He$ ratio, about 1 ppm of their contamination in the sediments would suffice to account for the isotopic ratio. However, the observed large variation in the ^{3}He content even among the sediments having a similar sedimentation rate is not consistent with the fallout hypothesis. Alternatively if we assume meteorite debris as the contaminating extra-terrestrial materials, a few ten to hundred ppm of gas rich meteorite such as Pesyanoe could account for the ^{3}He content and the isotopic ratio. The contamination of the meteorite debris in the sediments may be attributable to the meteorite impact on the ocean floor. However, it is then puzzling that the occurrence of the anomalous $^{3}He/^{4}He$ in sediments is so common in the Pacific ocean basin. Also, it is difficult to understand on the basis of the meteorite impact hypothesis the general tendency of the increase of ^{3}He content and $^{3}He/^{4}He$ isotopic ratio with the depth in the sediment cores.

We made detailed studies on one of the sediment cores which showed very high $^{3}He/^{4}He$ ratio ($> 5 \times 10^{-5}$). The core was obtained by R/V Hakuho-Manu (4), University of Tokyo in the western Pacific (KH75-3-5-2 : 26°00.8'N, 150°00.0'E). The total core length is about 9 m and we measured the $^{3}He/^{4}He$ ratio at about 1 m intervals. The core shows clear morphological distinction between the upper and the lower section; the upper section (0 - 4 m) has lighter colour and compact texture, while the lower section (4 - 9 m) shows dark colour and loose compaction. No fossil was found in the core. Both the ^{3}He content and $^{3}He/^{4}He$ ratio increase from the upper to the lower section, while the ^{4}He content is nearly constant throughout the core. Moreover, there appears a discontinuous change in the $^{3}He/^{4}He$ ratio and ^{3}He content between the upper (0 - 4 m) and the lower section (4 - 9 m) corresponding to the distinction in the morphology. Preliminary microscopic examination did not reveal the existence of any exotic materials in the sediments. Neutron activation analyses were made on two sections (400 - 416 cm, 850 - 870 cm). Slight increase in Ni content across the transition layer may be real, but no anomalous concentration of Co, Cr was observed in both sections. Ir was not detected. The core was obtained in the midst of the

Cretaceous-Quaternary hiatus region. It is tempting to speculate that meteorite impact is responsible to the origin of the hiatus as well as to the observed high $^{3}He/^{4}He$ ratio.

References

(1) Ozima, M. and F.A. Podosek (1983)
Noble gas geochemistry, pp257-261, Cambridge Univ. Press.
(2) Tolstikhin, I.N. (1974)
Earth Planet. Sci. Lett., 22, 75-84.
(3) Rujan, R.S., D.E. Brownlee, D. Tomande, P.W. Hodge, H. Farrar and R.A. Britten (1977)
Nature, 267, 133-134.
(4) Kobayashi, K., S. Tonouchi, T. Furuta and M. Watanabe (1980)
Bull. Ocean Res. Inst., Univ. of Tokyo, No. 13, 1-148.

43

CARBON-14 AGES OF ANTARCTIC METEORITES

Matsuda,E. and Kigoshi,K.
Department of Chemistry, Gakushuin University, Mejiro, Toshima-ku, Tokyo 171

The terrestrial ages of Antarctic meteorites ,Y-75102 and 74459, have been measured by their content of cosmic-ray-produced carbon-14. The stepwise heating method was used to remove terrestrial carbon contamination, mainly secondary carbonates, resulting from weathering.

Approximately 20 g of meteorite samples was pulverized in an airtite alumina crusher for 10 hours. The powdered sample in a platinum boat was put into a quartz tube and was evacuated for a few hours at 100°C. The sample was then heated at 600°C for 5 hours under vacuum(10^{-5}- 10^{-6}Torr) to remove terrestrial contaminants. The gases evolved were passed through a liquid nitrogen trap, where CO_2 and other condensible gases were recovered. Non-condensible gases, mainly CH_4 and CO, were then passed through the CuO furnace heated at 450°C - 550°C, where CO was converted to CO_2, and were recovered in the molecular sieve 4A cooled in liquid nitrogen. CO_2 gas condensed in a liquid nitrogen trap was separated from SO_2 and H_2O by distillation at -150°C and passing molecular sieve 3A cooled in dryice-methanol. CH_4 retained in molecular sieve 4A was circulated through the CuO furnace at 800°C for 40 minutes to oxidized to CO_2, and added to the previously recovered CO_2. After recovery the CO_2 gas of 600°C fraction was completed.

The sample was then heated at 1000°C for 5 hours under vacuum. CO_2 gas was recovered with the same procedure as in the case of 600°C. The residual sample was heated again at 1000°C for 3 hours in oxygen atmosphere. The CO_2 evolved in this step was collected as 1000°C fraction together with the previous one. The amount of the CO_2 gas was measured volumetrically.

The CO_2 gases of both fractions, 600°C and 1000°C, were converted to acetylene respectively. The acetylene was prepared through lithium carbide which was obtained by the reaction between metalic lithium and CO_2. The reaction of lithium carbide and tritium-free water gave acetylene.

The carbon-14 in the acetylene was counted in a proportional counter of 53.0 cm^3 which had a background of 0.373 ± 0.016 cpm.

The terrestrial ages of meteorites were obtained from the activities in the carbon extracted at 1000°C. The activities in the carbon of 600°C fraction may give the information about the terrestrial contamination.

COSMOGENIC TRACKS AND SPALLATION PRODUCTS IN ANTARCTIC METEORITES AND THEIR TERRESTRIAL AGES

Bhandari, N., Goswami, J.N., and Shukla, P.N.

Physical Research Laboratory, Ahmedabad 380 009, India.

Simultaneous measurements of various cosmic ray effects such as VH tracks, cosmogenic nuclides (^{53}Mn, ^{26}Al, ^{36}Cl, ^{14}C etc.) and stable isotopes such as ^{21}Ne and ^{22}Ne made in the same aliquot of meteorite samples are useful in resolving problems such as precompaction irradiation, exposure history of meteorites, cosmic ray intensity variations and terrestrial ages [1,2]. Using tracks and $^{22}Ne/^{21}Ne$ (NeR) data it has been shown that one can distinguish cases of single or multiple exposure of meteorites [3]. Furtheremore, a study of three isotope plot of ^{21}Ne, ^{53}Mn and ^{26}Al in meteorites of simple exposure indicates that the average GCR intensity over the past 1-2 m.y. has been the same as that during the past 10^7 yr [1] and a combined analysis of ^{53}Mn and track data allows one to confirm or rule out the proposed pairing of several antarctic meteorites [2]. Here we describe the results of track measurements in four antarctic meteorites and then discuss procedures of deducing their terrestrial ages using radionuclide data.

Track density measurements: Four Yamato meteorites viz. 74013 (DIO), 74097 (DIO), 74191 (L3) and 74647 (H4-5) were studied for their nuclear track records. The track data together with rare gas and ^{53}Mn data are given in Table 1. The shielding depths for various samples are given in the last column. Based on the model calculations of Bhandari et al [4] the preatmospheric radius (under assumption of spherical geometry) are calculated to be 10 cm and 12 cm for 74191 and 74647 respectively. The recovered pieces of 74013, 74097 together with 74037 and 74136 can be reconstructed into a single diogenite weighing 5.57 kg. A preatmospheric radius of 33 cm has been estimated for this multiple fall.

Terrestrial ages (T_E): Accurate estimation of T_E of antarctic meteorites is important in determining the frequency of meteorite falls in the past and for understanding their movement in the ice. Thermoluminescence and radionuclides produced by cosmic rays have been used for determining T_E but only in a few cases accurate or consistent results have been obtained. It is therefore desirable to take into account variations in production rates due to depth in and size of meteorites and base T_E on more than one isotope. We discuss here three isotope diagrams based on $^{21}Ne/^{26}Al$ - $^{21}Ne/^{53}Mn$, $^{53}Mn/^{36}Cl$ - $^{53}Mn/^{26}Al$ and $^{21}Ne/^{14}C$ - $^{21}Ne/^{26}Al$. The following production rates have been taken for constructing fig. 1, 2 and 3. ^{21}Ne (10^{-8}cc STP/g. m.y.) : ^{53}Mn (dpm/kg (Fe + 1/3 Ni)) : ^{26}Al (dpm/kg met.) : ^{36}Cl (dpm/kg (Fe + Ni)) : ^{14}C (dpm/kg metal) = 0.39 : 415 : 60 : 25 : 54, based on the available data in literature. These curves are not sensitive to change in isotope production with size and depth of the meteorite and are useful in identifying cases of multiple exposure. In addition they can be used to determine reliable values of T_E. The ^{21}Ne, ^{53}Mn, ^{26}Al, ^{36}Cl and ^{14}C data used here have been taken from [5,6,7] and references quoted therein. Although all the measurements are not in the same aliquot, they can still give a better estimate of T_E compared to the value derived on the basis of a single isotope.

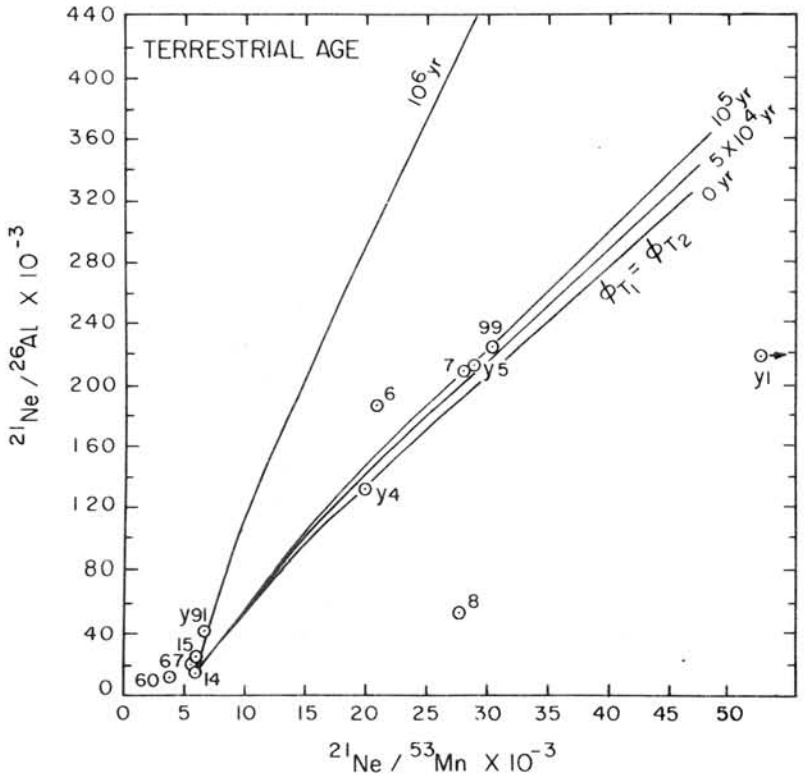

Fig.1. Calculated curves for different terrestrial ages. See table 2 for abbreviated symbols. Y is for Yamato and others are for Allan Hills.

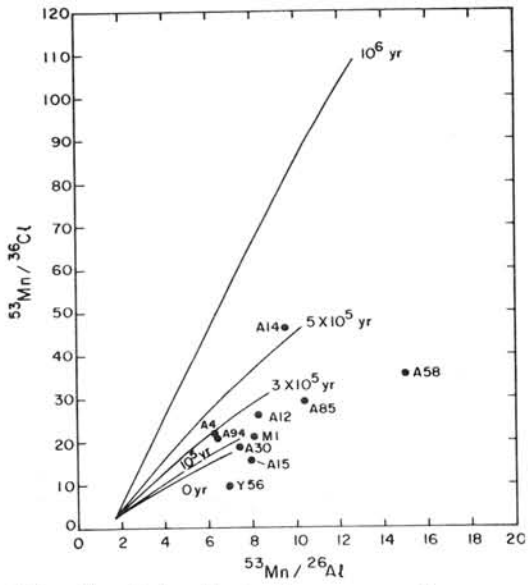

Fig.2. Calculated curves for different terrestrial ages.

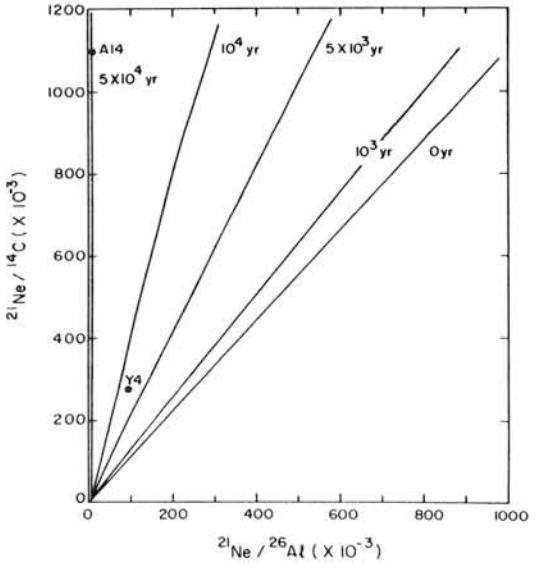

Fig.3. Calculated curves for different terrestrial ages.

In Table 2 we have summarized T_E obtained from these diagrams (fig. 1,2) alongwith the available literature values. In general, there is a good agreement between the two. In fig. 1, the meteorites ALHA 76008 and Y 7301 fall below the calculated line of zero terrestrial age indicating a complex exposure history and indeed a two stage irradiation for these meteorites have been proposed [5] to explain the radionuclide data. Based on this observation ALHA 78115 and Y 74156 also seem to belong to a case of complex exposure history (fig. 2). In fig. 3, based on ^{21}Ne, ^{26}Al and ^{14}C, we have given the calculated curves for various T_E and the meteorites belonging to terrestrial age group 10^3 - 10^4 yr could be better resolved from this diagram as can be seen for Y 7304 for which T_E of 6×10^3 yrs is deduced from fig. 3.

Table 1: Tracks, ^{21}Ne and ^{53}Mn data for antarctic meteorites

Sample	Measured Track density (#/cm²)	^{21}Ne exposure age (m.y.)	^{53}Mn exposure age (m.y.), (dpm/kg Fe)	Shielding depth (cm)	Pre-atmospheric radius (cm)
74013-1	2×10^5	32, 42[a]	>10(401 ± 37)	18.7	
74013-2	10^5			21.5	33
74013-3	1.5×10^5			19.7	
74013-4	6.7×10^4			23.0	
74097	6.8×10^4	34	>10(421 ± 38)	23.0	
74191-1	1.1×10^6	6.5, 9[a]	10(450 ± 32)	5.8	10
74191-2	1.06×10^6			5.8	
74647-1	5.1×10^5		8(329 ± 17)	7.0	12
74647-2	4.3×10^5			7.5	

(a) Modified values using [3].

Table 2: Terrestrial ages

Meteorite Class	Abbreviated symbol	Approx. Terrestrial Ages (yr) A	B	Literature*
A 77004 H4	A 4	-	3×10^5	$(1.8 \pm .8) \times 10^5$
A 76006 H6	A 6	5×10^5	-	$<3 \times 10^5$
A 76007 L6	A 7	10^5	-	$<5 \times 10^5$
A 78112 L6	A 12	-	2×10^5	$(2.3 \pm .8) \times 10^5$
A 78114 L6	A 14	-	6×10^5	$(4.6 \pm .8) \times 10^5$
A 77294 H5	A 94	-	2×10^5	$(3.0 \pm .2) \times 10^4$
A 77299 H3	A 99	10^5	-	$(.8 \pm .8) \times 10^5$
Y 7304 L5	Y 4	$<5 \times 10^4$ + 6×10^3+	-	$<10^5$
Y 7305 L5	Y 5	10^5	-	-
Y 74191 L3	Y 91	10^6	-	-

* From 5 and references therein. A - Based on fig.1, where the ratios $^{21}Ne/^{26}Al$ vs. $^{21}Ne/^{53}Mn$ are plotted. B - Based on fig.2, where the ratios $^{53}Mn/^{36}Cl$ vs. $^{53}Mn/^{26}Al$ are plotted. + - From fig.3.

We thank Dr. K. Yanai for kindly providing the meteorite samples.

References:

1. N. Bhandari, Lunar Planet. Sci. (1984), XV, 000.
2. J.N. Goswami and K. Nishiizumi, Earth Planet. Sci. Lett. 64 (1983) 1.
3. N. Bhandari and M.B. Potdar, Earth Planet. Sci. Lett. 58 (1982) 116.
4. N. Bhandari et al, Nucl. Tracks 4 (1980) 213.
5. K. Nishiizumi et al, Earth Planet. Sci. Lett. 45 (1979) 285; 62 (1983) 407.
6. E.L. Fireman et al., Lunar Planet. Sci. (1982), XIII, 219.
7. N. Takaoka and K. Nagao, Mem. Nat. Inst. Polar Res. Spec. Issue 8 (1978) 198; 12 (1979) 207.

RELATIONSHIP BETWEEN THE TYPE OF METEORITES AND THE CHARACTERISTICS OF Ar-DEGASSING

Kaneoka, I.

Geophysical Institute, University of Tokyo, Bunkyo-ku, Tokyo 113

So far, we have determined the ^{40}Ar-^{39}Ar ages of Antarctic meteorites which include both ordinary (L-, H-, LL-)chondrites and achondrites (eucrites, howardite, diogenite)(1-3). Antarctic meteorites are often found to have been weathered to some extent, which are resulted in the disturbed patterns in the ^{40}Ar-^{39}Ar age spectra. Such weathering effect does not always lower an apparent ^{40}Ar-^{39}Ar age. In effect, an example has been demonstrated where an anomalously old ^{40}Ar-^{39}Ar age was observed in Antarctic meteorites due to the weathering effect (4). The characteristics of Ar-degassing from a meteorite would be controlled by the type of meteorite which might reflect both the mineral and chemical compositions and the texture of the meteorite. It may also control the Ar-retentivity in a meteorite. Hence, it is important to get such information in order to evaluate the obtained ^{40}Ar-^{39}Ar age properly. Based on the data of Ar-degassing from Antarctic meteorites at each temperature, which were used to obtain ^{40}Ar-^{39}Ar ages previously, the characteristics of Ar-degassing has been examined for different type of meteorites.

By using the ^{39}Ar-degassing pattern, diffusion parameters for each meteorite can be determined approximately. The diffusion constants (D/a^2) are estimated to be $(0.5\sim2)\times10^{-5}$ sec^{-1} at 1000°C, but they do not show any systematic change with type of meteorite. The activation energies range from about 10 to 50 Kcal/mole, but most meteorites show the values between 20 to 40 Kcal/mole. It seems that non-equilibrated ordinary chondrites might have relatively lower activation energies compared with equilibrated ones.

The figures for integrated fractions of each Ar isotope against degassing temperatures indicate that ^{39}Ar and ^{40}Ar are degassed systematically in larger proportions than ^{37}Ar and ^{36}Ar up to the highest temperature. The differences are less, however, for achondrites than ordinary chondrites. This suggests that K and Ca are located in rather different phases in ordinary chondrites. Relatively complicated diffusion characteristics is observed for non-equilibrated ordinary chondrites compared with those of achondrites. This may reflect the occurrence of fine matrix in these meteorites. Hence, a non-equilibrated ordinary chondrite may be more easily affected than an achondrite by the weathering in its ^{40}Ar-^{39}Ar age.

References

(1) Kaneoka, I., Ozima, M. and Yanagisawa, M., Mem. Natl Inst. Polar Res., Spec. Issue, 12, 186 (1979).
(2) Kaneoka, I., ibid., Spec. Issue, 17, 177 (1980).
(3) Kaneoka, I., ibid., Spec. Issue, 20, 250 (1981).
(4) Kaneoka, I., Nature, 304, 146 (1983).

Isotopic Analysis of Noble Gas in ALH-77257(Ur).

Nobuo Takaoka
Department of Earth Sciences
Yamagata University

Elemental and isotopic compositions of noble gases in bulk and carbon fraction of ALH-77257 ureilite were measured by step heating. The carbon fraction was prepared from decomposition of powdered sample with HF + aqua regia in a Teflon bomb at 110 °C. X-ray defraction analysis shows that it contains diamond, graphite and quartz. The quartz seems to recrystallize from silicate solution.

Fig. 1 shows release patterns of He, Ar and Xe from the carbon. The isotopes of He appeared at low temperatures are mostly cosmogenic, produced from graphite carbon by cosmic-ray spallation. It should be noticed that most of gases including He were released at about 2000 °C. This means that these gases resided in diamond. Diamond is converted into graphite around this temperature and releases the occluded gases. The lowest $^{3}He/^{4}He$ ratio is 1×10^{-3} at 1900 °C. This value is significantly higher than that for trapped He in primitive meteorites. Most part(89%) of ^{3}He at 1900 and 2050 °C is spallogenic origin from diamond carbon.

Isotopic composition of Ne trapped in diamond resembles that of Ne-C (Black,1972), and Kr and Xe have the same isotopic ratios as those for the bulk sample, in agreement with those for Kenna bulk (Wilking and Marti,1976).

Radiogenic Ar was also appeared at low temperatures. Ninety seven percent of trapped Ar was released at temperatures higher than 1900 °C, and the lowest $^{40}Ar/^{36}Ar$ ratio of 1.2×10^{-3} was found at 2050 °C. The $^{38}Ar/^{36}Ar$ ratio is 0.192, typical value for ureilite trapped Ar. The trapped ^{36}Ar in the carbon fraction amounts to 3.55×10^{-4} cc/g. Except Dyalpur carbon, the ALH-77257 carbon contains the highest amounts of trapped gases (Göbel et al. ,1978).

Cameron(1973) have guessed the primordial $^{40}Ar/^{36}Ar$ ratio to be 2×10^{-4}. The present result is larger by six times.

Because the primordial $^{40}Ar/^{36}Ar$ ratio in ureilite diamond depends on the origin of its parent body, it can give a useful constraint on models of the origin.

References.

Black,D.C.(1972), Geochim Cosmochim. Acta,36,347.

Göbel,R. et al.,(1978), J. Geophys. Res.,83,855.

Wilking,L.L. and Marti,K. (1976), Geochim.Cosmochim. Acta, 40, 1465.

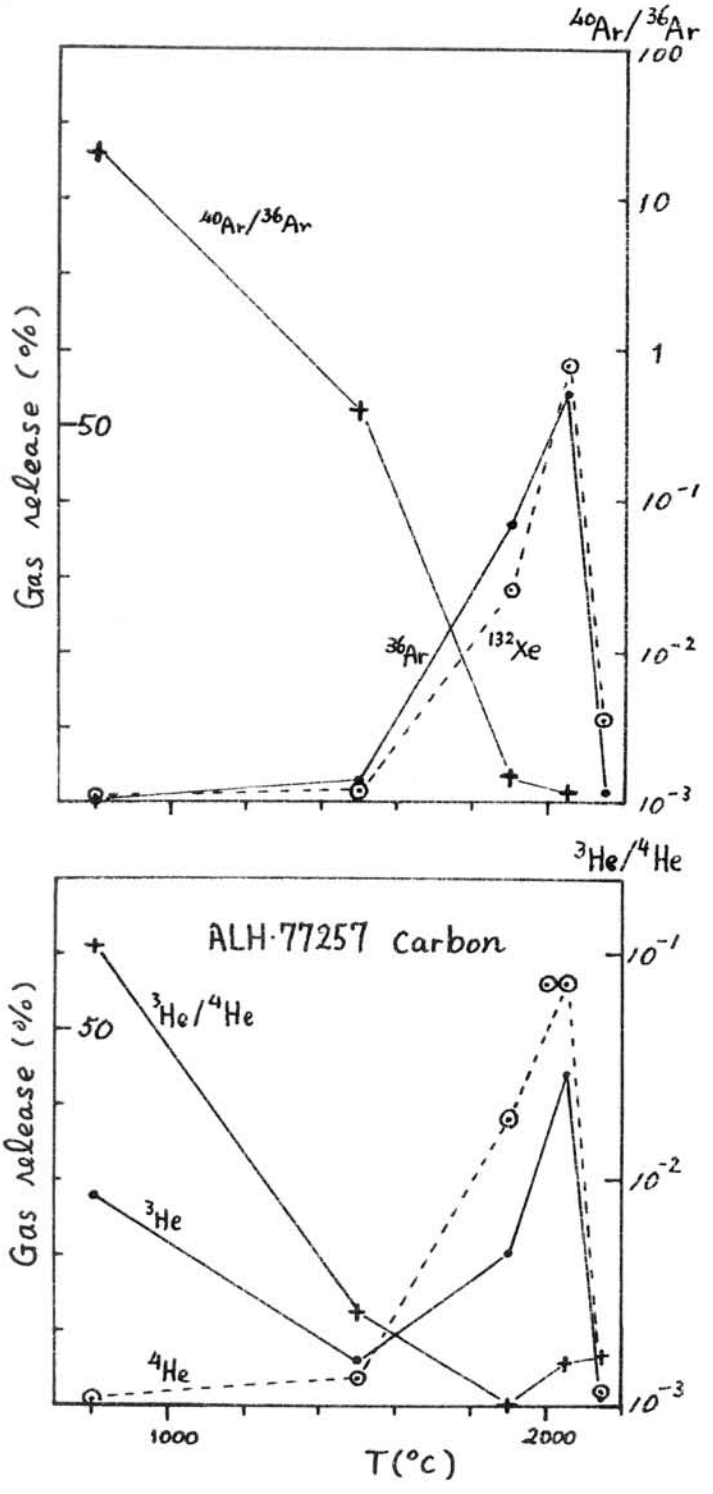

Fig. 1. Release pattern of He, Ar and Xe from carbon fraction of ALH-77257 (Ur).

RARE GAS STUDIES OF THE ANTARCTIC METEORITE: Belgica-7904 C2 chondrite

Nagao, K., Inoue, K. and Ogata, K.
Okayama University of Science, Ridai-cho 1-1, Okayama 700

Rare gas elemental and isotopic abundances in Belgica-7904 C2 chondrite have been analized by stepwise heating method. This carbonaceous chondrite was recovered by Yanai et al. on Dec 19, 1979 at Belgica Mountain, Antarctica. It consists of abundant dark phyllosilicate matrix containing chondrules, inclusions, and minerals(Meteorite News 1982, vol.1, No.1, Natl. Inst. Polar Res.).

Sample used in this work is fine grained matrix of 0.1696g containing no inclusions. Rare gas were extracted by stepwise heating, the temperatures were 700, 900, 1100, 1300, 1500 and 1800°C. Results are listed in Table 1 and Figs. 1.and 2.

He and Ne were released mainly at the temperatures of 900 and 1100°C, whereas the most part of heavy rare gases Ar, Kr and Xe were released at the higher temperatures of 1100 and 1300°C.

3He/4He ratio of 700°C fraction is 2.6×10^{-2}, which indicates the release of cosmogenic He. The ratios of higher temperature fractions are in the range of 10^{-4}, which are similar to the ratio of primordial He.

Neon isotopic ratios are plotted in Fig. 1. The ratios of 1100°C fraction are plotted lower than the line connecting the components of Ne-A and spallogenic neon. The point of 1100°C fraction strongly suggests a presence of Ne-E, the nearly pure 22Ne, in this C2 chondrite. The release temperature of Ne-E for this chondrite agree with that for other carbonaceous chondrites.

38Ar/36Ar ratios are as same as the ratio of trapped argon. 40Ar/36Ar ratios are very low relative to the atmospheric argon and the ratio for 1300 and 1500°C fractions are lower than 1. Argon in this meteorite is mainly composed of primordial component.

Since the isotopic composition of Xe in the lowest temperature fraction is similar to the ratios of atmospheric Xe, most part of xenon in this fraction is the atmospheric contamination. The ratios for higher temperature fractions consist of AVCC-Xe and fissiogenic Xe. The presence of fission Xe is evident in the fraction of 900°C, and its relative abundances subtracted AVCC-Xe are 130Xe:131Xe:132Xe:134Xe:136Xe=0 :0.146 : 0.083 :0.813 : 1. The abundances are similar to that for Allende C3 chondrite in which the abundance of 132Xe is lower than that of 131Xe (Lewis et al. 1975, Science 190, 1251).

Table 1. Rare gas abundances and isotopic compositions.
(preliminary results)

Temp.	4He#	3/4*	20Ne#	20/22	21/22	36Ar#	38/36	40/36	84Kr$	132Xe$
700	22	264	0.22	2.98	0.703	1.8	0.188	17.3	2.9	6.7
900	290	5.84	2.2	6.78	0.234	2.9	0.194	1.49	2.8	4.2
1100	350	2.17	4.7	5.97	0.135	26	0.188	2.94	25	25
1300	82	3.45	1.5	7.33	0.157	22	0.188	0.564	16	15
1500	8.0	9.96	0.44	7.36	0.386	7.0	0.192	0.892	5.8	6.5
1800				2.91	0.845					

* unit in 10^{-4}, # unit in $10^{-8}cm^3STP/g$, $ unit in $10^{-10}cm^3STP/g$.

Fig. 2. Plot of δ for Xe.

Fig. 1. Three isotope plot of Ne

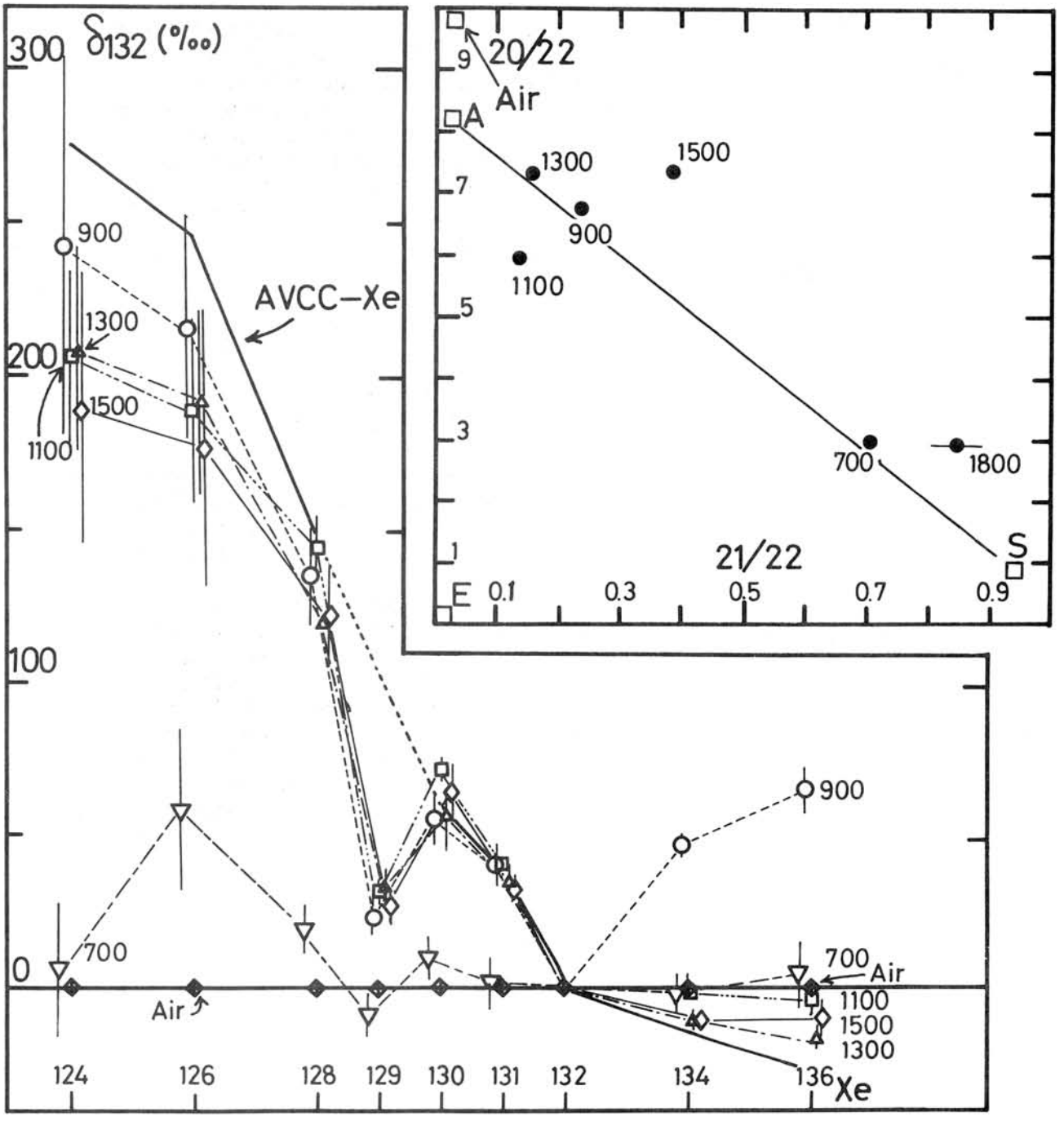

NON-DESTRUCTIVE MEASUREMENT OF RADIONUCLIDES IN YAMATO METEORITES

KOMURA, K., TAN, K.L. and SAKANOUE, M.
L.L.R.L., Kanazawa University, Tatsunokuchi, Ishikawa 923-12

Cosmic-ray induced Al-26, natural K-40 and artificial Cs-137 in six YAMATO meteorites have been measured by non-destructive gamma-spectrometry using low background Ge(Li) detector. In the present work, the detection efficiency of the Ge(Li) detector was calibrated by an improved method using mock-ups, prepared from the mixture of plasticine and nickel powder, having almost the same shapes and densities as those of the meteorite samples. Results are summarized in Table I.

The terrestrial ages of these meteorites were estimated from the present data together with the data of Mn-53 and their cosmic-ray exposure ages measured from Ne and/or K isotopes.

Table I. Al-26, K-40 and Cs-137 activities of YAMATO meteorites.

Meteorite Name	Type	Weight (g)	Al-26 (dpm/kg)	POTASSIUM (%)	Cs-137 (cpm)
YAMATO-					
74080	L6	249.6	38±2	0.069±.003	0.103±.006
74192	H5	347.3	60±4	0.059±.003	0.216±.010
74193	H5	128.2	33±3	0.065±.007	0.294±.010
74374	H6	113.3	61±5	0.074±.008	0.137±.005
74640	H6	125.9	43±4	0.064±.004	0.076±.006
74646	LL6	183.3	43±4	0.074±.004	0.427±.011

COSMOGENIC SCANDIUM 45 IN IRON METEORITES.

M.Honda,H.Nagai,K.Yamamuro,Y.Hayashida.

Department of Chemistry,College of Humanities and Sciences, Nihon University,Sakura-jōsui,Setagaya-ku, Tokyo,156.

Twenty six years ago, in1958 Wänke reported the contents of ^{45}Sc in iron meteorites and concluded that the most of them were due to cosmogenic products. The same author (1960) examined several specimens which have very low contents of cosmogenic stable nuclides and found that about 0.2 ppbSc,on the average, may be attributed to the natural origin, but up to ca.2 ppb can be attributed to be the products of cosmic ray irradiation for 10^8-10^9 years in space. Since 1960, however, no paper has been published on this problem.

Scandium is a monoisotopic element and the contents in meteorites could be due to natural scandium originally contained in irons or accidientally contaminated under terrestrial and laboratory conditions. To improve this ambiguity, the most important may be to eliminate any interference caused by contaminations and to prove that the blank in appropriate samples is really low, much lower than ppb levels. Recently some impurities found in iron meteorites have been reexamined for verious purposes. The presence of many lithophile elements, such as Mg,K,Ca,Ag, and U, has been attributed to the terrestrial contaminations, and these elements can be removed by careful samplings and pretreatments on the surface.

In this work, the surface layer of 1 - 2 gram size sample has been cleanced by extensive etchings before and after the irradiation of thermal neutrons. The doses of neutrons were at about 10^{17} n/cm^2 in a Triga II reactor at the Atomic Energy Inst., Rikkyo University. The cleaned samples were dissolved in aqua regia,and 1-5 mgSc carrier was added. Fe,Co,and others were removed by extraction and ion exchanges. Finally scandium fraction was eluted from a cation exchange column using 2N NH_4OAc (HOAc acidic), and the hydroxide was precipitated with ammonia. After the counting for ^{46}Sc by a Ge detector, the recoveries were determined by reirradiation of Sc or by weighing Sc_2O_3.

The samples examined so far are: Braunau, Canyon Diablo, Grant, Nativitas, Odessa (2 specimens), Trenton, Treysa, Toluca, Xhiquipilco, Yamato790517 and 790724. According to current results especially in our Odessa and Toluca samples which have extremely low contents of cosmogenic products, the contents of natural scandium in irons seem to be lower than 0.1 ppb. The limit of the detection sensitivity may easily be extended applying a higher neutron dose.

Based on these data, we may determine the dose of cosmic ray irradiation to the irons directly by this convenient method without any blank correction.

REFERENCE:
H.Wänke, Scandium-45 als Reaktionprodukt der Hoehenstrahlung in Eisenmeteoriten I, Z.Narurforschg.,13a,645(1958).
H.Wänke and H.König, Studies on Meteorites. Max-Planck Inst.f.Chem.,Mainz, p.54-57 (1960).

Magnetic Properties of Antarctic Polymict Eucrites

Takesi NAGATA and Minoru FUNAKI
National Institute of Polar Research, Tokyo.

The magnetic properties of achondrites have been very little known, mostly because rather few number of achondrites were recovered in the past. In Hey's Catalog of Meteorites (1966), only 69 achondrites in total have been listed. In a previous paper (Nagata 1980), 17 Antarctic achondrites are magnetically classified into 3 groups, namely, diogenites, ureilites and another group of eucrite + howardite + shergottite. The group of 5 Antarctic eucrites was magnetically characterized by a small content of ferromagnetic metal, i.e. 0.006～0.11 wt%, and the absolute domination of kamacite (80～100%) in the ferromagnetic metallic phase. All these five Antarctic eucrites are polymict eucrites. (Delaney et al 1982)

More number of polymict eucrites have been recovered from Antarctica since then. Figures 1 and 2 illustrate examples of two different thermo-magnetic characteristics of Antarctic polymict eucrites.

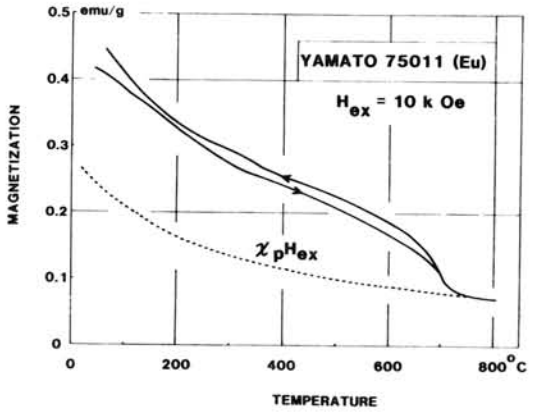

Fig. 1

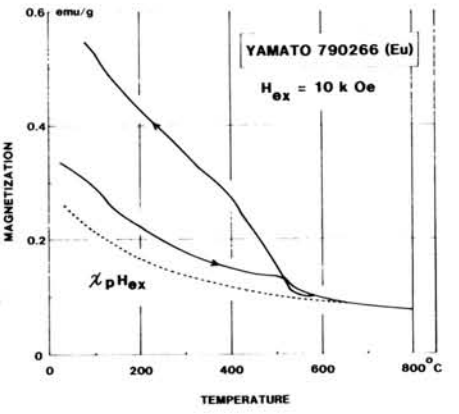

Fig. 2

A newly examined Yamato polymict eucrite (Fig. 1. Yamato 75011) can be thermomagnetically characterized by kamacite of 0.042 wt% in content, which is within the defined range of eucrites in the previously proposed magnetic classification scheme for achondrites. However, the thermo-magnetic (TM) curve of another Yamato polymict eucrite (Fig. 2. Yamato 790266) shows no presence of kamacite phase, but instead demonstrates presence of a ferromagnetic phase which has Curie point at 540°C and is thermally unstable, becoming enriched by heating up to 800°C in vacuum. Since the ferromagnetic phase of 540°C in Curie point, found in Yamato 790266 and Yamato 790122, tends to be enriched by a heat treatment and is apparently stable in succeeding heat treatments, this ferromagnetic phase could not be identified to plessite which is transformed to taenite by a heat treatment, but might be identified to either magnetite or taenite.

In Table 1, saturation magnetization (I_S), saturated remanent magnetization (I_R), coercive force (H_C), remanent coercive force (H_{RC}),

and Curie point (Θ_C) of 5 Yamato polymict eucrites and 3 Allan Hills polymict eucrites are summarized.

Table 1. Magnetic Properties of Antarctic Polymict Eucrites

Eucrite Sample	I_S (emu/g)	I_R (emu/g)	H_C (Oe)	H_{RC} (Oe)	Θ_C (°C)
(Yamato)					
YM-74159	0.061	0.0040	265	420	750
YM-74450	0.25	0.0044	58	70	758
YM-75011	0.084	0.0035	60	390	730
YM-790122	0.012	0.0016	45	550	538
YM-790266	0.0075	0.0013	35	240	538
(Allan Hills)					
ALH-76005	0.076	0.0009	15	-	750
ALH-77302	0.017	0.0017	42	780	(740, 585
ALH-78040	0.083	0.0072	90	560	(790, 575

According to Delaney et al (1982), YM-74159, YM-74450 and YM-75011 may be fragments of a single meteorite, because their petrography and mode are very similar to one another. ALH-76005, ALH-77302 and ALH-78040 also might come from a single meteorite, because of the same reason. The ferromagnetic characteristics of the three Yamato eucrites also are similar to one another. Although the magnetic properties of ALH-77302 are reasonably similar to those of ALH-78040, (to presume that they are fragments of a single meteorite), those of ALH-76005 are markedly different from those of the other two Allan Hills eucrites. The magnetic properties of YM-790122 and YM-790266 are similar to each other, but they are markedly different from the group of the other three Yamato eucrites in regard to their magnetic characteristics.

The ferromagnetic phases of 730～790°C in Curie point can certainly be identified to kamacite. The ferromagnetic phase in YM-790122 and YM 790266 has not yet been identified. Then YM-75011, YM-790122 and YM-790266 are examined with a reflection microscope for identifying opaque minerals and with EPMA for evaluating their chemical compositions. The results are summarized in Table 2. It will be almost definite that the ferromagnetic properties of YM-75011 are due to kamacite grains which are very close to metallic iron in their chemical composition. However, no metal can be detected in both YM-790122 and YM-790266, in which chemical compositions of ilmenite and troilite in the former are very similar to those in the latter. The chemical compositions of ilmenites in both eucrites are close to the stoichiometric $FeTiO_3$ and those of troilites to the stoichiometric FeS. The pyrrhotite phase as an impurity in FeS cannot correspond to the ferromagnetic phase of Θ_C=538°C, because Θ_C of pyrrhotite is 320°C.

Table 2. Chemical Composition of Opaque Minerals in these Yamato Polymict Eucrites

Eucrite Sample	Grain number	TiO_2 (wt%)	FeO (wt%)	Sum	Fe (wt%)	Ni (wt%)	Co (wt%)	S (wt%)	Sum
[YM-75011]									
(1)Ilmenite	4	54.94 (±0.45)	46.39 (±0.72)	100.33					
(2)Troilite	3				62.82 (±0.26)	0.001 (±0.00)	0.045 (±0.034)	35.97 (±0.27)	98.83
(3)Metal	7				98.74 (±0.37)	0.49 (±0.04)	0.50 (±0.13)	0.02 (±0.01)	99.74
[YM-790122]									
(1)Ilmenite	7	53.67 (±0.16)	45.85 (±0.63)	99.52					
(2)Troilite	8				63.64 (±0.47)	0.032 (±0.026)	0.14 (±0.10)	36.24 (±0.20)	100.06
[YM-790266]									
(1)Ilmenite	4	53.57 (±0.23)	45.86 (±0.38)	99.42					
(2)Troilite	5				63.63 (±0.47)	0.025 (±0.014)	0.006 (±0.01)	35.53 (±0.27)	99.16

The stoichiometric ilmenite is paramagnetic above liquid nitrogen temperature. However, there may be still a possibility that some titanomagnetite phases of TiO_2-FeO-Fe_2O_3 in chemical composition (e.g. Nagata 1961) can stand for the observed ferromagnetic phase.

Magnetic Properties of Antarctic Iron Meteorites

Takesi NAGATA*, Minoru FUNAKI* and Isamu TAGUCHI**
* National Institute of Polar Research
** R&S Laboratories - I, Nippon Steel Corporation

Chemical and metallographical studies on Antarctic iron meteorites have systematically started recently by a Japanese research group. Magnetic properties also are examined for these Antarctic iron meteorites whose chemical compositions have been known. Table 1 shows magnetic properties such as saturation magnetization (I_S), saturated IRM(I_R), coercive force (H_C), remanence coercive force (H_{RC}), transition temperature from α-phase to γ-phase in the heating process (Ⓗ*$\alpha \rightarrow \gamma$) and trnsition temperature from γ-phase to α-phase in the cooling process (Ⓗ*$\gamma \rightarrow \alpha$) together with the major chemical elements (Ni, Co, P) and typical rare elements (Ga, Ge, Ir) of three Antarctic iron meteorites, YM-790724, ALH-77263 and ALH-77289.

Table 1. Magnetic Properties and Chemical Compositions of Antarctic Iron Meteorites (I)

	YM-790724 (III-A)	ALH-77263 (I)(0g)	ALH-77289 (I)(0g)	
I_S	196.0	207.4	200.9	(emu/g)
I_R	0.12	0.06	0.07	"
H_C	3.0	2.0	2.0	(Oe)
H_{RC}	168	79	75	"
Ⓗ* $\alpha \rightarrow \gamma$	745	755	750	(°C)
Ⓗ* $\gamma \rightarrow \alpha$	592	618	616	"
Ni	7.47	6.78	6.74	(wt%)
Co	0.45	0.47	0.52	"
P	0.12	0.20	0.18	"
Ga	15.6	99.4	97.5	(ppm)
Ge	48.9	409	360	"
Ir	10.0	3.1	3.5	"

Both magnetic properties and chemical compositions of ALH-77289 are close to those of ALH-77263. It seems most likely therefore that these two iron meteorites are fragments of a single octahedrite mass of Group I.

Both magnetic properties and chemical composition of YM-790724 are definitely different from those of the two iron meteorites of Chemical Group I. Bases on the chemical composition YM-790724 can be classified into Chemical Group III-A. Corresponding to the chemical composition, Ⓗ*$\gamma \rightarrow \alpha$ value of ALH-790724 is considerably smaller than Ⓗ*$\gamma \rightarrow \alpha$ values of ALH-77263 and ALH-77289.

Two iron meteorites recovered from Allan Hills and two irons from

Derick Peak have been magnetically and chemically analyzed. Data of the analyses are summarized in Table 2.

Table 2. Magnetic Properties and Chemical Compositions of Antarctic Iron Meteorites (II)

	DRPA-78003	DRPA-78007	ALH-76002	ALH-77255	
I_S	211.2	200.0	212.2	188.2	(emu/g)
I_R	0.50	0.53	0.30	0.45	"
H	7.5	4.0	6.2	9.0	(Oe)
H_{RC}	67	272	130	223	"
ⓓ* $\alpha \rightarrow \gamma$	753	762	776	728	(°C)
ⓗ* $\gamma \rightarrow \alpha$	637	674	643	555	"
Ni	5.4	7.3	7.2	12.2	(wt%)
Co	0.51	0.38	0.60	0.61	"
P	0.40	0.75	0.40	0.03	"

DRPA-78003, -78007 and ALH-76002 are typical octahedrites, but ALH-77255 is an unusual iron meteorite, which consists of a large number of intergrowth of kamacite and taenite.

Saturday, March 24, 1984

0945 - 1150 Presentation, Auditorium

MICROSTRUCTURAL AND THERMOANALYTICAL CHARACTERIZATION OF SEVERAL ANTARCTIC METEORITES

M.Żbik[1], B.Lang[2], A.Grodziński[3] and L.Stoch[4]
1/ Warsaw University, Department of Geology, 02-089 Warsaw, Poland,
2/ Warsaw University, Department of Chemistry, 02-089 Warsaw, Poland,
3/ Institute of Electronic Materials, 02-075 Warsaw, Poland
4/ Technical University of Mining and Metallurgy, 30-059 Cracow, Poland.

An attempt is made to bridge the earlier studies of morphological features of pore spaces in a number of meteorites of various type [see Żbik, 1982; Żbik and Lang, 1983] and those of thermochemical behavior during heating of Yamato-74013 and -74010 diogenites [Lang et al., 1984 /in press/]. The present study covered 3 achondrites from Antarctica : Yamato-7308 howardite and Yamato-74450 and ALH-765 polymict eucrites. So, making allowance for our earlier work on diogenites we arrived at the thermoanalytical characterization of Antarctic HED /howardites-eucrites-diogenites/-achondrites - as they are termed by Takeda et al. [1983] . For reference to earlier obtained thermoanalytical curves [see Lang et al., 1981] our study covered also Yamato-75102 L-6 chondrite.

Some microstructural features of the examined meteorite samples were observed with SEM method. Our attention has been focused on microcracks and abundant intergranular void spaces - micro- and mesopores - in brecciated structures and between basaltic clasts and fine matrix material. Our observations are exemplified with microphotographs of the Yamato-75102 L-6 chondrite (Fig. 1, a, b) . Secondary mineralization from weathering process was observed in the Yamato-7308 howardite.

We obtained differential thermal /DTA/ and thermogravimetric /TG/ curves for the examined meteorite samples. The latter were heated at the rate of 10°C/min up to 1200°C. Two kinds of thermoanalytical curves were obtained. From heating in air the recorded response was strongly influenced by oxidation processes. At temperatures not exceeding 350°C the sulfides are affected by phase transitions, while at higher ones possibly oxidation of pyrrhotite to magnetite becomes important. However, these processes are weakly reflected on the TG-curves. Only at temperatures higher than 450°C a significant mass increase is observed. It substantiates oxidation of iron as the most sensitive component of the metal phase. Generally oxidation occurs in Fe-Ni-O system. For such a reason the total mass increase during heating in air is controlled by the abundance of FeNi in the meteorite composition.

Heating in argon suppressed the oxidation process as produced by oxygen from air, but in such a case thermogravimetric monitoring was not available. Heating in argon facilitates revealing features due to reversible processes as polymorphic transitions.

52 – 2

In Fig. 2a, b are given the thermoanalytical curves for the Yamato-7308 howardite. In Fig. 2a are shown the curves for air, while in Fig. 2b the DTA-curve for argon. In Fig. 3a, b are shown the thermoanalytical curves for the Yamato-75102 chondrite.

Compared with other thermoanalytical curves as received for various meteorites those for the examined Antarctic ones are markedly depleted in thermoanalytical features. Such a characterization argues for low importance in the composition of these meteorites of both sulfide and metal phase.

Oxidation of meteorites during heating in air must strongly depend upon access of oxygen to mineral components sensitive to oxidation. Open porosity components as microcracks and intergranular void spaces certainly make easier such an access. However in the examined Antarctic meteorites this expected effect appeared to weak to be recorded.

References

Lang, B., Grodziński, A. and Stoch, L. (1981) Meteoritics 16, 345 - 346.
Lang, B., Grodziński, A. and Stoch, L. (1984) Mem.Natl Inst. Pol.Res. Spec.Issue No.30 /in press/.
Takeda, H., Mori, H., Delaney, J.S., Prinz, M., and Harlow, G.E. (1983) Eight Symposium on Antarctic meteorites /abstract/, 27-1 - 27-3.
Żbik, M. (1982) Bull. Acad.Pol.Sci.,Ser.Sci.Terre 30, 59 -65.
Żbik, M., and Lang, B. (1983) Morphological features of pore spaces in chondrules in Chondrules and their origins, E.King, editor, LPI, Houston, p. 319 - 329

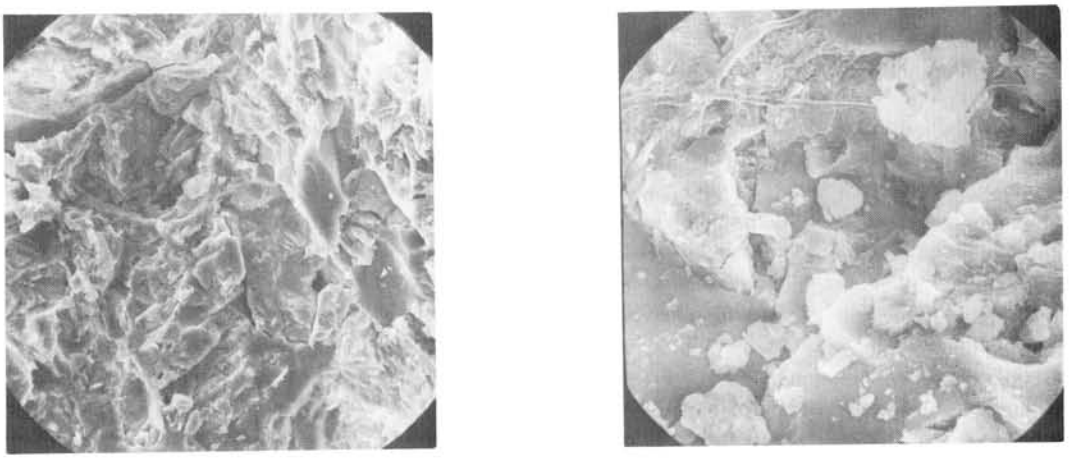

a b

Fig. 1

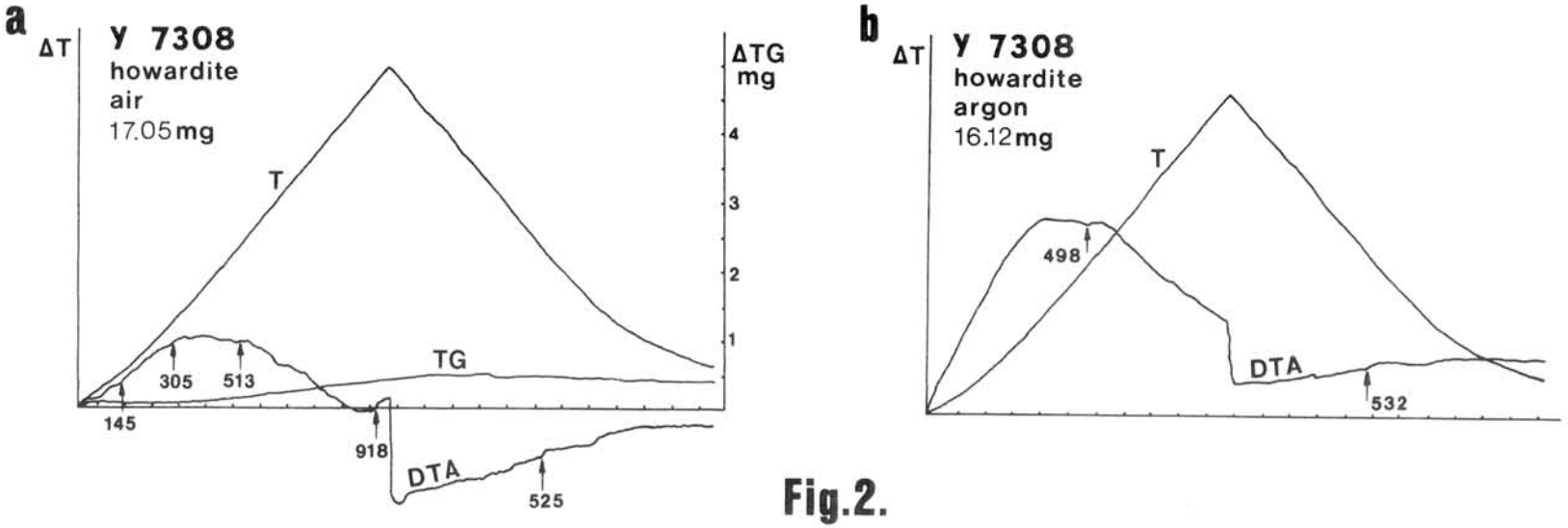
a
ΔT
y 7308
howardite
air
17.05mg
ΔTG
mg
T
TG
305
513
145
918
DTA
525
4
3
2
1
b
ΔT
y 7308
howardite
argon
16.12mg
T
498
DTA
532

Fig.2.

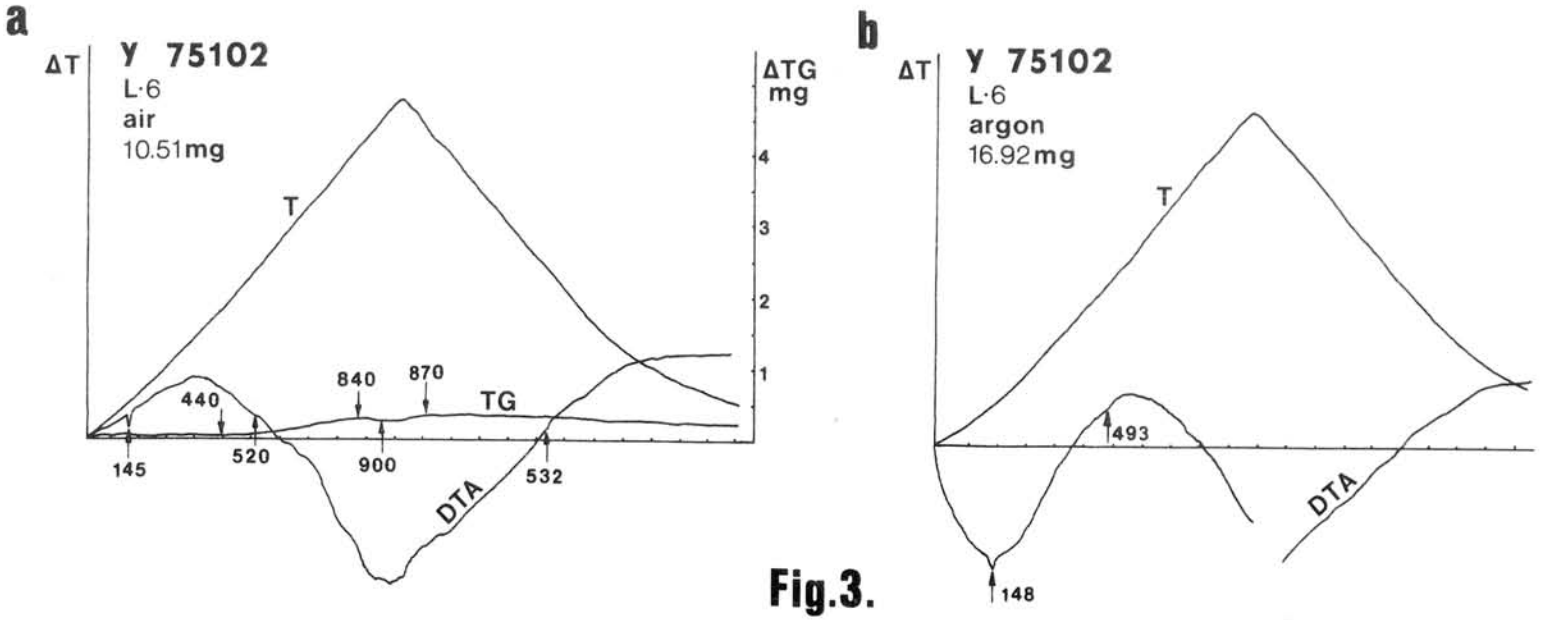
a
ΔT
y 75102
L·6
air
10.51mg
ΔTG
mg
T
840
870
440
TG
145
520
900
532
DTA
4
3
2
1
b
ΔT
y 75102
L·6
argon
16.92mg
T
493
148
DTA

Fig.3.

53－1

OBSERVATIONAL EVIDENCE RELATING NEAR-EARTH ASTEROID COMPOSITION TO METEORITES. McFadden, L.A.[1], Gaffey, M.J.[2], Takeda, H.[3]. [1]Univ. of Maryland, College Park, MD, USA, [2]Univ. of Hawaii, Honolulu, HI, USA, [3]Univ. of Tokyo, Tokyo.

Geochemical analyses of meteorites indicate that they are fragments of small solar system bodies. Efforts to identify their parent bodies are limited by the lack of extraterrestrial material for in situ laboratory studies and by limitations of existing remote sensing techniques. Nevertheless, careful analysis of remotely sensed data can contribute to an understanding of the relation between meteorites and objects currently in their own orbit around the Sun. A potential source of meteorites, the near-Earth asteroids, is currently under remote study from the Earth. Active programs exist to locate these small asteroids (1,2) and to characterize their physical (3) and chemical properties (4). Based on reflectance spectroscopy of 17 near-Earth asteroids and interpretation in terms of mineralogy and petrology (4) experimental evidence can begin to address the relation between these two solar system components.

The basis for this evidence is the fact that combinations of certain reflectance features (albedo, absorption bands and/or slopes) are characteristic of specific minerals which in turn can be related to meteorite classes. When an asteroid has the same spectral features as a meteorite class, its surface composition is inferred to be analogous to that of the meteorite, although it is not necessarily a fragment from any particular surface. Dynamical evidence can strengthen any suggested link between two objects. The spectrum of each meteorite class is characteristic of that class in the spectral region (0.33-2.5 μm) and with spectral resolution (1.5%) of the laboratory data. Laboratory spectra of meteorites have been measured for both non-antarctic (5) and antarctic meteorites (6). A comparison of main belt asteroids to meteorites was made prior to the availability of the antarctic meteorites (7). Most near-Earth asteroid spectra were measured between 0.33-0.96 μm with wavelength resolution of 0.025-0.030 μm, equivalent to 2.5-10% resolution. These observational limitations are due to the apparent faintness of the asteroids and the sensitivity of the detector. The spectra are scaled to 1.0 at 0.56 μm and are not calibrated to an absolute brightness. Albedo has been measured independently for some of these asteroids.

None of the observed near-Earth asteroids have spectra similar to irons, stony-irons, nor the rare achondrites such as Nakhla, Angra dos Reis, Chassigny, Novo Urei, Shergotty, or ALHA77005. Based on the presence of a strong UV absorption, position of the 0.90- μm band and albedo, 1915 Quetzalcoatl has a composition equivalent to diogenites. The spectra of polymict eucrites and recrystallized diogenites abundant in the antarctic collection do not have spectral features that differ from common eucrites and diogenites at the wavelength resolution of the asteroid data. The spectrum of 1862 Apollo has absorption bands in the same position and of the same strength and albedo as LL4 ordinary chondrites. 1980AA has the same characteristics as a shocked, black chondrite, a shock metamorphosed ordinary chondrite with a low albedo, weak 0.90 μm and a generally linear UV absorption. An albedo calculation of 1980AA will test this interpretation. There are no enstatite chondrite analogues measured to date. Among the antarctic collection are some black, fine-grained, vesicular, vitrified ordinary chondrites of LL bulk chemistry (8). Spectra of 433 Eros, 887 Alinda and possibly 1036 Ganymed, 1620 Geographos and 1981QA (although there is no or poor coverage of the 1.0 μm region for these asteroids) have similar spectral characteristics as these meteorites. Of these, 887 Alinda and 433 Eros have albedos of 0.166 and 0.125, consistent with the albedo of these glassy chondrites (albedo has not been determined for the others mentioned above). These meteorites indicate that a glassy matrix can also

suppress mafic silicate absorption bands and reduce the albedo of an asteroid in the same manner that small amounts of carbonaceous material does in C3 type meteorites without masking the UV band completely. 433 Eros has been interpreted as an H or L chondrite (9) and 887 Alinda has been interpreted as an H3 (10) and a C3 (11) chondrite. Spectral coverage to 2.5 μm can constrain some of these possible interpretations. The reflectance of 433 Eros is higher in the near-infrared than that of the glassy ordinary chondrites which would not support this interpretation without invoking optical alteration of Eros' regolith (which has to also be invoked for the comon ordinary chondrite interpretation (9)). The spectrum of 2100 Ra-Shalom has the features and albedo of a carbonaceous type 2 chondrite. The other known dark asteroid, 1580 Betulia, does not have the strong UV absorption edge of carbonaceous chondrites.

Experimental evidence indicates that some near-Earth asteroids are possible meteorite parent bodies. Based on existing data, the absence of irons is consistent with cosmic ray exposure ages indicating a longer surface residence time than the statistical mean lifetime of near-Earth asteroids (12). Unless optical alteration of asteroid regoliths is invoked, there are some near-Earth asteroids tha appear not to have sent fragments to the Earth (e.g. 1685 Toro, 1580 Betulia, 1943 Anteros, 1979VA, 2201 Oljato). Therefore, not all near-Earth asteroids are meteorite parent bodies. It is possible that meteoritic analogues of these asteroids have not been found yet on Earth. It is also possible that some of the meteoritic analogues not found among the near-Earth asteroids have not been discovered and/or measured yet either. The components of the dark, glassy chondrites found in Antarctica should be studied as mineral separates and compared to lunar agglutinates to enhance our understanding of asteroid regoliths.

We thank NIPR for supplying some of the meteorite samples.

References:

1) Helin, E.F. and Shoemaker, E.M. (1979), Icarus, 40, 321-328.
2) Gehrels et al. (1983) Bull. Am. Astr. Assoc., 15, 824.
3) Veeder et al. (1983) Bull. Am. Astr. Assoc., 15, 824.
4) McFadden et al. (1984) submitted to Icarus.
5) Gaffey, M.J. (1976) J. Geophys. Res., 81, 905-920.
6) McFadden et al. (1980) 13th Lunar and Planet. Symp., Tokyo, 173-180.
7) Chapman, C.R. and Salisbury, J.W. (1973) Icarus, 19, 507-522.
8) Sato et al. (1982) 7th Symp. on Antarctic Meteorites, Tokyo, 9-10.
9) Pieters et al. (1976) Icarus, 28, 105-115.
10) McCord, T.B. and Chapman, C.R. (1975) Astrophys. J., 197, 781-790.
11) Gaffey, M.J. and McCord, T.B. (1978) Space Sci. Rev., 21, 555-628.
12) Arnold, J.R. (1964) Isotopic and Cosmic Chemistry, ed. H. Craig et al., North Holland Publ. Co., Amsterdam.

54－1

Grain Formation of Primordial Materials of Meteorites

Hiroichi HASEGAWA and Takashi KOZASA
Dept. of Phys., Fac. of Sci., Kyoto Univ., Kyoto 606

Primordial grain materials of meteorites are produced originally in the gas envelopes around the mass loss stars. The main contribution for grains comes from the cool luminous stars such as M giants. According to the nucleation and growth theory, submicron Mg-silicate grains, Fe grains (a few tens of Å) are produced. These grains diffuse into the interstellar space. Observation of stellar extinction can be interpreted by these grains (sizes and composition). In the molecular clouds, the H_2O molecules condensate as mantles of Mg-silicate grains. Thus the primordial grains for the solar system are submicron Mg-silicate grains with H_2O ice mantles and finer Fe or Fe oxide grains.

In the primordial solar nebula, these grains suffer the reheating according as the location. Far from the protosun they are unchanged. In the inner region ice mantles are evaporated. In the more inner region Mg-silicates and FeO component are partially evaporated and Ca-Al component remains. In the innermost region all the grains are evaporated, and afterwards the refractory elements are recondenced when the solar nebula is cooled down. Two cases should be considered. In the first case Ca-Al minerals and Mg-silicates condence as grains separately. Because of the higher gas pressure (compared with the stellar envelope) grain size r(Å) for Mg-silicates is given by $\log r=2.3+0.84\log(p\tau)$ (p the total gas pressure and τ the cooling time). The size of Ca-Al mineral grains is about 1/10 as small.

In the second case the Mg-silicates condence on the Ca-Al minerals. Then the grains have complex composition similar to the original gas abundance with the size given by $\log r=1.6+0.77\log(p\tau)$.

Because of large surface tension (1800 erg/cm^2), iron would condence in the very supersaturated condition. The Fe gas can exist under the equilibrium temperature of Fe. Under this condition, the equilibrium temperature of Fe compounds such as FeO does not differ so much from the equilibrium temperature of metalic iron. On the other hand, the surface tension of Fe decreases very much due to the impurities especially sulphur. Thus the three processes of condensation of Fe are competing; the nucleation and growth of metalic Fe (impurity S), the nucleation and growth of Fe on the substrate of preexisting mineral grains and the gas-solid reaction between Fe gas and mineral grains. The first process supplies the metalic iron component and irons from the second and the third processes may be the sources of Fe^{++} in meteorites.

55－1

SHAPE ANALYSIS OF Fe-Ni GRAINS AMONG ANTARCTIC ORDINARY CHONDRITES

Naoyuki Fujii, Hiroyuki Takeuchi, Keisuke Ito, and Masamichi Miyamoto(*)
Dept. Earth Sci., Kobe Univ., Nada, Kobe 657.
(*)Dept. Pure & Appl. Sci., Tokyo Univ., Meguro, Tokyo 153.

Irregular shape of Fe-Ni grains among ordinary chondrites has expected to reflect some events of lithification and deformation processes during evolution, 'thermal' metamorphism and fragmentation of chondritic parent bodies. Fe-Ni grains mostly exist at boundaries among chondrules. In this paper, results of the shape analysis for Fe-Ni grains are presented by using the two-dimensional Fourier Descriptors and some statistical analyses of the grain shape distribution for selected Antarctic ordinary chondrites: ALH-77233 (L4), ALH-77115 (H6), ALH-77230 (L4), ALH-77105 (L6), and ALH-77231 (L6).

Three mutually perpendicular surfaces were cut and ground flat from each chondrite and named A, B and C, each of which covered with an area of about 3 x 5 mm. The computer-aided microscopic picture analyzing system was developed for the digitizing and processing procedure as reported previously.

Figs. 1a and 1b demonstrate examples of the digitized outlines of Fe-Ni grains from H4-A and L4-A, respectively. Instead of applying normally used polar angle co-ordinate, a radial distance R_j from the center of gravity is defined as a function of perimeter length. R_j is then expanded in a finite Fourier series as shown in Fig. 2, in which B_k and D_k are the Fourier Descriptors. Examples of R_j and B_k for Fe-Ni grains in H4-A and L4-A are shown in Figs. 3a and 3b, respectively. Both grains have large values of B_2, which indicate that an over-all outline can well be fitted to an elipse. However, the shape irregularity is evidently different. The shape parameter defined by $L/\sqrt{S}$ are 11.0 and 5.7 for grains from H4-A and L4-A, respectively, where L is the total perimeter length ($L=\langle \Sigma \Delta \underline{l} \rangle$) and S is the area. Values of $L/\sqrt{S}$ generally increase with the increase of S for each surface. However, no distinguishable difference of this correration among chondrites studied is observed, partly because of considerable scatter in the $L/\sqrt{S}$ vs S diagram.

The difference of mean values of axial ratios ($\underline{b}/\underline{a}$) between H4 and H6 would suggest that higher grade metamorphism could make Fe-Ni grains rounded (Fig. 4), in which $\underline{a}$ and $\underline{b}$ are calculated by using the principal component analysis for each sample surface and lengths of principal and semi-major axes, respectively. For L-chondrites, however, this difference is not clear partly due to small number of grains. Fig. 5 shows the average value of the shape parameter ($SP = \langle (\Sigma \underline{l} \cdot \sqrt{S}) / \Sigma S \rangle$) for each sample surface as a function of the number of grains, in which grains are numbered by decreacing order in S and n is the number of grains averaged. The value of SP for each surface tends to approach to a constant value as n increases. If the shape parameter of the larger grains represent the value of SP, the curves should be nearly horizontal and smooth as seen in the bottom in Fig. 5. It is noticed that H-chondrites have higher values of SP than those of L-chondrites and unequilibrated chondrites seem to contain more irregular shaped Fe-Ni grains and smaller axial ratios.

The shape irregularity of Fe-Ni grains is likely to be reduced as the deformation of chondrules and Fe-Ni grains proceed during the metamorphism in a chondritic parent body. Although there remain several difficulties to obtain physically meaningful averages of above parameters and to distinguish the differences among petrologic types and other physical properties, this approach could provide some clues to investigate the mechanisms of lithification and deformation processes within chondritic parent bodies.

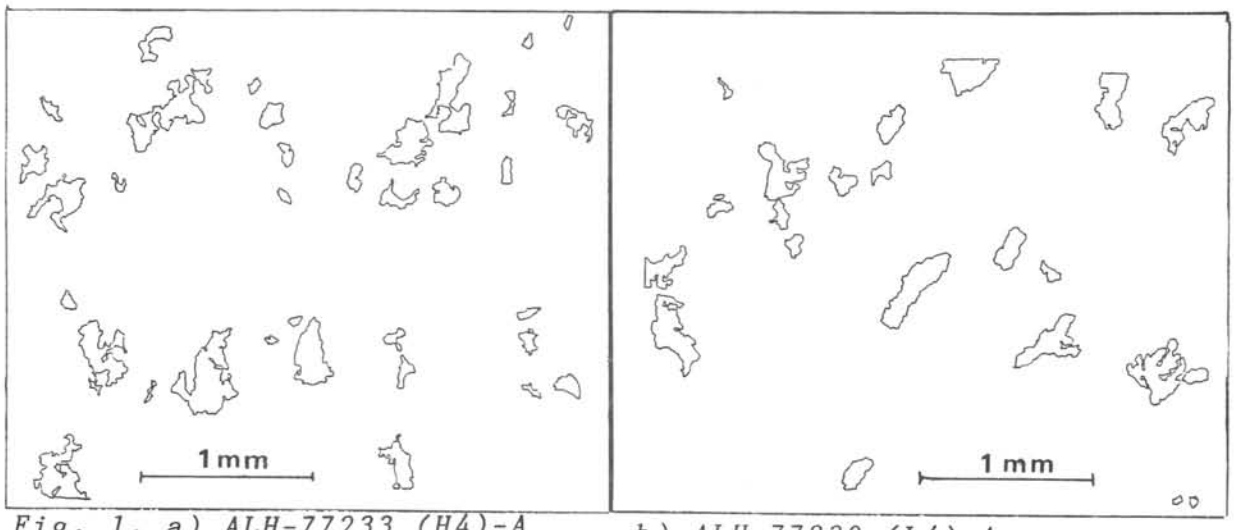

Fig. 1. a) ALH-77233 (H4)-A b) ALH-77230 (L4)-A

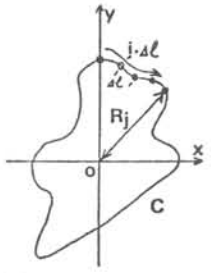

Fig. 2.

$$Rj = Ro + 2\sum_{k=1}^{(N-1)/2} Bk \cdot \cos(j \cdot k/N - Dk)$$

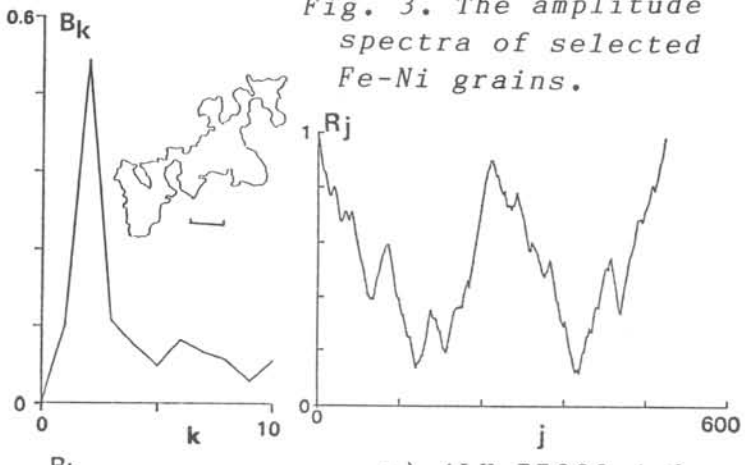

Fig. 3. The amplitude spectra of selected Fe-Ni grains.

a) ALH-77233, A-3.

b) ALH-77230, A-13.

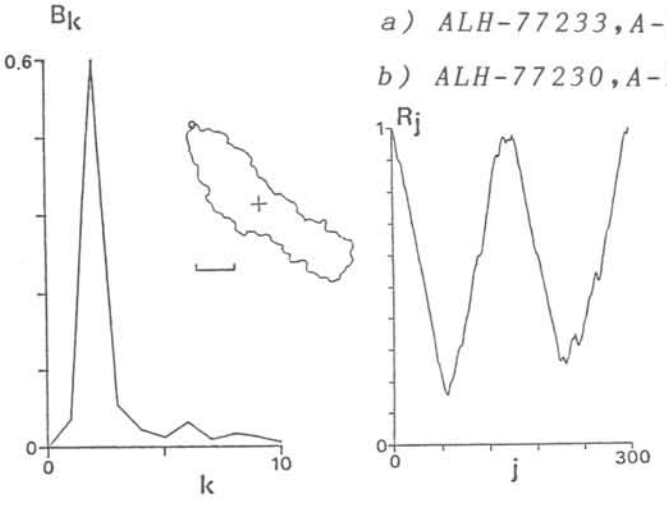

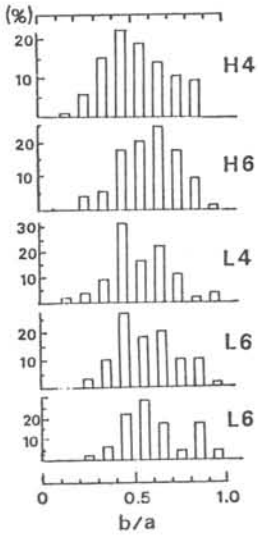

Fig. 4. Distribution of the axial ratio (b/a).

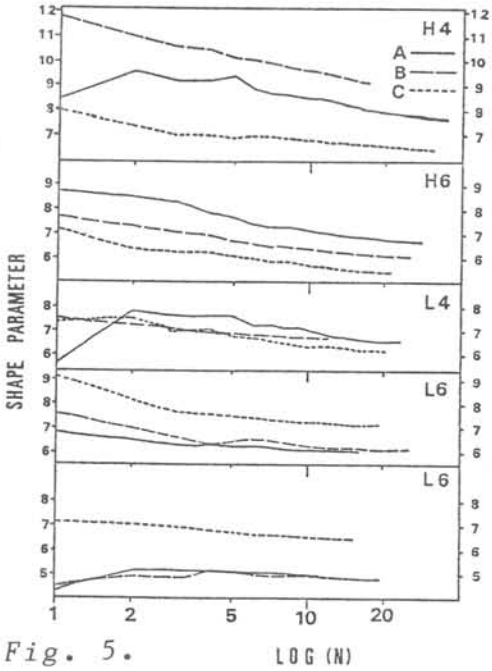

Fig. 5.

56

METEORITE as a possible guiding star for the creation of new materials under micro gravity

Tsuyoshi Tanaka
(Geological Survey of Japan, Higashi 1-1-3, Yatabe, Ibaraki 305, Japan)

Metal, polimer and ceramics are the fundamental materials of many industrial products. In recent progress of technology, many "new materials" with special physical and chemical features are required. One of the condition to create such materials is believed to be micro gravity field. In the micro gravity field, for example, mechanical mixing of two melts with different densities is easy. Many experiments under the micro gravity field are planned by using material testing rocket(NASDA) and Spacelab(NASA).

However, such special features created in space under micro gravity are observed in some meteorites and their constituents minerals. Definite example is pallasite, which is a mixture of two different materials with different densities. Wollastonite wiskers in Allende meteorite are considered as produced by gas diffusion (Miyamoto et al., 1979). $BaTiO_3$ is one of the "new materials" of electronics and also found in Allende meteorite (Tanaka and Okumura, 1977)..... Many analogous features and textures are recognized between meteoritic materials and "new materials" of technology(Tanaka, 1982,1983).

I would like to emphasize that more attention from technological view point should be paid on the studies of meteorite. Extensive studies of physical, mineralogical and chemical properties of meteorites and their constituent minerals will serve us many unknown informations on the technological experiments otherwise attained only by using expensive Spacelab or rocket.

Miyamoto, M. Onuma, N. and Takeda, H.(1979) Geochemical J. v.13, p.1-6.
Tanaka, T. (1982) Monthly Geology no. 333, p.24-30.
Tanaka, T. (1983) Industrial Science and Technology v.11, p.54-58.
Tanaka, T. and Okumura, K.(1977) Geochemical J. v.11, p.137-145.

The Martensitic Transformation and the Change of Thermo-Remanent Magnetization

Kan-ichi Momose[1], Hiroyuki Nagai[2] and Yoshitoshi Muraoka[3]

(1)Department of Geology, (2)Department of Physics, Faculty of Science and (3)Department of Physics, Faculty of Liberal Arts, Shinshu University, Matsumoto 390.

The martensitic transformations of Fe-Ni alloys occured by cooling, rolling or grinding. The phenomena depend on the sample shape besides the chemical composition. The experimental results are listed in Table 1.

In order to study the remanent magnetization of meteorite it is very important to investigate whether the remanent magnetization in fcc phase is preserved in bcc phase after the martensitic transformation, or not. The 29at%Ni-Fe alloy satisfied the following magnetic properties according to the thermal hysteresis of the magnetization of Fe-Ni alloys.

(i) The Curie temperature (T_c) of fcc phase is higher than room temperature (T_r).

(ii) The martensitic transformation temperature (T_{Ms}) is lower than T_r.

(iii) The fcc phase changes to bcc phase at 77K.

The thermo-remanent magnetization (TRM) of 29at%Ni-Fe alloy was magnetized at 650°C for 2hrs in vacuum of 10^{-3}pa in the heatproof brick. The direction and the intensity of the TRM of this alloy were measured before and after cooling at 77K. The results are as follows:

TRM	original	cooling at 77K in zero external field
Declination	-24.73°	-91.24°
Inclination	58.92°	8.30°
Magnetization J ($x10^{-3}$emu/gr)	11.494 ($=J_0$)	1.846

These results showed that the direction and the intensity of the magnetization changed markedly in magnitude ($J/J_0=0.161$).

Furtheremore, we investigated whether the martensitically transformed bcc phase could be magnetized in the magnetic field during the martensitic transformation. We used the 25at%Ni-Fe alloy because T_{Ms} is higher than T_c of fcc phase, namely, the martensitic transformation occurs in paramagnetic

fcc phase. The TRM of 25at%Ni-Fe alloy were as follows:

TRM	original	cooling at 77K in zero external field
Declination	-10.94°	-64.98°
Inclination	59.65°	2.88°
Magnetization J ($x10^{-3}$emu/gr)	7.208(=J_0)	3.036

The experimental results of 25at%Ni-Fe alloy show that the direction and the intensity of the magnetization changed markedly in magnitude (J/J_0=0.421).

Table 1. The experimental results of Fe-Ni alloys

Sample	Original	Annealing	Cooling at 77K	Rolling or Grinding
29at%Ni-Fe(b)	fcc(from melting P)	fcc(800°C-750°C)	bcc + fcc	bcc + fcc (R)
29at%Ni-Fe(p)	fcc(from melting P)	fcc(800°C,1-2hrs.)	fcc	bcc + fcc (G)
28at%Ni-Fe(b)	fcc(from melting P)	fcc(800°C-750°C)	bcc + fcc	bcc + fcc (R)
28at%Ni-Fe(p)		fcc(800°C,1-2hrs.)		bcc + fcc (G)
27at%Ni-Fe(b)	bcc>>fcc(quenched from 1150°C)	bcc>>fcc		bcc > fcc (R)
27at%Ni-Fe(p)		fcc(600°C,1hr.)	fcc>>bcc	
26at%Ni-Fe(b)	bcc>>fcc(quenched from 1150°C)	bcc>>fcc (750°C,24hrs.)		bcc (R)
26at%Ni-Fe(p)		fcc(600°C)	fcc > bcc	bcc > fcc (G)

* (b):block sample, (p):powder sample, (R):rolling, (G):grinding

NRM directions around a cm-size inclusion in Allende

N. Sugiura and D.W. Strangway
University of Toronto, Toronto, Canada

Natural Remanent magnetization (NRM) of a cm size inclusion and the surrounding matrix in Allende were measured to assess when this meteorite was magnetized.

Sample description: The sample (Fig. 1) has a light-grey coloured inclusion. Surrounding portions of the matrix are referred to as M1, M2 and M3 as shown in the figure. M1 and M2 are similar portions of chondrule-rich matrix. M3 is poor in chondrules and its boundaries with M1, M2 and the inclusion appear to be faults. A dark rim is seen along parts of the boundary between the inclusion and M1 and M2. The rim is most conspicuous at the boundary with M2 (hatched area in Fig. 1).

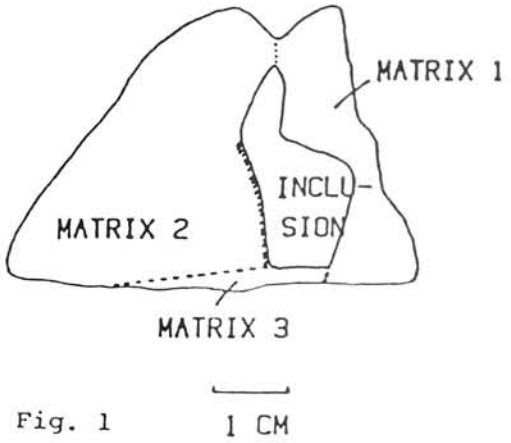

Fig. 1

Experiments: The NRM directions of small (200mg) specimens were measured with a superconducting magnetometer. A soft secondary component of NRM was detected in many specimens from the upper right corner illustrated in Fig. 1. This may be an IRM acquired by exposure to a magnet. Alternating field (AF) demagnetization was done to erase this IRM. In most cases less than 50 Oe was needed to erase the IRM. The NRM after the AF demagnetizations are shown in Fig 2. All the matrix and the inclusion samples have roughly the same NRM directions. But there are significant differences between M1, M2 and (M3 + inclusion). There is a systematic change in NRM direction among M2 specimens. Specimens from the left hand side of M2 (Fig. 1) show increasing inclinations approaching the boundary with the inclusion. The NRM direction of M2 samples near the boundary is similar to that in the M1 samples.

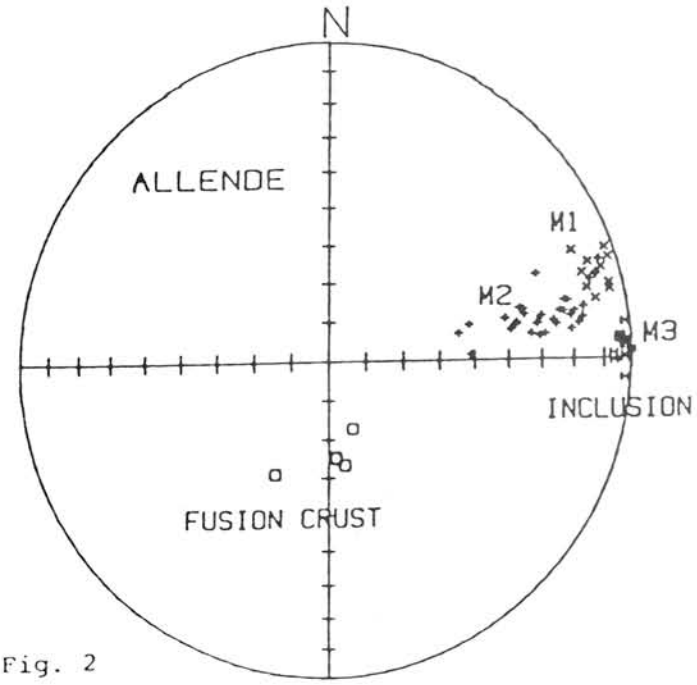

Fig. 2

Stepwise thermal demagnetization was done for many specimens. As the demagnetization temperature approaches 320 C (Curie point of pyrrhotite), the NRM directions start changing, and reach a stable direction at

temperatures above 320 C (Fig.3). This high temperature component of NRM is almost randomly distributed (Fig.4) except for the grouping shown by three specimens from the inclusion. The intensity of the high temperature component is very weak and is only several times 10^{-7} emu for each specimen.

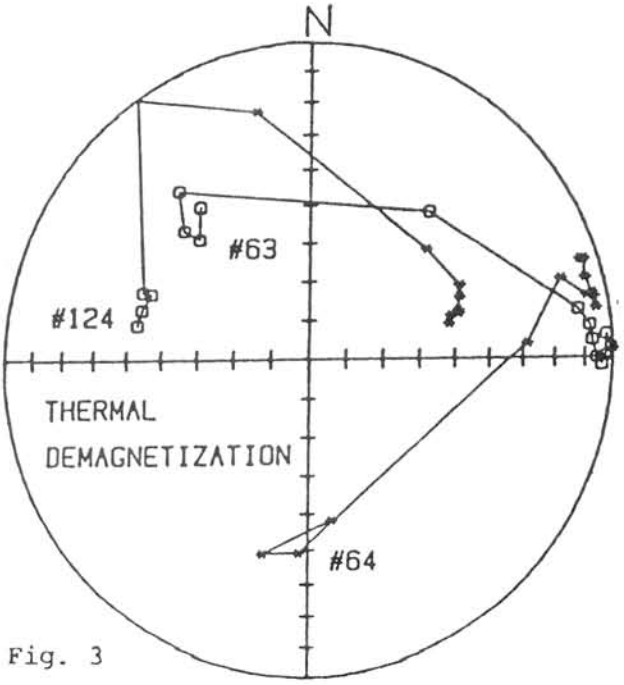

Fig. 3

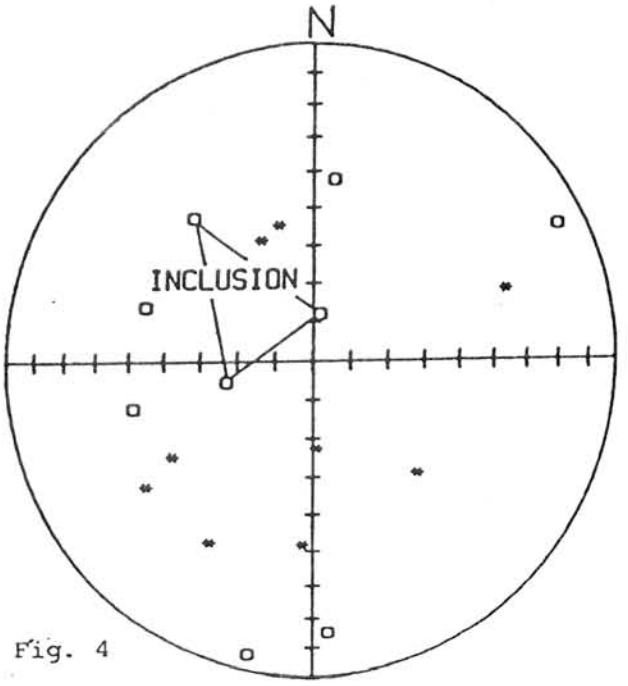

Fig. 4

NRM HIGH TEMPERATURE COMPONENT

Interpretation: Since the sample is almost homogeneously magnetized, we assume the sample was remagnetized (probably by chemical remanence) after accretion. Small differences among M1, M2 and (M3 + Inclusion) and the differences within M2 are thought to be a result of mechanical deformation which occurred when the faults were formed. Since the difference in NRM direction within M2 is as much as 40 degrees, quite a large deformation is required. This suggests that the matrix must have been soft and porous before the deformation.

Since the directions of the high temperature component of NRM are almost randomly distributed, the high temperature component is likely to be carried by chondrules which were magnetized before accretion (1). Intensities of the high temperature component are also well explained if they are carried by chondrules since our earlier studies showed that chondrules are weakly magnetized.

The dark rim surrounding the inclusion does not have the same high temperature component as that of the inclusion. This strongly suggests that the rim is probably not part of the inclusion.

A detailed study of individual chondrules in the present sample will be done in the near future. The present results confirm our previous interpretation that the previous magnetic fields existed (a) during the formation of chondrules, (b) during the formation of the inclusion, and (c) during the thermochemical event which remagnetized the whole sample, but the mechanical deformation which formed faults in Allende did not cause remagnetization.

REFERENCES

(1) N. Sugiura et al. (1979) Phys. Earth Planet. Interi. 20, 342-349.

Special Lecture

Saturday, March 24, 1984

1330 - 1530 : Robert N. Clayton, Professor of Chemistry, Enrico Fermi Institute and Department of Chemistry and the Geophysical Sciences, University of Chicago

Title: Isotopic Cosmochemistry of Oxygen and Silicon

Isotopic Cosmochemistry of Oxygen and Silicon

Clayton, R.N., Mayeda, T.K. and Molini-Velsko, C.A.

University of Chicago, Chicago, IL 60637

Simultaneous measurements of oxygen and silicon isotopes of individual chondrules and inclusions are used to search for correlated processes of isotopic fractionation and reservoir interaction during chondrule formation. Chondrules from the H3 chondrite, Dhajala, show heavy-isotope enrichment in silicon in smaller chondrules, probably associated with evaporative loss of silicon. The corresponding effect in oxygen is an ^{16}O enhancement due to exchange with nebular gas. Ferromagnesian chondrules from Allende show similar effects but require isotopically different precursor materials. Silicon isotope variations in refractory inclusions in Allende are ten times greater than in Allende chondrules, implying extensive evaporation and recondensation of silicon, as has also been concluded for magnesium and calcium in these inclusions. On three-isotope plots of $^{29}Si/^{28}Si$ versus $^{30}Si/^{28}Si$, silicon data in all three instances fall on a slope-1/2 line, indicating that ordinary mass-dependent fractionation processes are dominant. However, in all three cases, the plots of $^{17}O/^{16}O$ versus $^{18}O/^{16}O$ define trends with slope = 1, which are incompatible with mass-dependent fractionation, and probably result from interaction of isotopically distinct reservoirs. Thus, the two most abundant elements of the meteorites are governed by fundamentally different cosmochemical processes. In a few Allende inclusions (called FUN) even greater silicon, magnesium, and oxygen fractionation effects are observed, sometimes accompanied by nuclear anomalies in these and other elements. The origin of the FUN effects remains enigmatic.